

**STUDIES ON SUSTAINABLE TOUGHENED
POLYLACTIC ACID BASED MULTIPHASE SYSTEMS**

Thesis submitted to
Cochin University of Science and Technology
in partial fulfilment of the requirements
for the award of the degree of
Doctor of Philosophy
Under the Faculty of Technology



**COCHIN UNIVERSITY OF SCIENCE AND TECHNOLOGY
KOCHI - 22**

by
V. H. SANGEETHA



**CENTRE FOR BIOPOLYMER SCIENCE AND TECHNOLOGY
A UNIT OF CIPET (GOVT. OF INDIA),
ELOOR, UDYOOGAMANDAL P.O., KOCHI - 683 501**

December 2017

Studies on Sustainable Toughened Polylactic acid based Multiphase Systems

Ph.D. Thesis under the Faculty of Technology

Author

V. H. Sangeetha

Research Scholar

Centre for Biopolymer Science and Technology (CBPST)

A Unit of CIPET (Govt. of India), Eloor, Udyoogamandal P.O., Kochi - 683 501

Supervising guide

Dr. T O Varghese

Director & Head (HLC)

Centre for Biopolymer Science and Technology (CBPST)

A Unit of CIPET (Govt. of India),

Eloor, Udyoogamandal P.O., Kochi - 683 501

December 2017

सेन्टर फॉर बायोपोलिमर साईंस एण्ड टेक्नॉलाजी

(ए यूनिट ऑफ सिपेट)

रसायन एवं पेट्रोरसायन विभाग,
रसायन एवं उर्वरक मंत्रालय, भारत सरकार
जेएनएम कैम्पस, एलूर, उद्योगमंडल पी. ओ.
कोची, केरल - 683 501.

फोन: 0484-2541750, 2555750, फेक्स: 0484-2551740

ई-मेल: cbpst@cipet.gov.in, cbpst2012@gmail.com

वेबसाइट: www.cipet.gov.in



CENTRE FOR BIOPOLYMER SCIENCE & TECHNOLOGY

(A unit of CIPET)

Department of Chemicals & Petrochemicals,
Ministry of Chemicals & Fertilizers, Govt. of India
JNM Campus, Eloor, Udyogamandal P. O.
Kochi, Kerala - 683 501.

Ph: 0484-2541750, 2555750, Fax: 0484-2551740

Mob: 9496156777, 8129497181

email: cbpst@cipet.gov.in, cbpst2012@gmail.com

Web: www.cipet.gov.in

Certificate

This is to certify that the thesis entitled “**Studies on Sustainable Toughened Polylactic acid based Multiphase Systems**” is an authentic record of research work carried out by **V H Sangeetha** under my supervision and guidance at Center for Biopolymer Science and Technology, Kochi. No part of the work reported in this thesis has been presented for any other degree from any other institution. All the relevant corrections and modifications suggested by the audience during the pre-synopsis seminar and recommended by the Doctoral committee have been incorporated in the thesis.

Dr. T. O. Varghese
(Supervising Guide)

Declaration

I hereby declare that the thesis entitled “**Studies on Sustainable Toughened Polylactic acid based Multiphase Systems**” is based on the original research work carried out by me under the guidance and supervision of Dr. **T O Varghese**, Director & Head, Centre for Biopolymer Science and Technology, Eloor, Udyogamandal, Kochi-683501 and no part of the work reported in the thesis has been presented for the award of any degree from any other institution.

Kochi- 22
22/12/2017

V H Sangeetha

*Dedicated to
my dear parents and brother*

Acknowledgements

No achievements blossoms with the lone effort of a single person. There are many heads and hearts behind this work, to bring it to this final form, within the stipulated period, for which I would like to express my deep felt gratitude.

First and foremost, I would like to express my sincere gratitude to Prof. Dr. S. K. Nayak, Director General, CIPEET, for his permission and valuable help extended for accomplishing this work,

I would like to acknowledge my deepest sense of heartfelt gratitude, respect and obligation to my Research Guide, Dr. T. O. Varghese, Director & Head, CBPST for his kind-hearted support, invaluable guidance, motivation, constructive criticism and encouragement throughout the course of work,

I extend my sincere thanks to Dr. Syed Amanulla- Asst. Prof, Mr. K.A. Rajesh -Manager (P/T), Mr. Libin Roberts -Technical Officer, Mr. E Sivakumar- Lecturer, CBPST for giving necessary support for the research.

I owe my special thanks to Dr. V. Ravi Babu, Scientist, CECRI, former faculty CBPST, for his constant support and valuable help rendered for the successful completion of my research work,

I cherish the valuable advice and suggestions given by Prof. Dr. Sunil K Narayanan Kutty, Prof. Dr. K E George, Prof. Dr. Rani Joseph, Prof Dr. Thomas Kurian, Dr. G.S. Sailaja, Mrs. Saira Raj, Department of PS & RT for their whole hearted cooperation throughout my research work,

It is with great pleasure that I express my sincere token of gratitude to Processing Department members, Dr. Manoj Kumar, Shri. SKS Tomar, Sreeraj K.S., Mr. V N Santhosh Kumar, Mr. Bibin Paul for their timely help and inspiration to complete the research work, I also express my sincere thanks to Testing Department members, Mr. Alagu Sudalai. Mr. Abin Davis, Ms. Saranya Kartha, Mrs. Priyanka for all support during my work, Also I extend my sincere gratitude to

Librarians Mr. Nidhin P M and Mr. Bavijesh for timely help at CBPST. I take this time to acknowledge the help provided by former librarians Mrs. Nisha Raj and Ms. Renny also.

I express my special gratitude to my friend Jayavani S, Faculty, CBPST for her encouragement, suggestions and moral support throughout my research career. Also, my sincere gratitude to Arun M Panicker, Research Fellow, CBPST for his valuable suggestions throughout the course of my study.

I am very thankful to Dr. Harekrishna Dekha, Dr. R. Giri, Shri. K S Vidyasagar, Shri. Suraj Varma, Mr. Abin Kuriakose, Shri. Sunil Kumar, Mrs. C Rema, Mrs. Krishnambal, Mrs. Amutha T, Mrs. Usha., Mrs Gem, Augusty sir, Mr. Bharath K.L., Mr. Mohammed Shameem, Mr. Jewel, Mr. Sreejesh, Mr. Subin, Mr. Manoj, Mr. Antony Sibi, Mr. Ajesh, Mr. Prabulan and all my colleagues who rendered all help during the work.

I express my gratitude to STIC-CUSAT, CIPET-Chennai for characterization of the samples. Also I thankfully acknowledge ARSTPS Chennai for all the help provided during my research work. I express my sincere thanks to Mr. Binoop Kumar for the neat compilation of my thesis.

I would like to offer my sincere thanks to all my teachers and friends, who have helped me so much to bring out this work with their advices and discussions. Also, my special thanks to all my students for creating a pleasant atmosphere at CBPST for successful research work.

My heartiest gratitude to the entire dear and near who helped, supported and encouraged me in the fulfillment of this work. My deepest gratitude to my dear parents and my brother, relatives, who stood by me in all my hard times, prayed for me and helped me in this endeavour.

Last but not least I thank the God almighty who gave me the courage and strength for bestowing me with patience for the successful completion of this work.

V. H. Sangeetha

||| Preface |||

This thesis reports to the studies on sustainable toughened Polylactic acid based blends and nanocomposites. Polylactic acid (PLA), a renewable resource based biopolymer became an alternative to petrochemical derived polymer of fossil fuel origin. It is a linear, aliphatic, thermoplastic polyester produced either from L-lactic acid or D-lactic acid monomer via fermentation of carbohydrates by lactic bacteria mainly belongs to the genus *Lactobacillus*. PLA being a fully biodegradable plastic which possess the properties like good mechanical strength, low toxicity, excellent transparency, compostability, biocompatibility etc. have made its applications in packaging and other durable products. Despite PLA possess the above advantages, it cannot compete with the conventional plastics due to inherent brittleness, poor thermal resistance, slow crystallization rate and poor gas barrier properties. For widening the applications of PLA, properties like impact strength, flexibility, stiffness, barrier properties, thermal stability etc. needs to be improved.

Recently, several studies on PLA based blends and composites have emerged with improved chemical, mechanical, and biological properties equivalent or superior to conventional polymers. The most widely used strategies to modify the properties of PLA include polymer blending, copolymerisation, and nanocomposite technology. However, no systematic study has been noted to improve the properties of PLA by melt blending with other elastomers or nanocellulose materials in a cost effective way. In this study, modification of PLA was carried out with various flexible rubbery polymers used as toughening agents and their properties are investigated. Nanocellulose isolated from waste cotton was also used in various PLA based blends and studied their effect on thermo-mechanical properties of toughened PLA system.

Two different types of elastomers namely, Styrene Ethylene Butylene Styrene (SEBS), Ethylene Vinyl Acetate (EVA) and its modified forms namely MA-g-SEBS, EVOH are used to modify PLA by melt blending technique under various compositions and tested their properties such as mechanical, thermal, morphological and performance of the above blends and composites has been investigated.

SEBS is used as toughening agents in PLA, owing to its high impact strength, superior heat resistance, good flow characteristics etc. Modified SEBS, i.e. MA-g-SEBS was synthesized by melt grafting technique using twin screw extruder, was used as toughening agent in order to study the effect of maleation in SEBS for better interfacial adhesion with PLA.

EVA co-polymer offers the advantages of good clarity, gloss, low-temperature toughness, stress-crack resistance, ultra-violet resistance etc. Therefore, EVA and modified EVA (hydrolysed EVA) are used as toughening agents in PLA blends and their mechanical, thermal and morphological properties are investigated.

Nanofibrillated cellulose shows considerable interest in preparing biocomposites owing to its improved mechanical and barrier properties of biopolymers. Nanofibrillated cellulose is isolated from waste cotton by steam explosion technique and used as reinforcing agent in toughened PLA. Both the toughened PLA systems are reinforced with nanofibrillated cellulose at three different compositions and studies carried out in its effect on mechanical, morphological, and thermal properties.

The investigations are presented in **nine** chapters as follows:

A concise prologue to the topic of study is presented in **chapter 1**. Literature review on Polylactic acid based blends and composites with special reference to improvement in impact strength are briefly discussed. Motivation and objectives of the present work are also discussed in this chapter.

The details of the materials used and the experimental procedure for the preparation of PLA based blends and nanocomposites are outlined in **chapter 2**. The various characterization techniques employed for the investigation of modified toughening agents, mechanical, thermal and morphological analysis of PLA blends and nanocomposites are also described in this chapter.

Chapter 3 describes the usage of Styrene Ethylene Butylene Styrene (SEBS) and Maleic anhydride grafted SEBS (MA-g-SEBS) as toughening agents in PLA and studied their effect on property improvement of PLA, especially impact strength. Maleic anhydride was grafted on SEBS by twin screw extruder using dicumyl peroxide initiator. The grafting efficiency and acid number of maleated SEBS was found out by titration method. PLA/SEBS and PLA/MA-g-SEBS blends were prepared under four different compositions (5,10,15 and 20 wt%.) by melt mixing technique using a co-rotating twin screw extruder after optimizing the mixing conditions. Also, the effect of these toughening agents on mechanical, thermal and morphological behaviour of PLA has been investigated.

In **chapter 4**, the isolation of nanofibrillated cellulose from waste cotton using Steam explosion technique is discussed in detail. Nanocellulose was characterized by different analysis techniques like TEM, SEM and XRD.

Chapter 5 deals with the effect of nanocellulose on maleated SEBS toughened PLA blends. Nanocomposites have been prepared by melt blending and were characterized by different techniques like TGA, DSC, SEM, TEM etc. The properties of the blends such as mechanical, thermal and morphological behaviour were also investigated.

Chapter 6 describes the blends of PLA/EVA prepared via melt-mixing technique. The influence of EVA content on the toughening of

PLA has been investigated. Also, kinetic studies for PLA/EVA blends are performed using Flynn–Wall–Ozawa and Kissinger models. The quantitative assessment of non-isothermal melt crystallization behaviour for PLA/EVA blends are also discussed in this chapter.

Chapter 7 deals with the preparation of PLA/EVA/EVOH ternary blend system via melt blending. The effect of degree of hydrolysis of EVA on compatibility, impact strength and crystallization properties of PLA/EVA/EVOH blends are evaluated with PLA/EVA blend and neat PLA. Thermal degradation kinetics of EVA toughened PLA blends were studied using Coats–Redfern method for the better understanding of degradation behaviour. The non-isothermal cold crystallization temperature for PLA and PLA/EVA/EVOH blends are also investigated.

Chapter 8 explains the preparation of PLA /EVA/ EVOH/nanocellulose multiphase composites using melt mixing method. The effects of nanofibrillated cellulose on the mechanical, thermal and surface morphology of PLA nanocomposites are also investigated.

The summary, conclusion and future scope of the study are presented in **chapter 9**

Contents

Chapter 1

INTRODUCTION.....	01 - 68
1.1 Introduction.....	01
1.2 Biopolymers.....	03
1.2.1 Classification of Biopolymers.....	03
1.2.2 Bioplastics.....	05
1.2.3 Classification of Bioplastics.....	06
1.2.4 Advantages of Bioplastics.....	08
1.3 Modification of Biopolymers.....	08
1.3.1 Polymer Blending.....	08
1.3.2 Addition of nanoparticles.....	09
1.4 Nanocellulose.....	10
1.4.1 Cellulose Nanofibrils (CNF).....	11
1.4.2 Cellulose nanocrystals (CNC).....	14
1.4.3 Bacterial cellulose (BC).....	15
Literature Review.....	15
1.5 Polylactic acid (PLA).....	15
1.5.1 PLA Chemistry.....	18
1.5.2 Structure of PLA.....	19
1.5.3 Synthesis of PLA.....	19
1.5.4 Properties of PLA.....	21
1.5.4.1 Physical and chemical properties.....	21
1.5.4.2 Barrier properties.....	21
1.5.4.3 Mechanical properties.....	22
1.5.4.4 Crystallinity and thermal properties.....	23
1.5.5 Processing of PLA.....	24
1.5.6 Blends of PLA.....	25
1.5.6.1 PLA - Starch Blends.....	25
1.5.6.2 PLA-Copolymer Blends.....	27
1.5.6.3 PLA-Acrylonitrile Butadiene Styrene (ABS) Blends.....	29
1.5.6.4 PLA-Natural Rubber (NR) Blends.....	30
1.5.6.5 PLA-Copolyester Blends.....	32
1.5.6.6 PLA-Polycaprolactone (PCL) Blends.....	32
1.5.6.7 PLA-Poly butylene succinate (PBS) Blends.....	35
1.5.6.8 PLA - Polyhydroxyalkanoate Blends.....	36
1.5.6.9 PLA - Poly (butylene adipate-co-terephthalate) (PBAT) Blends.....	36
1.5.6.10 PLA-thermoplastic Blends.....	37
1.5.7 PLA based green composites.....	40
1.5.7.1 PLA - Kenaf Fiber Biocomposites.....	40
1.5.7.2 PLA - Hemp Fiber Biocomposites.....	41

1.5.7.3	PLA- Jute Fiber Biocomposites	42
1.5.7.4	PLA - Bamboo Fiber Biocomposites	43
1.5.8	PLA based nanocomposites	45
1.5.8.1	Polylactic Acid - Montmorillonite Nanocomposites	45
1.5.8.2	PLA-silica nanocomposites	49
1.5.8.3	Polylactic Acid Micro/Nanocrystalline Cellulose Nanocomposites	50
1.5.9	Applications of PLA based Blends and Composites	52
	Motivation for the present work:.....	53
	Objectives	57
	References	58

Chapter 2

MATERIALS AND EXPERIMENTAL TECHNIQUES 69 - 90

2.1	Materials	69
2.1.1	Polylactic Acid (PLA)	69
2.1.2	Styrene Ethylene Butylene Styrene (SEBS)	70
2.1.3	Ethylene vinyl acetate (EVA)	70
2.1.4	Waste Cotton.....	71
2.1.5	Other Chemicals.....	71
2.2	Methodology	72
2.2.1	Blend and Composite preparation	72
2.2.1.1	Melt Blending.....	72
2.2.2	Preparation of test specimen	74
2.2.3	Characterization Techniques	75
2.2.3.1	Fourier Transform Infrared Spectroscopy (FTIR)	75
2.2.3.2	X ray diffraction (XRD).....	75
2.2.3.3	Scanning Electron Microscopy (SEM)	76
2.2.3.4	Transmission Electron Microscopy (TEM)	76
2.2.3.5	Thermogravimetric analysis (TGA)	77
2.2.3.6	Differential Scanning Calorimetry (DSC).....	78
2.2.3.7	Mechanical properties	79
2.3	Isolation of nanocellulose by steam explosion technique	86
2.3.1	Characterisation of cellulose nanofibers.....	87
2.3.1.1	Fourier Transform Infra Red Spectroscopy (FTIR)	87
2.3.1.2	X- ray Diffraction (XRD).....	88
2.3.1.3	Scanning Electron Microscopy	88
2.3.1.4	Transmission Electron Microscopy.....	88
2.3.1.5	Thermo-gravimetric Analysis (TGA)	88
	References	89

Chapter 3

POLYLACTIC ACID (PLA) /STYRENE

ETHYLENE BUTYLENE STYRENE (SEBS) AND

PLA /MA-g-SEBS BLENDS91 - 111

3.1	Introduction	92
3.2	Experimental	96
3.2.1	Materials	96
3.2.2	Grafting of maleic anhydride on SEBS	96
3.2.2.1	Melt Blending	96
3.3	Analysis and Characterisation	97
3.3.1	Analysis of Maleated SEBS	97
3.3.2	Thermal Characterisation	98
3.3.3	Scanning Electron Microscopy	99
3.3.4	Fourier Transform Infrared Spectroscopy	99
3.3.5	Mechanical Properties	99
3.4	Results and discussions	100
3.4.1	Chemical structure characterisation of MA-g-SEBS	100
3.4.2	Mechanical Properties	101
3.4.3	Blend morphology	102
3.4.4	Thermal Properties	105
3.5	Conclusion	109
	References	110

Chapter 4

ISOLATION AND CHARACTERISATION OF

NANOFIBRILLATED CELLULOSE FROM WASTE

COTTON USING STEAM EXPLOSION PROCESS 113 - 126

4.1	Introduction	114
4.2	Materials	115
4.2.1	Isolation of nano fibrillated cellulose from waste cotton using steam explosion	116
4.3	Analysis and Characterisation	117
4.3.1	Fourier Transform Infra Red Spectroscopy (FTIR)	117
4.3.2	X- ray Diffraction (XRD)	118
4.3.3	Scanning Electron Microscopy	118
4.3.4	Transmission Electron Microscopy	118
4.3.5	Thermo-gravimetric Analysis (TGA)	118
4.4	Results and Discussions	119
4.4.1	FTIR Analysis of treated and untreated waste cotton and nano cellulose	119
4.4.2	X-ray diffraction analysis of nanocellulose	121

4.4.3 SEM Analysis of treated and untreated waste cotton, nano cellulose and its nanocomposites	121
4.4.4 Transmission Electron Microscope Analysis	123
4.4.5 Thermogravimetric Analysis (TGA)	123
4.5 Conclusion	124
References	125

Chapter 5

EFFECT OF NANOCELLULOSE ON MA-g-SEBS

TOUGHENED PLA SYSTEM 127- 144

5.1 Introduction.....	128
5.2 Experimental	131
5.2.1 Materials	131
5.2.2 Fabrication of Toughened PLA Nanocomposite	131
5.2.3 Analysis and Characterisation	132
5.2.3.1 X ray Diffraction (XRD)	132
5.2.3.2 Scanning Electron Microscopy (SEM)	132
5.2.3.3 Transmission Electron Microscopy (TEM)	132
5.2.3.4 Thermal Characterisation	132
5.2.3.5 Testing of Mechanical Properties	133
5.3 Results and Discussions	134
5.3.1 XRD analysis of PLA, toughened PLA and its nanocomposites	134
5.3.2 SEM Analysis of nanocomposites.....	135
5.3.3 TEM analysis of PLA nano composites	136
5.3.4 Mechanical properties	137
5.3.5 Thermal properties	138
5.4 Conclusions	141
References	142

Chapter 6

POLYLACTIC ACID (PLA)/ ETHYLENE VINYL

ACETATE (EVA) BLENDS 145 - 175

6.1 Introduction	146
6.2 Experimental	148
6.2.1 Materials	148
6.2.2 Preparation of PLA-EVA Blends	148
6.2.3 Characterization	149
6.2.3.1 Scanning Electron Microscopy	149
6.2.3.2 Mechanical Properties	149
6.2.3.3 Thermal Properties	150
6.3 Results and Discussion	151

6.3.1 Scanning Electron Microscopy Analysis	151
6.3.2 Mechanical Properties	152
6.3.3 Thermal Properties	154
6.3.4 Thermal degradation Kinetics of PLA and PLA-EVA blend.....	156
6.3.5 Differential Scanning Calorimetry (DSC)	163
6.3.6 Non isothermal melt crystallization of PLA and PLA/EVA blends	166
6.4 Conclusions	172
References.....	173

Chapter 7

PLA /EVA/EVOH TERNARY BLEND SYSTEM: EFFECT OF DEGREE OF HYDROLYSIS OF

ETHYLENE VINYL ACETATE 177 - 206

7.1 Introduction.....	178
7.2 Experimental	180
7.2.1 Materials	180
7.2.2 Modification of EVA.....	180
7.2.3 Determination of hydroxyl content of hydrolysed EVA.....	181
7.2.4 Blend Preparation	182
7.2.5 Characterization Techniques	183
7.3 Results and Discussion	184
7.3.1 EVA Hydrolysis	184
7.3.2 FTIR Analysis	185
7.3.3 Mechanical Properties	187
7.3.4 Toughening mechanism via surface morphology of impact fractured surface	189
7.3.5 Thermogravimetric Analysis	192
7.3.6 Differential Scanning Calorimetry (DSC)	200
7.4 Conclusions	203
References.....	204

Chapter 8

EFFECT OF NANOCELLULOSE ON TOUGHENED PLA / EVA /HYDROLYSED EVA TERNARY

BLEND SYSTEM..... 207 - 220

8.1 Introduction	208
8.2 Experimental	209
8.2.1 Materials.....	209
8.2.2 Preparation of Nanocomposites	209

8.3	Testing and characterization	209
8.3.1	Mechanical Properties	209
8.3.2	Scanning Electron Microscopy	210
8.3.3	Transmission Electron Microscopy	210
8.3.4	Thermal properties	210
8.4	Results and discussions	211
8.4.1	Mechanical Properties	211
8.4.2	Scanning Electron Microscopy (SEM)	214
8.4.3	Transmission Electron Microscopy (TEM)	215
8.4.4	Differential Scanning Calorimetry	216
8.4.5	Thermogravimetric analysis (TGA)	217
8.5	Conclusions	219
	References.....	219

Chapter 9

SUMMARY AND CONCLUSION	221 - 226
-------------------------------------	------------------

LIST OF PUBLICATIONS.....	227 - 228
----------------------------------	------------------

CURRICULUM VITAE	229
-------------------------------	------------

||| List of Abbreviations and Symbols |||

ASTM	American Society for Testing and Materials
CNF	Cellulose Nanofibrils
CNC	Cellulose nanocrystals
DSC	Differential Scanning Calorimetry
EVA	Ethylene Vinyl Acetate
EVOH	Ethylene Vinyl Alcohol
FTIR	Fourier Transform Infrared Spectroscopy
LA	Lactic Acid
MA-g-SEBS	Maleic Anhydride grafted SEBS
NFC	Nanofibrillated Cellulose
PLA	Poly(lactic acid)
SEBS	Styrene Ethylene Butylene Styrene
XRD	X ray Diffraction
UTM	Universal Testing Machine
F-W-O	Flynn-Wall-Ozawa
A	pre-exponential factor
α	conversion factor
α_{\max}	degree of conversion
β	heating rate
ϕ	heating rate
E_a	apparent activation energy
n	order of reaction
R	relative gas constant
T	absolute temperature
T_{\max}	temperature at which occurs maximum weight loss
$t_{1/2}$	Crystallization half-time
X(t)	relative crystallinity

- 1.1 *Introduction*
- 1.2 *Biopolymers*
- 1.3 *Modification of Polymers*
- 1.4 *Nanocellulose*
- 1.5 *Poly(lactic acid) (PLA)*

1.1 Introduction

Plastics play an important role in everyday life for its prospective usage in numerous applications such as automobiles, construction, electronics, biomedical, packaging, agriculture etc. [1]. This is because of the positive attributes of plastics such as relative inexpensiveness, easy processability, light weight, non-corrosive nature, high mechanical performance, design flexibility, good barrier properties, heat sealability, resilience, resistance to moisture and chemicals, good aesthetic appearance etc. [2-7]. Packaging remains as the major application in which a large volume of plastics is consumed due to its ease of handling, storage efficiency, attractiveness, light weight, low cost and prolonged product display. It also protects food from spoilage by microbial contamination, physical damage and bio-chemical reactions during storage [8]. Plastics also convey many public health benefits like hygienic drinking water

supplies and also facilitate medical devices like surgical equipments, drips, aseptic medical packaging and blister packs for pills. Transportation vehicles contain about 20 per cent plastics usually as parcel shelves, door liners, steering wheels, etc. [7]. Plastics can also improve the performance and reduce the costs of construction materials including lightweight fixings, windows, door frames, fixtures and insulation materials.

At present, majority of plastics used for various applications are derived from petrochemical sources. Though plastics have brought considerable benefits to the society, it is admitted that our environment is continuously troubled due to its non-degradable nature. The approaches taken up to make free our environment from plastic waste pollution includes i) dumping of plastic waste materials at landfill sites, (ii) use of waste plastics through incineration and recycling process [9]. However, burial of waste plastic materials cannot be practiced in actuality due to the non availability of suitable landfill sites. The drawback associated with the incineration process includes the production of huge quantity of carbon dioxide and other toxic gases, which in turn contributes to pollution and global warming. Recycling process also requires segregation and the process is inconvenient and it comes with high cost. Therefore, the development of eco-friendly plastic materials from renewable energy resources has become an essential task for mankind in this context [10]. The renewable plastics possess superior biodegradation property unlike the conventional polymers and hence, they could be readily composted to natural degradation product like carbon dioxide, water, methane etc. Thus, research and development units in academia and industries are nowadays

more attracted towards the development of environmentally benign plastics which are biodegradable in nature and safe to the environment [11, 12].

1.2 Biopolymers

Biopolymers are polymers produced from living organisms [13]. The molecular structure of biopolymers are made up of repeating units of saccharides, nucleic acids, amino acids and various other chemical side chains imparting their functionalities. These may be polysaccharides, proteins or lignin that act as energy reserves or have a structural function for cells or whole organism [14]. It can also be derived from monomers like lactic acid via chemical, biochemical methodologies to produce polymers namely, Polylactic acid (PLA) [15] or synthesized from microorganisms as in the case of Polyhydroxyalkanoates synthesized from genetically modified microorganisms [16]. Chitosan is yet another common linear polysaccharide composed of randomly distributed β -(1-4)-linked D-glucosamine (deacetylated unit) and N-acetyl-D-glucosamine (acetylated unit). It is obtained by treating the chitin shells of shrimp and other crustaceans with alkaline substance like [17].

1.2.1 Classification of Biopolymers:

Biopolymers are classified according to their source and synthesis process as shown in scheme 1.1 [18].

(i) Biopolymers from biomass:

These polymers are derived from biomass products like polysaccharides and proteins. The major polysaccharides include starch, chitin, chitosan, lignocelluloses etc. Proteins are agro-polymers produced

by plants, animals, and bacteria. Soy protein, corn protein and wheat proteins are among the major plant proteins whereas casein, collagen, gelatin, and keratin are important animal proteins. Lactate dehydrogenase, chymotrypsin, fumarase etc. forms main bacterial proteins [18].

(ii) Biopolymers developed from microorganisms:

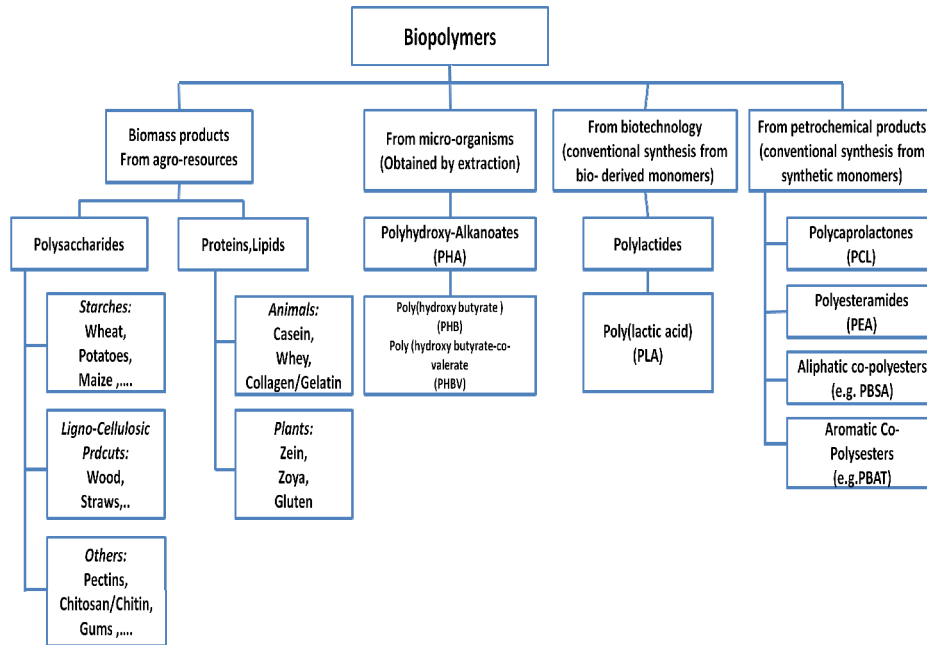
Polyhydroxyalkanoates (PHAs) are family of intracellular biopolymers produced by bacteria as intracellular carbon and energy storage granules. PHA family includes poly hydroxybutyrate homopolymer (PHB), poly(hydroxybutyrate-co-hydroxyalkanoates) etc [19].

(iii) Biopolymers whose monomers obtained from agro-resources:

An example of this type of biopolymer is PLA whose monomer lactic acid obtained by fermentation of carbohydrates by lactic acid bacteria belonging to the genus *Lactobacillus*, or filamentous fungus like *Rhizopus* etc. [20]. The fermentation process requires a bacterial strain, a carbon source (like carbohydrates), a nitrogen source (yeast extract, peptides), mineral elements to allow the growth of bacteria and the production of lactic acid.

(iv) Biopolymers whose monomers are from conventional fossil resources:

A large number of biodegradable polyesters are made from petroleum resources obtained chemically from synthetic monomers which include polycaprolactone, aliphatic copolyesters, and aromatic copolyesters etc [21].



Scheme 1.1 Classification of Biopolymers [18]

1.2.2 Bioplastics

A plastic material is considered as a bioplastic if it is either biobased, biodegradable, or features both properties [22]. At present, bioplastics represent about one per cent of 300 million tonnes of plastic produced annually. The global market size of bioplastics & biopolymers was USD 2.66 Billion in 2015 and is projected to reach USD 5.08 billion by 2021. The market is projected to witness a compounded annual growth rate of 12.0%, in terms of value, during the forecast period [23]. Bioplastics are made partly or completely from polymers derived from biological resources such as sugarcane, potato starch, corn starch or cellulose from cotton, straw etc. Some of them degrade biologically in open air whereas others do so in compostable medium in presence of

micro organisms. Apart from this, there are a few bioplastics that imitate the robustness and durability of conventional plastics like polyethylene, polypropylene, poly (ethylene terephthalate) etc. Bioplastics with lower *carbon footprint* and the capability to degrade completely to carbon dioxide and water are vital and budding complement to conventional petroleum based plastics. As oil becomes limited, the value of bioplastics would increase yet further in the coming years. Bioplastics serve as an alternative for almost every conventional plastics and its corresponding application. Bioplastics have similar properties as the conventional plastics with additional advantages such as reduced “*carbon footprint*” and waste management options such as composting.

1.2.3 Classification of Bioplastics

Bioplastics may be classified into three groups each according their individual characteristics as given below:

i) Bio-based (or partly bio-based), non-biodegradable plastics:

The material or product is partly derived from renewable resources like corn, sugarcane, cellulose etc. Their monomers are biological in origin but the final plastic product is non biodegradable. Bio-based polyethylene is a bioplastic produced from ethanol (from sugarcane), whereas the traditional polyethylene uses fossil resources such as oil or natural gas [24]. Many conventional plastics like polypropylene and poly(vinyl chloride)can also be made from renewable resources, such as bioethanol [25]. The product named ‘Plant Bottle’ uses 30 per cent plant-based materials for its manufacture with the same characteristics as traditional bottle and are non biodegradable and completely recyclable

[26]. Bio-polyamides (PA) and biopolyurethanes are also derived partially by plant based materials which are non-biodegradable [27].

ii) Bio-based and biodegradable plastics

These plastics are derived from different natural sources including plants, cellulose, protein, chitin (prawn shells), bacteria etc. Bio-based plastics in terms of production, renewability and biodegradability include PLA, PHAs etc. Recent development in bacteria synthesized plastics like PHA and the utilization of nature's own building block such as proteins, fats, carbohydrates, lignin, etc. obtained from agricultural feedstocks and agro-wastes which made a major advancement towards bio-based plastics. PLA's increasing popularity has seen its usage from primarily food packaging to a wide range of applications including medical, textile, automotive, cosmetic and household applications. PHA is fully biodegradable under compostable conditions which is non-toxic, and can be used in a wide range of applications from food packaging to medical implants.

iii) Plastics based on fossil resources and biodegradable

These plastics are derived from fossil fuels but are still biodegradable and include polymers such as polybutylene adipate terephthalate (PBAT), which is a random copolymer made up of adipic acid, 1,4 -butanediol and dimethyl terephthalate. It is a fully biodegradable under composting conditions and possesses properties similar to LDPE such as high elasticity, fracture resilience and flexibility and thereby forms a viable alternative for use in packaging. It is particularly suited for manufacturing garbage bags or disposable packaging due to its ability to decompose in compost

within a few weeks [28]. Other synthetic biodegradable polyesters are poly (ethylene succinate) , poly (propylene succinate), poly(butylene succinate), polycaprolactone etc [29].

1.2.4 Advantages of Bioplastics

The bioplastics industry is fast-growing, laden with the capability to resolve economic growth from resource depletion and negative environmental impact and help to convey better economic and environmental outcomes by replacing fossil feedstock with renewable ones. They also contribute to increased resource competence by applying the principles of the circular economy and make sure plastics to re-enter the economy as precious technical material or as biological nutrients [22]. Bio-based plastics have some unique advantage over conventional plastics with the competence to reduce the dependency on limited fossil resources, reduce greenhouse gas emissions, saving fossil resources, and for substituting them gradually. Furthermore, biodegradability is an add-on property of certain types of bioplastics and offers additional means of recovery at the end of life of a product.

1.3 Modification of Polymers

There are several approaches to modify biopolymers which include plasticization, physical blending, copolymerization, incorporation of fillers and reinforcements etc.

1.3.1 Polymer Blending

Polymer blending is a suitable method for developing new polymeric materials which combine the advantages of more than one constituting polymers [30]. The properties of the resulting polymer

blends are also tunable through the selection of blending components and the variation of blend compositions. Blending can be carried out by using conventional processing machines such as extruder, internal mixer etc. Wide range of property attributes can be achieved by this approach to meet the requirements of the targeted application in relatively short span of time and at low cost. The goal of blending is to bring about improvement in material properties and to maximize its performance for a suitable application. Biopolymers have been blended with various plasticizers and polymers in order to improve the performance of the polymer. Polymer blends are prepared generally by melt mixing technique, latex mixing [31] and solution mixing. Melt blending technique is more convenient, much more cost effective than other techniques.

1.3.2 Addition of nanoparticles

Addition of nanoparticles to an immiscible blend improves the compatibility of blends. Nanoparticles act as interfacial modifiers to strengthen the interfacial adhesion and thus blend performance. The incorporation of nanoparticles can create high performance material that combines the advantages of polymer blends and the virtues of polymer nanocomposites. Therefore, tailoring phase morphology of immiscible blends by addition of nanoparticles represents a universal way of preparing polymer nanocomposites with improved properties. The nanoscale fillers, such as carbon nanotubes (CNTs) [32] or inorganic nanoparticles [33] have been used to reinforce polymer matrices. Their high specific surface area enables the formation of a large interphase in the composite and strong filler-matrix interactions. In the same way, the

addition of nanoclays to fiber-reinforced thermoplastic composites has been reported to improve damping properties, fatigue life, toughness, and wear resistance [34]. Nanocellulose is often being regarded as a renewable reinforcement for the production of high performance biocomposites [35].

1.4 Nanocellulose

Nanocellulose is one of the most fascinating nature-based materials derived from lignocellulosic biomass which is used in biomaterials, engineering, medicine, optoelectronic devices, textiles, cosmetics etc. It offers inherent renewability, availability, flexibility, printability, low density, high porosity, optical transparency and extraordinary mechanical, thermal and physico - chemical properties [36]. Most lignocellulosic biomass comprises mainly cellulose, hemicelluloses and lignin. Cellulose is the most abundant polymer in nature and it accounts for approximately 40% of lignocellulosic biomass which may be either cellulose nanofibers (CNF), nanocrystalline cellulose or cellulose nanocrystals or bacterial nanocellulose. Nanocellulose films have been used for diverse applications like food packaging [37], electronics etc. it is used in paper and paperboard industry to enhance the bond strength and to have reinforcement effect on paper [38]. The native crystallinity, high strength, and moderate to high aspect ratio of nanocellulose are important for stress-transfer and load-bearing applications in thermoplastics, such as polyvinyl alcohol (PVA)[39], PLA [40], polycarbonate (PC) [41], polyurethane [42], polymethyl methacrylate (PMMA) [43] etc. It can form emulsions and dispersions and is used as thickeners and stabilizers in food products [44]. It has good absorption properties and therefore

used in diapers and other hygienic products and are inherently suitable for tissue engineering scaffolds, membranes, hydrogels, electrospun nanofibers and other medical applications. Another area of use of nanocellulose based materials is for drug delivery in the form of membranes, tablet coatings etc. They are extensively used as reinforcing fillers in thermoplastic polymeric matrices to produce cost-effective, high performance materials, with a 'greener' footprint.

1.4.1 Cellulose Nanofibrils (CNF)

Cellulose nanofibrils (CNF) are those materials containing fibrils with length in micrometer and width in the nanometric range forming a network structure. They can be 20–50 nm in width and 500–2000 nm in length [45]. CNFs are prepared by mechanical methods via high shearing followed by homogenization at high pressure. They are mainly produced using equipments like high pressure homogenizers, refiners, grinders, cryo-crushers and microfluidizers. Cellulose nanofibers (CNF) act as potential materials for various applications like optoelectronic conversion, energy storage, packaging, drug delivery, bioimaging and biomedical materials, nanofillers, protective coatings, barrier membranes filtration media, transparent films, antimicrobial activity, pharmaceuticals etc [46][47][48].

The isolation of nanocellulose from different cellulose sources occurs in two stages: The first stage consists of purification, homogenization and pretreatment of the cellulosic material. The pretreatment depends on the cellulose source and involves the complete or partial removal of wax, pectin, hemicelluloses, lignin, etc. and subsequent isolation of individual

fibers. The second stage involves the isolation of purified cellulose into microfibrillar and crystalline components. There are several approaches to isolate cellulose particles. The three basic approaches are mechanical treatment, acid hydrolysis, and enzymatic hydrolysis. Mechanical processes such as high-pressure homogenization, grinding/refining, cryocrushing, high intensity ultrasonic treatments, and microfluidization have been used to extract cellulose fibrils from different sources.

a) High Pressure Homogenization

It is a widely used method for bulk production of cellulose nanofibrils, which involves forcing of the suspension through a very narrow orifice using a piston under high pressure of about 50–2000 MPa. The resultant high suspension streaming velocity causes an increase in the dynamic pressure and successive reduction in the static pressure below the vapor pressure of the aqueous phase which leads to the formation of gas bubbles that collapse immediately and subsequently cause disruption of cellulose fibrillar structure [49].

b) Microfluidization

Unlike the homogenizer which operates at constant pressure, the microfluidizer operates at a constant shear rate. The fluid slurry is pumped through a z-shaped chamber, where it reaches a high shear force and pressure as high as 276 MPa approximately [50].

c) Cryocrushing

Cryocrushing is a mechanical fibrillation method which produces fibrils with relatively large diameters, ranging between 0.1 and 1 μm

[51]. In this process, water-swollen cellulose fibers are frozen in liquid nitrogen and subsequently crushed [52]. This procedure is applicable to various cellulose materials and can be used as a fiber pretreatment process before homogenization.

d) Steam explosion

It is a thermo-mechanical process that breaks down the structural components of cellulose using steam. Steam at high pressure penetrates deep into the lignocellulosic biomass through diffusion and thereby releases hemicelluloses from cell walls and makes them available to chemical and biochemical degradation. Both steam and acetic acid (released from the biomass during steam explosion) activate the hydrolysis of hemicelluloses. The sudden release of pressure generates shear force which hydrolyzes the glycosidic bond and hydrogen bonds between the glucose chains, leading to the formation of nanofibers. Figure 1.1 shows the schematic of lignocellulose macromolecular structure before and after pre-treatment.

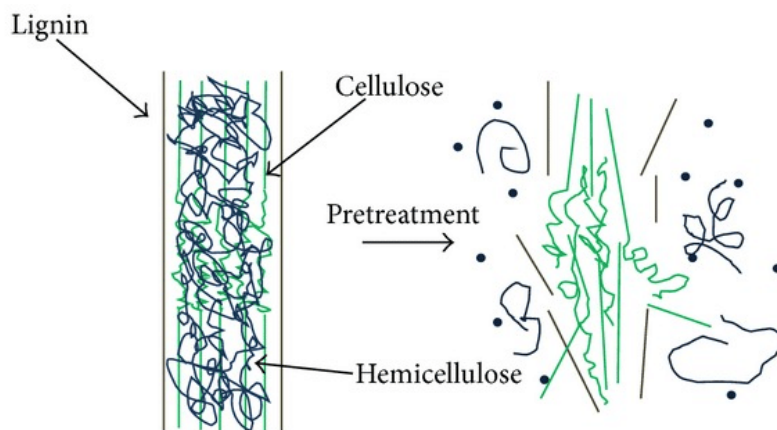


Figure 1.1 Deconstruction of lignocellulose into cellulose, hemicellulose, and lignin [45]

The general advantages of steam explosion pretreatment are that (1) use of limited chemicals except water (2) avoids excessive degradation of monosaccharides (3) minimum corrosion of equipment is generated at mild pH reaction media (4) less energy requirements than mechanical process (5) cost effective and (6) steam-exploded biomass is quite liable to the action of enzyme like cellulases. However, steam explosion also has some economical problems, i.e. incomplete destruction of lignin-carbohydrate complex, possible generation of fermentation inhibitors, weight losses of initial dry mass, etc [53-56].

1.4.2 Cellulose Nanocrystals

CNCs formed by acid hydrolysis are spheroid, spherical or rod-like crystals of cellulose particles with high aspect ratio (3–5 nm wide, 50–500 nm in length), and are highly crystalline (54–88%), hundred percentage cellulose with a high fraction of beta crystal structure (68–94%) [57]. These particles are also called as nanocrystalline cellulose, cellulose whiskers and cellulose nanowhiskers. They resemble whiskers because of the tapering ends of the crystals and most likely result from the acid hydrolysis [58]. The isolation of CNCs from plant sources is generally conducted in three steps. The first step is the purification of raw material to remove non-cellulose components from the plant material and to isolate purified cellulose. The purification can be performed with sodium or potassium hydroxide followed by bleaching with sodium chlorite or sodium hypochlorite. This process is repeated several times for more effective purification of cellulose. The second step is a controlled chemical treatment, generally acid hydrolysis,

followed by mechanical or ultrasound treatment that separates CNCs. Different strong acids including hydrochloric and sulphuric acids have been extensively used to disrupt cellulose fibers. Strong acid hydrolysis treatment applied to cellulosic fibers allows the disintegration of amorphous domains. During the acid hydrolysis process, the hydronium ions penetrate into the cellulose chains in the amorphous regions resulting in the hydrolytic cleavage of glycosidic bonds and releases individual crystallites after mechanical treatment like ultrasonication.

1.4.3 Bacterial cellulose (BC)

Bacterial nanocellulose is produced by microorganisms extracellularly, with *Gluconacetobacter xylinum* being one of the most efficient in producing cellulose. BC is synthesized as pure cellulose BC is produced in the form of twisting ribbons with cross-sections of 3–4 nm \times 70–140 nm and a length of more than 2 μ m [59].

Literature Review

1.5 Polylactic acid (PLA)

PLA is the most widely used biodegradable material that has the largest possibility to replace the position of the conventional plastics in the current scenario of oil scarcity. The production cost of PLA is coming close to the cost of traditional plastics and with the strong extension of market applications, will get soon accepted globally. The latest statistics in 2012 shows that in the next 10 years, the average annual growth rate of lactic acid and PLA will be 18.7% [60]. PLA market is expected to acquire \$5.2 billion by 2020, registering a

compound annual growth rate of 19.5% during the forecast period 2013-2020[61]. Currently the total production capacity of PLA globally is about 180,000 tonnes and the leading producers in the world are the United States, Japan and Germany. American Nature Works LLC is the world's largest PLA manufacturer, with an annual capacity of 140,000 tonnes [60]. Favourable compostable and degradation characteristics, its ability to maintain carbon dioxide balance after its decomposition are the various factors that contribute to the success of PLA as a substitute to traditional petroleum-based plastics [62,63]. Currently, annual crops such as corn, sugarcane and sugarbeets prevail as plant based feedstock in the commercial production of PLA. PLA, being derived from renewable resources such as corn, wheat, or rice is biodegradable, recyclable, and compostable and its production also consumes less carbon dioxide [15, 64, and 65]. The characteristics like sustainability and eco-friendly make PLA an attractive biopolymer. The most noticeable aspect of PLA, especially with respect to biomedical applications, is its biocompatibility. A biocompatible material should not produce toxic or carcinogenic effects in local tissues. PLA has better thermal processibility compared to other biopolymers such as poly(hydroxy alkanates) (PHAs), poly(ethylene glycol) (PEG), poly(caprolactone) (PCL), etc. It can be processed by injection molding, extrusion blown film, blow molding, thermoforming, fiber spinning, and film forming. Lower energy use makes PLA production potentially beneficial with respect to cost as well.

Despite its advantages, PLA is a very brittle material with very less elongation at break (less than 10%) [66,67]. Although its tensile strength and elastic modulus are comparable to poly(ethylene terephthalate)

(PET), poor toughness limits its wide range of applications [68]. The rate of degradation of PLA via hydrolysis of ester back bone depends on crystallinity, molecular weight, molecular weight distribution, morphology, water diffusion rate into the polymer, and the stereoisomeric content of PLA [69]. The degradation rate is an important selection criterion for biomedical applications [70]. The slow degradation rate leads to a long *in vivo* life time, which could be up to years in some cases [71]. PLA is relatively hydrophobic, with a static water contact angle of approximately 80° that results in low cell affinity, and inflammatory response from the living host on direct contact with biological fluids. PLA is chemically inert with no reactive side-chain groups making its surface and bulk modifications difficult. The brittleness of PLA can be modified via several approaches like copolymerisation of lactic acid with other monomers such as α -caprolactone and by blending PLA with a second polymer or a plasticiser [72]. Extensive efforts have been made to modify the properties of PLA via the first approach. Nevertheless none of these PLA copolymers are commercially available in the market. Blending PLA with other flexible biodegradable or non biodegradable polymers present a more pragmatic and economic way of toughening the material. PLA has been blended with a number of polymers such as polycaprolactone (PCL), polyhydroxyalkanoate (PHA), and polyethylene (PE). Many of these PLA blends are immiscible or only partially miscible and may need compatibilisers to improve their compatibility [73, 74]. This will improve the dispersion of the minority phase, the adhesion between the blend components and stabilise the blend morphology resulting in better mechanical properties. Compatibilizers can be introduced by adding a

premade block or graft copolymer, or by *in situ* reactive formation during melt processing. The flexibility and ductility of PLA can also be improved by blending PLA with a plasticiser. Several low molecular weight compounds have been employed as plasticizers for PLA, for example, glycerol triacetate citrate and polyethylene glycol. Another method to improve the mechanical and thermal properties of PLA is the addition of fillers or filler materials. PLA/plant fiber green composites were widely investigated and it has been found that they exhibit significant improvement in properties.

1.5.1 PLA Chemistry

The gifted feedstock for the production of PLA is lactic acid (2-hydroxy propionic acid), which contains a chiral centre. Lactic Acid (LA) can be produced by fermentation from renewable resources such as corn, potato, sugarcane molasses and beet sugar. The LA produced contains both D and L forms, and the L-form is predominant. L-lactide monomer, a cyclic dimer of LA, is presently being distilled from corn biomass, which naturally contains L-lactic acid, oligo-L-lactide. The 90% pure commercial grade LA contains impurities such as arsenic (<1 ppm), iron (<5 ppm), heavy metals (<5 ppm), chloride (<10 ppm), sulfates (<10 ppm), sulphated ash (maximum 0.05%), reducing sugar, methanol and methyl ester. Stereochemical purity of LA is an important factor in deciding the properties of PLA. The stereoisomers of LA are shown in Figure 1.2 [75].

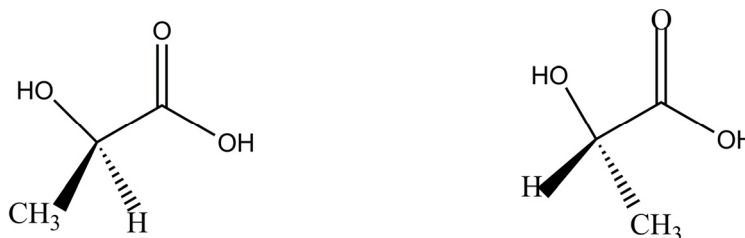


Figure 1.2 Stereoisomers of lactic acid

1.5.2 Structure of PLA

The structural formula of PLA is shown in Figure. It is a chiral polymer in which molecules with asymmetric carbon atoms have a helical orientation. PLLA and PDLA are the two optical isomers of PLA. In 1968, de Santis and Kovacs reported the pseudo-orthorhombic crystal structure of PLLA [76]. The crystal structure of PLA is based on an orthorhombic base-centered unit cell with two $10/3$ helical chains arranged along the c axis. PLA shows hexagonal packing. The point group of PLLA crystal is D_2 [77].

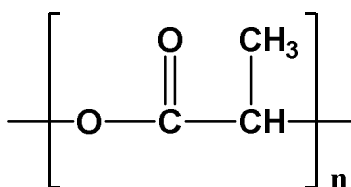


Figure 1.3 Structure of PLA

1.5.3 Synthesis of PLA

The synthesis of LA into high-molecular-weight PLA follows two different routes of polymerization, as depicted in Figure. Lactic acid is polymerized via condensation to yield a low-molecular-weight, brittle and glassy polymer. The molecular weight of this condensation polymer

is low due to the presence of water which should be removed. The second route of producing PLA is ring-opening polymerization (ROP) of lactide to yield high-weight average molecular weight ($M_w = 100,000$ Da) PLA. The lactide method is used for producing pure, high-molecular-weight PLA. Mitsui Toatsu Chemicals recently commercialized a process wherein LA and catalyst undergoes azeotropic dehydration in a refluxing, high-boiling, aprotic solvent under reduced pressures to obtain PLA with weight-average molecular weights greater than 300,000 [78-80]

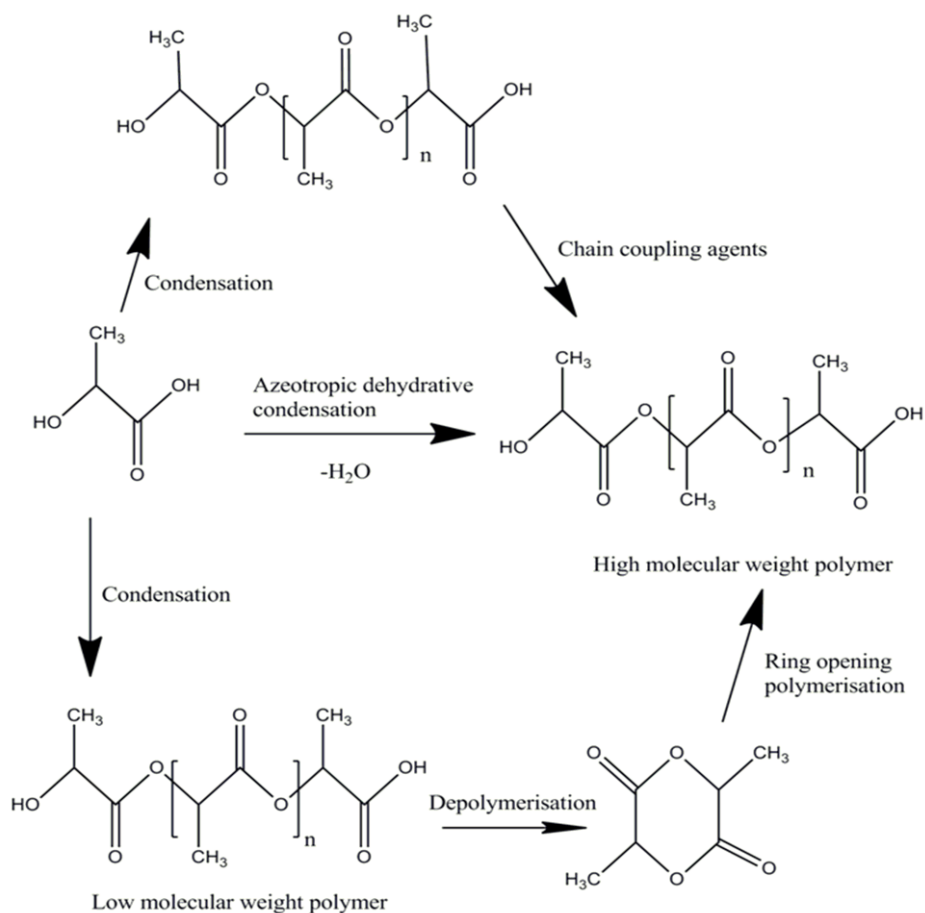


Figure 1.4 Synthesis routes of PLA

1.5.4 Properties of PLA

1.5.4.1 Physical and chemical properties

Several distinct forms of polylactide exist due to the chiral nature of lactic acid. Poly-L-lactide (**PLLA**) is the product formed from polymerization of L,L-lactide (also known as L-lactide). PLLA has a crystallinity of around 37%, a glass transition temperature of 60–65 °C, and melting temperature in the range 173–178 °C. The surface energy of PLA made up of 92 per cent l -lactide and 8 per cent meso-lactide was found to be 49 mJ m⁻², with dispersive and polar components of 37 and 11 mJ m⁻² respectively indicating a relatively hydrophobic structure compared with that of other biopolyesters. The best solvent for PLA is chloroform. Other solvents are chlorinated or fluorinated organic compounds, dioxane, and furan. They are also soluble in many other organic solvents like acetone, pyridine, ethyl lactate, tetrahydrofuran, xylene, ethyl acetate, dimethylformamide, methyl ethyl ketone. Among non solvents, the most relative compounds are water, alcohols (*e.g.* methanol, and ethanol) and alkanes (*e.g.* hexane and heptane) [81].

1.5.4.2 Barrier properties

PLA finds a lot of packaging applications and its barrier properties on gases like carbon dioxide, oxygen and water vapour have been mostly investigated. The CO₂ permeability coefficients for PLA polymers are lower than those reported for polystyrene at 25°C and 0 per cent relative humidity (RH) and are higher than those for PET. The oxygen permeability for PLA film was 3.5×10^{-18} and 11×10^{-18} at 5 and 40°C respectively which are almost to similar to PET. Auras *et. al* have shown

that the permeability for 98% L-Lactide polymers is almost constant over the range studied despite PLA being a polar polymer [82].

1.5.4.3 Mechanical properties

The mechanical properties of PLA can vary from soft and elastic materials to stiff and high strength materials according to its crystallinity, polymer structure and molecular weight, material formulation and processing characteristics. For instance, commercial PLA, with 92 per cent l-lactide, 8 per cent meso-lactide has a modulus of 2.1 GPa and an elongation at break of 9 per cent. After plasticization, its Young's modulus decreases to 0.7 MPa and elongation at break rises to 200 per cent, with a corresponding shift in T_g from 58°C to 18°C. This indicates that mechanical properties can be readily tuned to suit different applications. The typical values of mechanical properties of PLA (Ingeo Biopolymer 3001 D) are displayed in Table 1.1 [83].

Table 1.1 Mechanical properties of PLA (Nature works -Ingeo Biopolymer 3001 D [Taken from mechanical data sheet of Nature works Ingeo Biopolymer 3001 D]

Physical Properties	Ingeo Resin	ASTM method
Specific Gravity	1.24	D792
MFR, g/10 min (210°C, 2.16kg)	22	D1238
Clarity	Transparent	
Mechanical properties		
Tensile Yield Strength, psi (MPa)	9,000 (62)	D638
Tensile Elongation, %	3.5	D638
Notched Izod Impact, ft-lb/in (J/m)	0.3 (16)	D256
Flexural Strength (MPa)	15,700 (108)	D790
Flexural Modulus (MPa)	515,000 (3600)	D790
Heat Distortion Temperature (°C)	55	E2092

1.5.4.4 Crystallinity and thermal properties

The properties of PLA depend on its molecular characteristics such as crystalline thickness, crystallinity, spherulite size, morphology and degree of chain orientation. The physical properties of polylactide are related to the enantiomeric purity of the lactic acid stereo-copolymers. PLA can be totally amorphous or with up to 40 per cent crystalline. PLA resins containing more than 93 per cent of l -lactic acid are semi-crystalline, but when with 50–93% is entirely amorphous. Generally, most PLAs are made up of l and d, l -lactide copolymers, since the reaction media often contain some meso-lactide impurities. Depending on the preparation conditions, PLLA exists in different crystalline forms. The α -form exhibits a well-defined diffraction pattern. This structure, with a melting temperature of 185°C is more stable than its β - counterpart which melts at 175°C. The latter form can be prepared at a high draw ratio and a high drawing temperature. The γ - form is formed by epitaxial crystallization. The crystallization kinetics of PLA is found to be rather slow, and it exhibits properties similar to poly(ethylene terephthalate) (PET). The rate of crystallization increases with a decrease in the molecular weight and it depends on the copolymer composition. PLLA can crystallize in the presence of d -lactide but as the structure becomes more disordered, the rate of crystallization decreases. PLA can be oriented by processing and chain orientation increases the mechanical strength of the polymer. If orientation is performed at low temperature, the resulting PLLA has higher modulus without any considerable increase in crystallinity. The crystallinity level of PLA can be determined by Differential Scanning Calorimetry (DSC).

The crystallization of thermally crystallizable, but amorphous PLA, can be initiated by annealing it at temperatures between 75°C and the melting point. Annealing crystallizable PLA copolymers often produces two melting peaks [84] and different hypotheses have been put forward to explain this feature. The typical PLA glass transition temperature (T_g) ranges from 50°C to 80°C, whereas its melting temperature ranges from 130°C to 180°C.

1.5.5 Processing of PLA

The processing of PLA is much more challenging than that of commodity plastics due to its hygroscopic nature and relatively poor melt stability. The commonly used processing techniques such as injection moulding, stretch blown film, extrusion blown film, thermoforming etc. can also be applied for PLA. The properties of the polymer will therefore depend on the specific conditions during processing steps. The main parameters during melt processing are temperature, residence time, moisture content and atmosphere.

The various means for improving the processability of PLA can be divided into those performed in the melt as a finishing process and those carried out as a subsequent and independent processing step. The process performed in the melt such as catalyst deactivation is mainly concentrated on improving the melt stability. Deactivators used for PLA are phosphorous containing compounds, antioxidants, acrylic acid derivatives and organic peroxides. Pre drying of the polymer is generally recommended prior to the processing of PLA in order to minimize the thermo - hydrolysis and consequent molecular weight reduction during melt processing. Suggested

drying conditions for PLA are 60 °C under vacuum or under hot dry air. Typically the polymer is dried to less than 100 ppm (0.01%, w/w moisture content). Natureworks LLC, one of the main suppliers for PLA polymers, recommended that resins should be dried to 250ppm (0.025%, w/w) moisture content or below before extrusion. Processes that have long residence times or high temperature approaching 240 °C should dry resins below 50ppm to achieve maximum retention of molecular weight [85].

1.5.6 Blends of PLA

1.5.6.1 PLA - Starch Blends

Starch being a hydrophilic material, fine dispersion in a hydrophobic polymer matrix is difficult. Generally, the mechanical properties of starch-related blends are not so good due to the poor affinity between starch and the other component. Thus, great efforts have been made to blend PLA and starch in order to produce a completely biodegradable plastic derived from natural renewable resources. Blending starch and PLA could drastically reduce the cost and enhance the biodegradability of blends.

Wootthikanokkhan et al. [86] studied PLA grafted with maleated thermoplastic starch (PLA-*g*-MTPS) and also compatibilizing efficiency of these copolymers in PLA/thermoplastic starch (TPS) blends. Maleated thermoplastic starch (MTPS) was first prepared by reacting cassava starch with glycerol and maleic anhydride. MTPS was later grafted onto PLA molecules using peroxide as initiator. The mechanical properties of the blend were improved considerably compared to those when PLA-*g*-MTPS was prepared with lesser amount of peroxide.

Kun-yu et al. [87] prepared blends of PLA with acetylated thermoplastic starch (ATPS) via melt mixing. The miscibility, thermal, mechanical and rheological properties were studied as a function of acetylated starch. It was found that the impact strength increased thrice with increase in percentage of acetylated starch (40 wt. %) than that of pure PLA. With increase in ATPS content, the percentage elongation increased significantly compared to virgin PLA. The glass transition temperature of PLA/ATPS blends decreased with increase in the amount of ATPS, indicating partial miscibility between the two phases. DSC studies showed that the crystallisation and melting temperature decreased with increase in ATPS content. DMA studies also supported the enhancement of cold crystallisation and ductility of PLA with the incorporation of acetylated starch.

Zhang et al. [88] reported a layer-like microstructure along flow direction (FD) in PLA/starch blends via pressure-induced flow (PIF) processing. The impact and tensile strength for PLA/starch blends with the layer-like microstructure was improved by 200% and 40% respectively. DMA and DSC results shows that the confinement of molecular chain in amorphous phase of PLA and the interphase between starch particles and PLA for pressure induced flow samples significantly increased compared with non-PIF samples

Xiong et al. [89] evaluated the efficiency of the effect of renewable tung oil anhydride (TOA) as a plasticiser on PLA/starch blends. Neat PLA or PLA/starch blends with and without TOA were prepared via melt blending in a twin screw extruder. The properties of PLA/starch blend

changed with the addition of only 5 wt. % of TOA in PLA/starch blend. The elongation at break and impact strength increased to ~ 17% and ~ 41 KJ/m² respectively whereas the tensile strength decreased up to ~ 30 MPa. Thus, TOA acted well as a plasticizer to alter PLA/starch blend from brittle to ductile state. A reduction in tensile properties was noticed when the content of TOA exceeded 7 wt. %. But, the impact strength of PLA/starch/TOA blends was not much changed with the increase in amount of TOA above 7 wt. %.

1.5.6.2 PLA-Copolymer Blends

Blending PLA with other polymers renders an economic path to obtain toughened products. Blending PLA with other biodegradable polymers is particularly interesting to keep the integrity of biodegradability.

Yao et al. [90] studied blends of PLA/poly(propylene carbonate) (PPC) using maleic anhydride (MA) to modify its properties. The melt compounding was done using a Haake Rheomix internal mixer. The toughness was improved while the strength was almost kept constant by adding a very low content of 0.9% of MA into the blends. PLA/MA-g-PPC blends noted stress whitening accompanied by necking with the addition of MA. The strain-at-break was also markedly increased compared with PLA/PPC binary blend.

Zhang et al. [91] prepared PLA/MBS blends by melt mixing with methyl methacrylate-butadiene-styrene(MBS) content of 5%, 7%, 10%, 25% w/w respectively. The addition of MBS changed the tensile behavior of PLA significantly. The impact strength was increased twenty

one times than neat PLA. Shear yielding in PLA matrix was indicated by the cavitation of MBS particles. The increase in viscosity and elasticity of PLA/MBS blends at low shear rate range can be attributed to the interfacial adhesion between MBS and PLA. Thus, MBS could be used as an effective impact modifier for PLA.

Afrifah et al. [92] conducted impact modification of PLA with biodegradable Ethylene/Acrylate Copolymer (EAC) with varying compositions of the blends 0, 3, 5, 10, 15, 20, and 30 wt% respectively). The addition of EAC up to 5 wt. % into PLA matrix affected neither the ductility, nor the energy to break the samples. Whereas, above this concentration, a significant increase in both ductility and energy to break occurred. Tensile strength and modulus of PLA decreased almost linearly with increase in EAC content. Tensile strength and modulus decreased by 38 and 31% respectively, by the addition of 20 wt% EAC in the blends.

Ma et al. [93] melt blended PLA and Ethylene Vinyl Acetate (EVA) using HAAKE Rheometer (at 170°C, 40 rpm, 4 min). Two series of blends PLA/EVA (80/20) blends in a fixed ratio, but with varying vinyl acetate content in EVA copolymers from, and 100/0, 95/05, 90/10, 85/15, 80/20 and 70/30 were studied. The incorporation of 20 wt% of EVA copolymer increased the elongation at break of PLA dramatically meanwhile the yield strength dropped out enormously. The compatibility between PLA and EVA was improved with the increase in vinyl acetate content. The toughness of the PLA/EVA (80/20) blends at first increased with VA content up to 50 wt% and then decreased. At low VA content

large EVA particle size and weak interfacial adhesion compromised on the toughness of the PLA/EVA blends. Impact toughness of PLA/EVA50 blends was noticeably improved by the addition of 15 wt% EVA.

Su et al. [94] used glycidyl methacrylate (GMA)-grafted POE (mPOE) as a toughening agent for PLA. Both the elongation and notched Charpy impact strength increased consistently with mPOE content. The impact strength was increased seven times that of neat PLA with the use of compatibiliser. The impact strength was increased to 54.7 kJ/m² with further addition of m POE to 45 wt%.

Taib et al. [95] melt blended PLA with varying amounts of ethylene acrylate copolymer as impact modifier. The tensile modulus of PLA also decreased with the increase of impact modifier content. The elongation at break of PLA slightly decreased with the addition of 3 and 5 wt% impact modifier. A significant increase in the elongation at break was observed with 10 wt% impact modifier. Later it levelled off up to 30 wt% impact modifier. The elongation at break increased amazingly with 40 and 50 wt% impact modifier contents in PLA. SEM results revealed that a debonding initiated shear yielding mechanism was involved in the toughening of PLA using ethyl acrylate.

1.5.6.3 PLA-Acrylonitrile Butadiene Styrene (ABS) Blends

NatureWorks [96] recently identified toughening agent called BlendexTM 338, for PLA, an effective toughening agent among various impact modifiers. The impact strength and elongation was increased upto 20% with the use of BlendexTM 338 compared to neat PLA

whereas tensile yield strength decreased from 62 MPa for neat PLA to 43 MPa.

Shimizu et al. [97] introduced styrene acrylonitrile glycidyl methacrylate copolymer (SAN-GMA) as a reactive compatibilizer and ethyltriphenylphosphonium bromide (ETPB) as a catalyst to enhance the compatibility between PLA and ABS during melt blending. The compatibilized PLLA/ABS blends exhibited improved impact strength and elongation but showed slight reductions in modulus and tensile strength. On adding 5 phr SAN-GMA to PLLA/ABS (70/30, W/W) blend increased elongation and impact strength. The elongation and impact strength of the blend was increased by further inclusion of 0.02 phr ETPB.

1.5.6.4 PLA-Natural Rubber (NR) Blends

NR is a renewable polymer containing 91–94 wt% polyisoprene with high modulus and outstanding mechanical strength and makes it ideal for toughening PLA.

Jaratrotkamjorn et al. [98] toughened PLA by blending with natural rubber, epoxidized natural rubber (ENR) and NR grafted with poly(methyl methacrylate) (NR-g-PMMA). The Young's modulus of the blends containing NR-g-PMMA and ENR was found to be higher than that of PLA/NR blend. The yield stress of PLA dropped out largely when blended with 10% of NR and on addition of 5wt% ENR. The lower stress at break in these blends may relate to their lower ductility. NR gave higher tensile strength and ductility than ENR; although ENR is more compatible to PLA than NR. The addition of ENR and NR-g-

PMMA reduced flexural properties of PLA. NR was found to be the best toughening agent compared to NR-g-PMMA and ENR.

Zhang et al. [99] grafted natural rubber (NR) with butyl acrylate (BA) by emulsion polymerization using potassium persulfate as initiator. Natural rubber grafted polybutyl acrylate, NR-g-PBA/PLA and NR/PLA blends were both prepared with various rubber contents (NR-g-PBA and NR contents were 1%, 3%, 5%, 10% and 20% by weight of PLA) in a Haake internal melt mixer (60 rpm, 170°C for 10 min). NR-g-PBA was melt blended with PLA for a toughening modification and compared with NR/PLA blends. SEM micrograph of the blends of NR-g-PBA/PLA showed no obvious interface. However many spherical globules can be observed in the NR/PLA blends, which established less compatibility between NR and PLA. Both NR/PLA and NR-g-PBA/PLA blends showed enhanced impact strength and elongation at break accompanied by reduced tensile modulus and strength. NR-g-PLA showed a better toughening effect on PLA than that of ungrafted NR.

Tanrattanakul et al. [100] studied the mechanical properties of PLA natural rubber blend in a twin screw extruder. Polyvinyl acetate (PVAc) was grafted on natural rubber with different contents of 1, 5 and 12% by emulsion polymerisation technique. The notched Izod impact strength and tensile properties were determined using compression molded specimens. All the binary blends showed improved Izod impact strength compared to PLA particularly 5 % PVAc showed a four-fold increment. The tensile properties also increased with the addition of PVAc. 5% PVAc became the best compared to 1 and 12% impact

modifier in terms of impact strength whereas 12% grafted seemed to be the best compatibilizer for enhancing the elongation at break of the blend. Thus, NR-g-PVAc could be used as a toughening agent for PLA as well as a compatibilizer for PLA/NR blend.

1.5.6.5 PLA-Copolyester Blends

Odent et al. [101] synthesized random aliphatic copolyesters by ring opening polymerisation of ϵ -caprolactone (CL) and δ -valerolactone(VL) by melt blending using a DSM twin-screw micro compounder at 200 °C and 60 rpm for 1 min. The copolyesters were added at 10 wt. % to virgin PLA to assess their effectiveness as impact modifier. The addition of 10 wt. % of copolyesters into PLA improved its impact strength. The impact strength of materials obtained by compression molding was found significantly higher than those obtained by injection molding at the same molar composition. SEM results supported the use of elastomeric phase in improving the impact strength of PLA. The use of copolyesters of higher molar mass with a molar composition of 45/55 mole % (CL/VL) resulted in the improvement of impact strength compared to neat PLA.

1.5.6.6 PLA-polycaprolactone (PCL) Blends

Polycaprolactone (PCL), a biodegradable polymer with a low T_g is perhaps the most widely studied toughening agent for PLA. Studies have shown that blending PLA with PCL resulted in significant increase in PLA ductility and toughness but the strength and modulus of PLA were substantially reduced.

Wang et al. [102] reactively blended PLA and polycaprolactone (PCL) using three coupling agents in a Haake twin screw mixing chamber. Triphenyl phosphate (TPP) showed best results as a coupling agent. It is apparent that for the reactive blends with PLA/PCL composition of 80/20, the tensile strength at break, elongation and elastic modulus increased with molecular weight of PCL. Elongation at break increased initially for a PCL content of 20%, then decreased upto 50%, and again increased to a maximum for 100% PCL. The addition of 2 phr TPP to PLA/PCL (80/20, w/w) during melt blending resulted in higher elongation and tensile modulus but lower tensile strength at break.

Semba et al. [103] prepared PLA/PCL blends under different melt-compounding conditions (internal mixers, twin-screw extruder) using dicumyl peroxide (DCP). Compression moulded film of PLA/PCL (70/30, W/W) blend showed greater elongation than neat PLA. The elongation of the resulting films increased to 130% on addition of 0.1 to 0.2 phr DCP. Further addition of DCP beyond the optimum amount showed a contradictory effect on elongation. The addition of 0.3 phr DCP resulted an increase in impact property of PLA/PCL (70/30, W/W) blend than that of neat PLA. From DMA data, it was found that DCP improved the viscous property in PCL phase that agreed with ductility and impact strength. The close values of tensile modulus and strength to those of rule of mixture indicated compatibility between the two phases. Stress whitening phenomenon was observed in tensile and impact fracture surfaces, which supported improved interfacial adhesion resulting from DCP addition.

Harada et al. [104] conducted a comparative study on the compatibilizing effects of lysine triisocyanate with four other reactive processing agents on PLA/ PCL (80/20, W/W) blends. Four isocyanates namely, lysine triisocyanate (LTI); lysine diisocyanate (LDI); 1,3,5-tris(6-isocyanatohexyl)-1,3,5-triazinane-2,4,6-trione (Duranate TPA-100); 1,3,5-tris(6-isocyanatohexyl)biuret (Duranate 24A-100)-and an industrial epoxide-trimethylolpropane triglycidyl ether (Epiclon 725)-were used as reactive processing agents. The use of LTI resulted in superior unnotched Charpy impact strength of PLA/PCL blend .The presence of LDI or TPA-100 fairly increased the impact strength of the PLA/PCL blend. The addition of Epiclon 725 did not show any improvement in the impact strength of binary blend. The impact strength increased considerably at 20 wt. % of PCL. The melt flow rate values of PLA/PCL blends decreased with increasing LTI. The morphological studies showed that PLA/PCL blends in presence of LTI showed sea-island morphology in which PLA forms a continuous phase and PCL forms a dispersed phase which contributed to an increment in physical properties.

Rao et al. [105] prepared blends of biodegradable PLA and PCL using Hakee Rheomix and characterized for its different properties. It was found that with 10 wt% of PCL, the elongation of the blend tremendously increased up to 19 % and the elongation increased with increase in PCL content upto 20 wt. % of PCL and subsequently it got reduced. Tensile strength of PLA/PCL blends decreased with increasing PCL. Tensile strength decreased by 35% for neat PLA with that of 20% PCL blend. Flexural strength decreased gradually with the addition of PCL. An increase in PCL content resulted in a gradual increase in

toughness up to 20% wt. of PCL and afterwards it decreased. PLA/PCL blend in the ratio of 80:20 exhibited the highest elongation and impact property. Rheological results revealed that the melt elasticity and viscosity of the blends increased with increase in concentration of PCL.

1.5.6.7 PLA-poly butylene succinate (PBS) Blends

Vannaladsaysy et al. [106] studied the melt blending of PLA and PBS and their reactive compatibilization using lysine diisocyanate (LDI) and lysine triisocyanate (LTI). PLA/PBS binary blend of composition 90:10, w/w displayed a slightly higher elongation and almost the same unnotched Charpy impact strength compared with neat PLA. The addition of 0.5 wt % LDI or 0.15 wt% LTI increased elongation of the PLA/PBS (90/10, w/w) blend to more than 150%. It was found that the magnitude of impact strength of the blends was independent of the molecular weight of PBS but got altered by concentrations of LTI and PBS. For the blends with 10-15 wt. % PBS content, the impact strength sharply increased with the addition of LTI. Addition of LTI as low as 0.15 wt. % significantly increased the impact strength of the PLA/PBS (80/20, W/W) blend. LTI was found to be more effective agent to increase the toughness of the PLA/PBS blends.

Lee et al. [107] investigated thermal, rheological, morphological and mechanical properties of binary blends of PLA and poly(butylene succinate adipate) (PBSA). The thermal stability of blends was found lower than that of pure PLA and PBSA. The tensile strength and modulus of blends decreased with PBSA content. Also, the impact strength of PLA / PBSA (80/20) blend increased significantly. However, at 20 wt. % PBSA content,

the impact strength increased much higher than pure PLA. Tg decreased for blend containing 80 wt. % PBSA indicating active interaction between PLA and PBSA chains. The melting temperature of PLA / PBSA blend raised up to 167 °C at 40 wt. % PBSA contents and slightly decreased at more than 40 wt. % PBSA contents. The crystallization temperature of PBSA was slightly increased with increasing PLA content but the heat of crystallization of PBSA per unit mass was decreased. The blend containing 80 wt. % PBSA showed highest biodegradation rate.

1.5.6.8 PLA - Polyhydroxyalkanoate Blends

Schreck et al. [108] investigated the impact toughness of blends of PLLA with Nodax H6 containing 7 mol% of 3-hydroxyhexanoate. PLLA/Nodax H6 (85/15, W/W) blend showed a two fold increase in notched Izod impact strength compared with PLLA. 5 wt. % of PLLA-b-Nodax H6 block copolymer was added to the binary blend to promote interfacial adhesion and impact performance of the binary blend system. Addition of Nodax increased the notched Izod impact resistance of the binary blends compared to that of PLLA.

1.5.6.9 PLA – poly (butylene adipate-co-terephthalate) (PBAT) Blends

PLA can be toughened by flexible poly(butylene adipate-co-terephthalate) (PBAT) at the cost of loss of tensile strength and modulus. Jiang et al. [109] prepared PLA/PBAT blend using a co-rotating screw extruder. PBAT was evenly dispersed in PLA even without the use of compatibilizers. When PBAT content was increased to 20 wt. %, elongation of the blend increased to more than 200%. On the other hand,

tensile strength and modulus decreased with PBAT content with 20 wt. % of PBAT.

1.5.6.10 PLA-thermoplastic blends

Imre et al. [110] prepared blends of PLA with thermoplastics namely, polystyrene (PS), polycarbonate (PC) and poly(methyl methacrylate) (PMMA). PMMA blends were found to be the strongest, while PS blends had the smallest tensile strength and that of PC blends runs in between. The strongest interactions were developed in PMMA while the weakest in PS blends. PLA/PS blends were brittle and failed at very small elongations. The elongation at break of PMMA blends changed continuously with composition, not very large, but larger than that of PS blends.

Choudhary et al. [111] melt blended PLA with polypropylene (PP) at various ratios to improve the melt processability of PLA. Maleic anhydride grafted PP (MAH-g-PP) and glycidyl methacrylate were used as reactive compatibilizers to induce miscibility in the blend. The disappearance of absorption peak of anhydride group present in MAH-g-PP and the emergence of a new absorption signal signifying the carbonyl group of ester linkage at 1758 cm^{-1} indicated interaction of MAH-g-PP with PLA/PP blend. The incorporation of PP matrix to the tune of 10 –70 wt. % within the PLA matrix decreased tensile strength in the resultant blends due to high polarity difference between the constituent polymers. The tensile modulus and stress at break of the blend increased at blend ratio of 90:10, to the tune of 11 and 18%, respectively, compared to those of virgin PLA. The maximum thermal stability was found for

PLA/PP/MAH-*g*-PP blend with the support of TGA. Dynamic mechanical analysis exposed an increase in both glass transition temperature and storage modulus with the addition of MAH-*g*-PP. Scanning electron microscopy of impact-fractured samples showed a decrease in the size of the dispersed phase with the incorporation of MAH-*g*-PP, which enhanced the compatibility between PLA and PP.

Lai et al. [112] investigated rheological and mechanical properties of PLA / polystyrene (PS) blends. PLA/PS blends in different ratios were prepared using a single screw extruder to obtain granules. From rheological studies, it was found that PLA/PS blend exhibited a typical shear-thinning behavior. Also, the viscosity of the blend decreased with increase in PLA content. The mechanical results showed immiscibility between PLA and PS in the blend system.

Li et al. [113] blended PLA with PU elastomer. From the $\tan\delta$ curves, all the blends showed two glass transitions, for PU at about 50°C and for PLA at about 70 °C, indicating that the blends are thermodynamically not miscible. However, the Tg of both PU and PLA shifted towards each other with varying compositions, suggesting partially miscibility and certain kind of molecular interactions between PU and PLA. The storage modulus at room temperature for PLA/PU blends gradually decreased with increasing content of rubbery PU. Thus, the addition of PU elastomer lowered the cold-crystallization temperature of PLA in the blend. The elongation at break continuously increased with increase in PU content while the tensile strength and modulus decreased with the addition of PU elastomer. SEM

analysis of tensile and impact fractured surfaces also supported the improvement in toughness.

Nature works [114] reported the toughening of PLA using a PCL based PU elastomer produced by Dow Chemical Company, Pellethane™ 2012-75 A. With the incorporation of 30% of Pellethane™, the notched Izod impact strength and elongation of PLA blend increased while the tensile yield strength was reduced with respect to virgin PLA.

Han et al. [115] conducted the melt blending of PLA and TPU with an aim to toughen PLA matrix. The elongation at break of the blends showed a small increment with the addition of 10 wt. % TPU and a prominent increase when the elastomeric content was further increased to 30 wt. %. Also, the yield strength of the blends decreased with increasing TPU content.

Feng et al. [116] conducted studies on PLA/TPU blends and investigated its morphological and mechanical properties. PLA and TPU were compounded at appropriate proportions by a Haake torque rheometer (30 rpm at 170 °C for 5 min). The stress - strain behavior of PLA varied noticeably with the addition of TPU. Also, PLA/TPU blends showed yielding and necking. The tensile strength declined slowly with increasing TPU content, whereas the elongation at break increased rapidly above 5 wt. % of TPU, while the tensile strength was still maintained above 40 MPa. The impact strength of the blend increased with TPU content. Thus, TPU improved the toughness of the blend without a significant drop in the tensile strength.

1.5.7 PLA based green composites

The wide use of petro - polymers in many industrial and domestic applications causes massive ecological problems connected with their consumption. The importance of biodegradable plastics is that they can be composted with organic wastes and returned to enrich the soil. They also reduce the labour cost for the removal of plastic debris in the environment. They can also be recycled to useful monomers and oligomers by microbial and enzymatic treatment. As a result, the use of natural fiber reinforced composites has been rapidly extended due to the availability of natural fibres derived from annually renewable resources, for use as reinforcement in both thermoplastic and thermosetting matrix composites.

1.5.7.1 PLA - Kenaf Fiber Biocomposites

Taib et al. [117] studied the properties of kenaf fiber (KF)/PLA biocomposites using polyethylene glycol (10 wt. %) as plasticiser. The weight loadings of KF were varied between 0 and 40 wt. %. The fiber length distribution was unique for plasticised PLA composite with 40 wt. % KF (p-PLA/ 40KF composite). The addition of kenaf fiber into p-PLA resulted in a significant change in its tensile properties. p-PLA/KF composites experienced initial decrease of tensile strength at 10 wt.% fiber loading. Beyond 10 wt. % fiber loading, the tensile strength increased almost linearly with fiber loading to values higher than that of p-PLA demonstrating kenaf fiber as an effective reinforcement for p-PLA. The tensile modulus of p-PLA increased linearly whereas the strain at break decreased with fiber loading. The addition of 10 wt. % KF decreased the strain at break from 42% to 6%

which may be due to the stiffening effect kenaf fiber that restricts the mobility of PLA chains. Also, the impact strength of p-PLA/KF composites decreased with increase in fiber loading.

Garcia et al. [118] fabricated eco composites using natural fibers. PLA was blended with kenaf and rice husks and the effect of the nature of fibers on various properties were measured. Also, high density polyethylene (HDPE) was blended with wood fibers of different length and the properties of the composites were compared with PLA. They also added maleated-PLA in the composites as compatibilizer. Young's modulus was increased dramatically on addition of kenaf fibers and it increased with increase in fiber content. Tensile strength reduced after the addition of fibers, especially with rice husk. However, the flexural modulus and flexural strength increased by the addition of kenaf fiber. Kenaf composites gave rise to much better mechanical performance than rice husk composites.

1.5.7.2 PLA - Hemp Fiber Biocomposites

Chemical modification of hemp fibre with acetic anhydride, alkali and silane compound was carried out and the influence of the same on the thermal properties of PLA was investigated [119]. Thermal degradation kinetic study was done using Flynn-Wall-Ozawa method. The hemp fibre treated with acetic anhydride exhibited 10-13% greater activation energy compared to silane and alkali treated hemp fibres incorporated PLA composites. The high bond energy between acetic anhydride treated hemp fibre and PLA led to improvement in the thermal stability for the composites.

PLA/hemp fibre composite was fabricated via twin-screw extrusion technique and the effect of different loadings (10-40 wt %) of hemp fibre on mechanical properties of the composites was examined [120]. At 40 wt% loading of hemp fibre, a maximum enhancement in the mechanical properties of PLA was noticed. The presence of hemp fibre in the PLA matrix resulted in ~40% and ~90% improvement in the tensile strength and tensile modulus, respectively. Also, the flexural strength and flexural modulus were improved compared to neat PLA.

1.5.7.3 PLA- Jute Fiber Biocomposites

Goriparthi et al. [121] studied the effect of surface modification of jute fibers on mechanical and abrasive properties of jute/PLA composites. The surface of jute fiber was modified by alkali, permanganate, peroxide and silane treatments. The treatment of jute fiber with trimethoxy methyl silane improved tensile strength and modulus by 35% and 38% respectively. The impact strength of treated composites was slightly lower than untreated composite. The storage modulus of surface modified jute fiber reinforced composites was higher than that of untreated jute fiber composite. Also, the incorporation of jute fiber into polymer matrix resulted in the shift of T_g towards a higher side, may be due to lower molecular mobility of matrix chains in presence of fibers. Untreated composites exhibited a higher tan δ peak value as compared to treated composites.. Alkali, permanganate and peroxide treatments resulted in the decrease of thermal stability as compared to PLA/untreated jute fiber composites. Modification of jute fiber surface with silane coupling agents slightly improved the thermal stability of the composites.

Hu et al. [122] investigated aging behaviors of short jute fiber/ PLA composite material in hygrothermal environment. The short jute fiber/PLA composite were fabricated by film stacking hot press method. For coated samples, the moisture absorption rate reached to 0.35% in 22 h, upto 17.5% that of uncoated sample (2.0%) at the same time. A steady moisture absorption increasing stage followed until inflexion appeared at 125th hour of ageing. The moisture absorption rate increased very rapidly since then. For coated specimen, the tensile strength does not show significant difference after 24 h ageing compared to that of specimens without ageing. The load–displacement curve for aged samples revealed that the load bearing capacity and elongation of the samples have greatly decreased with aging time.

Vijay Baheti et al. [123] wet pulverized waste jute fibers to nanoscale using high energy planetary ball milling and incorporated under different weright loadings (1,5 and 10 %) into PLA. The maximum improvement in mechanical properties was observed in case of 5 wt% composite film.

1.5.7.4 PLA - Bamboo Fiber Biocomposites

Lee et al. [124] studied the effects of lysine-based diisocyanate (LDI) as a coupling agent on the properties of biocomposites of PLA, PBS with bamboo fiber (BF). The micrographs of PLA/BF and PLA/PBS composites with LDI of 0.65% showed that BF appeared to be coated within the matrix polymer due to the compatible effect of graft copolymer with LDI. In the case of PLA/BF composite, as isocyanate content increased to 0.33%, tensile strength and Young's modulus also increased

and then levelled-off. However, there was no significant effect of LDI addition on the elongation at break. Similarly, the tensile strength of PBS/BF composites increased steeply from 21 to 34 MPa with isocyanate contents of 0.33% and then levelled-off. However, Young's modulus was not much changed by the addition of LDI. Elongation at break increased slightly by the addition of LDI, but still showed value less than 10%. It was also found that the absorption amount increased in all composites as bamboo fiber content increased. Also, the incorporation of BF in PLA matrix significantly affected the thermal stability. The composites showed a lower degradation temperature than PLA and a two-stage decomposition curve was observed for all composites.

Wang et al. [125] blended bamboo flour (BF) with PLA using PLA-g-glycidyl methacrylate (PLA-g-GMA) as compatibiliser. GMA was grafted on PLA using benzoyl peroxide and tertiary butyl peroxy benzoate as initiators. FTIR confirmed the grafting of epoxy groups in GMA on to PLA. . The tensile strength and tensile modulus of PLA/BF composites prepared with PLA-g-GMA as compatibiliser were improved compared with those without PLA-g-GMA. The tensile strength and modulus increased initially and then decreased with increase in compatibilizer content. The impact strength of the PLA/BF composite was improved with the use of PLA-g-GMA as compatibilizer. With increasing PLA-g-GMA concentration, the impact strength of the composite material increased initially and then decreased.

Fazita et al. [126] studied the recyclability and biodegradability of bamboo fabric-reinforced PLA. Recycled BF-PLA composite showed

decrease in tensile properties and an increase of flexural properties. The increased flexural properties may be because of short and dispersed bamboo fabric yarn in the composites during injection molding. The drop of the impact strength of the recycled BF-PLA composites was due to the composites turning brittle with the recycling. The biodegradation half-life of BF-PLA composites (46 days) was found to be longer than that of the virgin PLA (25 days), indicating that the reinforcement of bamboo fabric in PLA matrix minimizes the rapid microbial decay of BF-PLA composite. BF-PLA composite has the potential to be use in product packaging for providing eco-friendly and sustainable packaging.

1.5.8 PLA based nanocomposites

The association of a 100% bio-originated material and nanomaterials paves way for becoming independent from petrochemical-based polymers and also from environmental and health concerns. Recently, nanocomposites have received considerable attention as an alternative to conventional filled polymers. PLA based nanocomposites have gained its importance in the current era of science and technology.

1.5.8.1 PLA - Montmorillonite Nanocomposites

Ayana et al. [127] prepared thermoplastic starch (TPS) / PLA /sodium montmorillonite (NaMMT) nanocomposites by an eco-friendly approach, involving in-situ gelatinization of potato starch in presence of dispersed nanoclay followed by melt mixing with PLA. An increase in mechanical and thermal properties was clear in presence of PLA and the presence of clay influenced positively in enhancement of properties. The

water absorption was significantly decreased in presence of clay in the nanocomposites.

Ogata et al. [128] prepared PLA-Organically Modified Layered Silicate (OMLS) blends by dissolving the PLA in hot chloroform and dimethyl distearyl ammonium modified montmorillonite (MMT). Wide angle X-ray diffraction and small angle X-ray scattering (SAXS) results showed that the silicate layers could not be intercalated using solution casting.

Pluta et al. [129] investigated the morphological and thermal properties of nanocomposites and microcomposites of PLA. They found that the unmodified clay filled PLA formed a microcomposite with a phase-separated microstructure. TGA studies revealed the thermal stability of the nanocomposites. XRD indicated good affinity between organomodified clay and PLA to form intercalated structure in the nanocomposite.

Nam et al. [130] prepared PLA-layered silicate nanocomposites by melt extrusion of PLA and organically modified MMT. The incorporation of very small amounts of oligo(α -caprolactone) (o-PCL) as compatibilizer in PLA led to a better stacking of the silicate layers and also resulted in stronger flocculation due to the hydroxylated edge-edge interaction of the silicate layers.

Maiti et al. [131] investigated the effect of organic modifiers of various chain lengths in different types of clays like smectite, MMT, and mica in PLA. It was found that the nanocomposites of MMT and mica

are intercalated and well-ordered compared to smectite type. The layered structure and gallery spacing of organoclay in PLA nanocomposites showed that with a modifier of the same chain length, the gallery spacing of the organoclay was largest for mica and smallest for smectite. However, the increment of the modulus in a smectite nanocomposite was higher than MMT or mica nanocomposite due to better dispersion in a smectite system for the same weight loading. Smectite nanocomposites showed better gas barrier properties than the MMT or mica systems, which were larger in size but stacked in nature in their nanocomposites.

Lee et al. [132] studied the detailed crystallization behaviour and morphology of pure PLA and PLA-C18-MMT nanocomposites. It was observed that the overall crystallization rate of neat PLA increased after nanocomposite preparation with C18-MMT. Dispersed MMT particles acted as a nucleating agent for PLA crystallization in the nanocomposites.

Di et al. [133] investigated the thermal and mechanical characteristics of the PLA nanocomposite scaffold. The crystallization temperature of quenched PLA and its nanocomposites decreased by the addition of MMT clay and they acted as effective nucleating agents for crystallization of PLA.

Krikorian et al. [134] studied the effect of compatibility of different organic modifiers on the overall extent of dispersion of aluminosilicate layers in PLA matrix. Three different commercially available MMTs were used as a reinforcement phase. By TEM and XRD studies, an increase in miscibility of the organic modifier with PLA matrix increased the tendency of the aluminosilicate layers to exfoliate.

Pluta et al. [135] revealed that the exfoliation of MMT in PLA matrix was achieved due to the strong interaction between MMT and polymer matrix. They also stressed that the high surface area of MMT layers had reduced molecular mobility of PLA leading to unique properties for the PLA-MMT nanocomposites. The exfoliated MMT platelets acted as nucleating agents at low content by increasing the crystallization rate of PLA.

Peterson et al. [136] compared the mechanical, thermal and barrier properties of PLA based nanocomposites by incorporating 5 wt% of each bentonite and microcrystalline cellulose via solution casting method. The bentonite nanocomposite showed greater tensile modulus and yield strength compared to MCC nanocomposite. The results showed that there was a difference in exfoliation and interaction with the PLA matrix between layered silicates and MCC. Dynamic mechanical thermal analysis (DMTA) explored an improvement in storage modulus for both the nanoreinforcements.

Pluta et al. [137] studied the structure dielectric, viscoelastic and thermal properties of PLA-MMT nanocomposites by incorporating 3wt% and 5 wt% of nanoclay. The X-ray analysis showed the presence of exfoliated nanostructure in 3 wt% clay loaded nanocomposite. DMTA showed an increase in storage and loss modulus with the increase in organoclay content and dispersion.

Farahani et al. [138] prepared binary nanocomposites of poly lactic acid (PLA) with montmorillonite modified with trisilanol polyhedral oligomeric silsesquioxanes (Trisilanolisooctyl POSS) by solution-

blending and coated on paper by bar coating and compress hot melt coating methods. The dispersion and phase behavior of modified montmorillonite in PLA matrix was revealed by Transmission Electron Microscope. The water vapour permeability of PLA nanocomposites was decreased by 74% compared to those of paper coated with pure PLA. WVTR results indicated that the compress hot melt coating of nanocomposites is an effective method to improve the water vapor resistance of coated paper.

K. Fukushima et al. [139] made PLA based nanocomposites based on 5 wt.% of an organically modified montmorillonite (CLO), unmodified sepiolite (SEP) and organically modified zirconium phosphonate (ZrP) by melt blending. DSC analysis showed that the addition of ZrP could promote extent of PLA crystallization, whereas the presence of CLO and SEP did not significantly affect the crystallization and melting behaviour of PLA matrix. Also, the oxygen permeability of PLA were not affected by the addition of SEP and ZrP nanoparticles.

1.5.8.2 PLA-silica nanocomposites

Wu et al. [140] reinforced PLA with silica nanoparticles and investigated the effect on the thermal and mechanical properties of PLA. For PLA/silica nanocomposites, the maximum improvement in the elongation-at-break (%) and Young's modulus was observed at silica loading below 1.5 wt%. The addition of silica nanoparticles in the PLA matrix improved the HDT significantly by 25 °C, due to the high thermal stability of silica. Tsai et al. [182] employed sol-gel process to fabricate PLA/SiO₂/Al₂O₃ nanocomposites. The uniform distribution of

reinforcement was confirmed by morphological analysis. Positive influence on thermal expansion coefficient was reflected by the filler. However, the thermal stability of PLA decreased with increase in Al_2O_3 .

Yuzay et al. [141] studied the effect of zeolite 4A and chabazite zeolite on the thermal properties of PLA. Both the zeolites enhanced the nucleation sites and improved the crystallinity of PLA composites, whereas, the glass transition and melting temperatures remained unaffected. The activation energy was reduced for both the zeolite containing PLA composites as compared to pristine PLA, indicating decreased thermal stability of PLA after reinforcement.

1.5.8.3 PLA- Micro/Nanocrystalline Cellulose Nanocomposites

Hafiz et al. [142] prepared polylactic acid composites reinforced with microcrystalline cellulose (MCC) from oil palm biomass by solution casting. Fourier transform infrared spectroscopy showed no significant changes in chemical structure of PLA. The thermal decomposition temperature at 50 % improved with the addition of MCC, showing an increase in thermal stability of the composites. The Young's modulus increased whereas the tensile strength and elongation at break for composites decreased with the addition of MCC.

Mathew et al. [143] prepared biodegradable composites of PLA with microcrystalline cellulose (MCC) with a particle size of around 10–15 μm . The tensile strength for wood flour and wood pulp composites were better than for MCC composite. The elongation at break decreased in the composites compared to pure PLA, being in the order $WP > WF >$

MCC. The elongation was highest for PLA/WP system followed by PLA/WF and lowest for PLA/MCC system. SEM study revealed that the wood pulp acted as single fibers with higher aspect ratio than WF or MCC and also fiber pullouts were observed. The higher aspect ratio of wood pulp and wood flour enhanced the mechanical performances than with MCC. The higher crystallinity of PLA in WP and WF composites compared to MCC resulted in better mechanical performance of WF and WP composites. Also, all the composites showed higher thermal stability than pure PLA.

Qu et al. [144] prepared nanocomposites of PLA with cellulose nanofibrils using PEG as the compatibiliser to improve their interaction.. The tensile strength and elongation increased by 56.7 and 60 % respectively by the addition of PEG compared with PLA /cellulose nanofibrils. SEM studied revealed that the cellulose nanofibrils were homogenously dispersed in PLA matrix and thus PEG effectively reinforced the interfacial adhesion and miscibility between them.

Peterson et al. [145] prepared nanocomposites of poly(lactic acid) (PLA) and cellulose nanowhiskers (CNW) by solution casting method. The whiskers were either treated with tertiary butanol(B-CNW) or with a surfactant (S-CNW) prior to freeze drying. The S-CNW whiskers showed flow birefringence in chloroform. Both the whiskers and composites of PLA were found to be thermally stable upto 220 °C. DMTA analysis showed that all whiskers were able to improve the storage modulus of pure PLA at higher temperatures.

Arrieta et al [146] investigated on the thermal and crystallization properties of PLA/poly(hydroxyl butyrate) (PHB). Cellulose nanocrystals (were prepared using acid hydrolysis and the effect of pristine CNC and surfactant modified CNC on PLA/PHB blend was studied. It was observed that the presence of surfactant modified CNC enhanced the thermal stability of the PLA/PHB blend and the maximum improvement in the thermal degradation temperature of ~10 °C was obtained for the PLA/PHB/SCNC nanocomposite system. DSC analysis revealed that the reinforcement acted as a nucleating agent by improving the crystallinity of the system.

Cao et al. [147] prepared composites of poly(lactic acid) (PLA) with poly(butylene succinate) (PBS) and microcrystalline cellulose (MCC) as reinforcement of the polymer matrix by melt blending. As a reactive compatibilizer, a chain extender, ADR-4370 was used to improve the interfacial adhesion and their by mechanical properties. The addition of ADR-4370 improved the mechanical properties, particularly, tensile and impact strength and this improvement was proportional to the percentage of chain extender. However, the elongation at break decreased when the chain-extender percentage was over 0.5% because of slighter crosslinking within the resin matrix.

1.5.9 Applications of PLA based Blends and Composites

The demand for green and renewable materials continues to rise. PLA based blends and composites have occupied major applications in green packaging. Although these are emerging as alternatives to existing petroleum based plastics, the present low level production and high cost

restrict their widespread applications. PLA combined with organically modified clays will result in environmental friendly nano composites. The need for green and biodegradable plastics has been increased during the past decade due to its environmental concerns. PLA has been extensively used in many aspects due to its good biocompatibility, biodegradability, compostability etc. One way to improve the mechanical and thermal properties of PLA is the addition of fibers or filler materials. Both synthetic and natural fibers are used as reinforcement to improve the mechanical strength of PLA. PLA is currently used in a number of biomedical applications, such as sutures, stents, dialysis media and drug delivery devices. It is also being evaluated as a material for tissue engineering. It can also be useful in the preparation of loose-fill packaging, compost bags, food packaging and disposable dinnerware. PLA has also many potential uses in the form of fibers and non-woven textiles, upholstery, disposable garments, feminine hygiene products etc. Due to its high production costs, in the initial stages of development, PLA was used in limited areas such as preparation of medical devices. As its production cost has been lowered by new technologies, the application of PLA has been extended to other commodity areas such as packaging, textiles and composite materials.

Motivation for the present work:

In the past few decades, the usage of plastics has increased tremendously for its specific and advantageous properties such as light weight, high strength, easy moldability, product design flexibility, durability, non corrosive nature, processability, and high energy effectiveness and

henceforth versatile applications ranging from household articles to the aeronautic-space sector. It is difficult to avoid plastics even in ever growing realization for environmental friendly alternatives for exhaustible non-renewable sources of energy and materials; despite them being derived from crude oils and natural gas. According to statistics, from 1950 onwards, 9 % of growth has been seen globally in the production and consumption of plastics. In 1950, the overall production of plastic was 1.5 million tonnes while it reached 322 million tonnes in 2015 [148]. Subsequently, the problems created by plastic, viz, non-biodegradable wastes, an unmaskable high carbon foot print, depletion of non renewable petroleum resources, in addition to the associated heavy green house gas emissions triggered the interest in the development of biosourced, biodegradable plastics. It can be disposed off and will not remain for centuries in a landfill, or as litter which is one of the tenets driving the recent interest in 'green' technologies.

Among the various biodegradable, PLA is considered as one of the most promising material with several ideal properties such as light weightiness, tunable biodegradability, good printability, easy moldability, besides mechanical and thermal properties comparable to the common use petroleum based commodity plastics. PLA is a biodegradable aliphatic polyester, produced from renewable resources and has received much attention in the research of alternative biodegradable plastics. Commercial PLA is synthesized by ring opening of lactides which are the cyclic dimers of lactic acids. These lactic acids can be obtained from fermentation of renewable resources, the fermentation of crop like corn starch and sugar feed stocks etc. [149]. PLA has been found to be

environmentally biodegradable through a two - step process that begins with the high molecular weight polyester chains hydrolyzing to lower molecular weight oligomers under an appropriate temperature and moisture environment. In the second step, microorganisms convert these lower molecular weight components to carbon dioxide, water and humus.

In spite of all these advantages, PLA suffers from property defects viz, inherent brittleness, a low percentage elongation, and poor thermal stability which severely limits its application and versatility prospects. For wide range applications, properties like impact strength flexibility, stiffness, barrier properties, thermal stability needs to be improved. The most widely used technique to modify properties of PLA includes polymer blending, copolymerization, and nanocomposite technology. Chemical copolymerization is an important way of modifying properties of homopolymers. A variety of commercially important copolymers have been made via macromolecular design and chemical copolymerization. With respect to structure-property relationships, new materials with tunable properties can be prepared by cautious selection of monomers and by varying copolymer ratios.

Polymer blending is a method for achieving commercially viable product through either unique properties or lower cost than the individual polymers. Blending of PLA with other polymers offers the possibility of changing the properties, for example, the degradation rate, permeability characteristics, thermal and mechanical properties etc. Examples of polymers used to blend with PLA are poly (butylene

succinate adipate)[150], poly(butylene adipate-co-terephthalate)[151], poly- ϵ -caprolactone[152], poly (ethylene succinate)[153] etc.

Blending PLA with elastomeric disperse phase is one technique to improve toughness of PLA. Toughness is a measure of resistance to fracture. It is an important requirement in most load bearing applications of materials. In order to achieve the desired properties the polymer blends should in general be miscible. Immiscible blends are, however, preferred when elastomeric toughening phase is dispersed in polymers. Many of the PLA blends that have been studied are immiscible or partly miscible and may require some sort of compatibilizer in order to make them miscible. The goal of such technique is to combine the stiffness and processability of brittle plastic matrix with the fracture resistance of elastomers. Elastomers are widely used to improve toughness of brittle plastics.

Although many works have been reported on the PLA blends and composites, no systematic studies have been noted on modification of PLA by elastomeric toughening agents such as ethylene vinyl acetate (EVA), Ethylene vinyl alcohol (EVOH), Styrene Ethylene Butylene styrene (SEBS) and /or maleic anhydride grafted SEBS (MA-g-SEBS). This work presents a detailed study of synthesis, characterization and optimization parameters of PLA blends with the aforementioned modifiers. The thermal degradation kinetics and crystallization kinetics of toughened blend system is studied in detail in the subsequent chapters.

Objectives

The main objectives of this work are:

- To modify PLA by blending with various toughening agents such as SEBS, MA-g SEBS, EVA, EVOH and nanofibrillated cellulose
- To synthesize MA-g-SEBS by melt grafting technique and its characterization
- To synthesize hydrolysed EVA by chemical method and its characterization
- To prepare PLA/SEBS and PLA/MA-g-SEBS blends via melt blending technique and its characterization by FTIR, XRD, SEM etc.
- To prepare PLA/EVA and PLA/EVA /EVOH blends by melt mixing technique and its characterization by FTIR, XRD, SEM etc.
- To evaluate the thermo-mechanical property of toughened PLA blends
- To isolate and characterize nanofibrillated cellulose from waste cotton
- To perform crystallization and kinetic study of PLA blends
- To prepare nanofibrillated cellulose reinforced PLA composite and its performance study

Literature review of PLA included in this chapter has been published

“State of the art and future prospective of Poly (lactic acid) based blends and composites” VH Sangeetha, H Deka, TO Varghese, SK Nayak, Polymer Composites 39 (1), 2016, 81-101.

References

- [1] B. Zhang, Q. Wan, J. Agric. Food Chem., 60 (2012) 4162.
- [2] S.S. Ali, X. Tang, S. Alavi, J. Agric. Food Chem. 59, (2011) 12384.
- [3] B.R.T. Simoneit, P.M. Medeiros, B.M. Didyk, Environ. Sci. Technol. 39 (2005) 6961.
- [4] W. Amass, A. Amass, B. Tighe, Polym. Int. 47(1998) 89.
- [5] R. Chandra, R. Rustgi, Prog. Polym. Sci. 23 (1998)1273.
- [6] A.K. Mohanty, M. Misra, G. Hinrichsen, Macromol. Mater. Eng. 276(2000)1.
- [7] V. Siracusa, P. Rocculi, S. Romani, M.D .Rosa. Food Sci Technol 19 (2008) 634.
- [8] W. M. A. Mullan (2002) Science and technology of modified atmosphere packaging. <http://www.dairyscience.info/map-science.asp>.
- [9] S. J. Huang. J. Macromol. Sci., Part A Pure and Appl.Chem. (2006) 593
- [10] L.A. Anthony, M A. Neal, Phil. Trans. R.Soc.B. 364 (2009) 1977.
- [11] M. Alexandre, P. Dubois, Mater. Sci. Eng., 28 (2000)1.
- [12] K.K. Yang, X.L Wang, Y.Z. Wang, J. Ind. Eng. Chem., 13 (2007) 485. 16.
- [13] M. Niaounakis, Biopolymers applications and Trends, Elsevier (2015).
- [14] M. Thielen, Bioplastics: Basics, applications, markets, Polymedia publishers, Germany, First edition 2012.
- [15] R. E. Drumright, P. R. Gruber and D. E. Henton, Polylactic acid technology, Adv. Mater. 12, (2000) 1841.
- [16] Y. M. Varsha, Savitha R., J. Microb. Biochem.Tech., 3, (2011) 99.

- [17] M.N.V.R. Kumar, *Polymers* 46 (2000) 1.
- [18] L. Averous, N. Boquillon, *Carbohy. Polym.* 111 (2004) 56.
- [19] E.Pollet, L. Averous, *Production, chemistry and properties of polyhydroxy alkanoates*, Wiley Interscience Publishers 2011, Page 65-67.
- [20] Y-J Wee, J-N Kim, H-W Ryu, *Food Technol. Biotechnol.* 44(2006) 163.
- [21] M. Okada *Prog. Polym. Sci.*, 27 (2002)87.
- [22] <http://en.european-bioplastics.org/about-us>
- [23] <http://www.marketsandmarkets.com/Market-Reports/biopolymers-bioplastics-market>
- [24] <http://www.braskem.com>
- [25] http://bio-based.eu/market_study/media/files/13-06-21MSBiopolymersExcerpt.pdf
- [26] <http://www.coca-colacompany.com/plantbottle-technology>
- [27] http://www.bio-based.eu/market_study/media/16-12-16-Bio-based-Building-Blocks-and-Polymers-short-version.pdf
- [28] B.W. Chieng, N. A. Ibrahim, W. M. Z. W. Yunus *eXPRESS Polymer Letters*,4, (2010) 404.
- [29] <http://polymerdatabase.com/polymer%20classes/Biodegradable%20Polyester%20type.html>
- [30] L. A. Utracky, *Polymer Blends Handbook* , Springer (2002).
- [31] R.P. Sigh, *Polymer blends and alloys*, Asian Publishers Pvt. Ltd (2002).
- [32] H. Qian, E.S. Greenhalgh, M.S.P. Shaffer, A. Bismarck, 20 (2010) 4751.

- [33] G Lin, G. Xie, G. Sui, R. Yang, *Compos. Part B.* 43, (2012) 44.T. Naghdi, A. Merkoç, *Chem. Mater.*, 29 (2017) 5426.
- [34] M. Hussain, A. Nakahira, S Nishijima, K. Niihara, *Compos. Part A.*31 (2000) 173.
- [35] J.F. Timmerman, B.S. Hayes, J.C. Seferis, *Compos. Sci. Technol.* 62 (2002) 1249.
- [36] K.Y. Lee, Y. Aitomäki, L. A. Berglund, K. Oksman, A. Bismarck, *Compo. Sci.and Tech.* 105, (2014) 15. E.E Brown, M.P.G. Laborie, *Biomacromolecules*, 8 (2007) 3074.
- [37] F. Li, P. Biagioni, M. Bollani, A. Maccagnan, L. Piergiovanni, *Cellulose* 20 (2013) 2491.R. Müller, C. Jacobs, O. Kayser, *Adv. Drug Delivery Rev.*, 47 (2001) 3.
- [38] Westman G, Hasani M. Modified cellulose fibers. Sweden. Patent No.: EP2428610. 2012–03–14.A. Alemdar, M. Sain, *Bioresour. Technol.*, 9, (2008) 1664.
- [39] M. Ago, K. Okajima, J.E. Jakes, S. Park, O.J. Rojas, *Biomacromolecules* 13, (2012) 918.H. V. Lee, S. B. A. Hamid, S. K. Zain, *Scientific world journal* (2014).
- [40] A-L Goffin, J-M, Raquez, E, Duquesne, G. Siqueira, Y. Habibi, A. Dufresne , P. Dubois, *Biomacromolecules* 12 (2011) 2456.N. Saddler, L.P. Ramos, C. Breuil, *C.A.B. International* (1993) 73.
- [41] V. Khoshkava, M.R. Kamal, *Biomacromolecules* 14 (2013)
- [42] M. Floros, L. Hojabri, E. Abraham, J. Jose, S. Thomas, L. Pothan,A.L. Leao, S. Narine , *Polym. Degrad. Stab.* 97 (2012) 1970.
- [43] S. Maiti, S. Sain, D. Ray, D. Mitra, *Polym. Degrad .Stab* 98 (2013) 635.
- [44] G, Ström, C, Öhgren, M. Ankerfors, *Nanocellulose as an additive in foodstuff.* Innventia Report No.: 403; June 2013.

- [45] H. Kargarzadeh, M. Ioelovich, I.Ahmad, S. Thomas A, Dufresne, Handbook of Nanocellulose and Cellulose Nanocomposites, Methods for Extraction of Nanocellulose from Various Sources, Wiley First Edition (2017).
- [46] T. Naghdi, A. Merkoç, Chem. Mater., 29 (2017) 5426.V. Khoshkava, M.R. Kamal, Biomacromolecules 14 (2013) 3155.
- [47] R.J. Moon, A. Martini, J. Nairn, J. Simonsen, J. Youngblood, Chem.
- [48] M. Paakko, M. Ankerfors, H. Kosonen, A. Nykänen,S. Ahola, M. Osterberg, J. Ruokolainen, J. Laine, P. T. Larsson, O. Ikkala, T. Lindstrom, Biomacromolecules. 8 (2007) 1934.
- [49] J.S.Stevanic, C. Joly, K.S. Mikkonen, K. Pirkkalainen, R. Serimaa, C. Rémond, G. Toriz, P. Gatenholm, M. Tenkanen, L Salmén 122 (2011) 1030.
- [50] R. Müller, C. Jacobs, O. Kayser, Adv. Drug Delivery Rev., 47 (2001) 3.
- [51] H. A. Khalil, Y. Davoudpour, M.N. Islam, A. Mustapha, K. Sudesh,
- [52] A. Alemdar, M. Sain, Bioresour. Technol., 9, (2008) 1664.
- [53] G. Garrote, H. Dominguez, J.C. Parajo, Hydrothermal processing of lignocellulosic materials. Holzforschung, 57 (1999), 191.
- [54] N. Saddler, L.P. Ramos, C. Breuil, C.A.B. International (1993) 73.
- [55] K. Wang RC.: Sun RC., Cereal straw as a resource for sustainable biomaterials and biofuels. Oxford: Elsevier (2011)
- [56] L.P. Walker, D.B .Wilson, Bioresour. Technol. (1991)36,3-14..
- [57] Y. Habibi, L. A. Lucia ,O. J. Rojas, Chem. Rev., 110 (2010),3479.
- [58] P. Podsiadlo, S.Y. Choi, B.Shim, J.Lee, M. Cuddihy, N.A. Kotov,Biomacromolecules 6 (2005) 2914.

- [59] M. Roman, W.T. Winter, *Biomacromolecules* 5 (2004) 1671.Y. Tokiwa, B. P. Calabia, *Appl. Microbiol. Biotechnol.*, 72 (2006) 244.
- [60] http://english.jl.gov.cn/Investment/Opportunities/Industry/syhg/201302/t20130227_1422950.html
- [61] <https://www.alliedmarketresearch.com/polylactic-acid-market>
- [62] D. J. Garlotta, *J. Polym. Environ.*, 9 (2001) 63.
- [63] R. Auras, L. T. Lim, S. E. M. and H. S. Tsuji, *Poly (lactic acid): Synthesis, Structures, Properties, Processing and Applications*, John Wiley & Sons, Hoboken, New Jersey (2010).
- [64] J. R. Dorgan, H. J. Lehermeier, L. I. Palade and J. Cicero, *Macromol Symp*, 175, (2001) 55.
- [65] E. T. H. Vink, K. R. Rábago, D. A. Glassner and P. R. Gruber, *Polym. Degrad. Stab.*, 80, (2003). 403.
- [66] R. M. Rasal, D. E. Hirt, *J. Biomater. Sci., Polym. Edn.*, 88(2008) 1079.
- [67] H. M. Vainio, P. Varpomaa, J Seppala, P Tormala, *Macromol. Chem. Phys.* 197 (1996) 1503.
- [68] D. W. Grijpma, A. J. Nijenhuis, V. Wijk and A. J. Pennings, *Polym. Bull.*, 29, 5715.
- [69] A.V. Janorkar, A.T. Metters and D. E. Hirt, *Macromolecules*. 37 (2004).
- [70] Y. Tokiwa, B. P. Calabia, *Appl. Microbiol. Biotechnol.*, 72 (2006) 244.
- [71] J. E. Bergsma, W. C. De Bruijn, F. R Rozema, R. R. M. Bos and G. Boering, *Biomaterials*, 16 (1995) 25.
- [72] W. M. Gramlich, M. L. Robertson and M. A. Hillmyer, 43 (2010) 2313.
- [73] H. T. Oyama, *Polymer*, 50 (2009) 747.

- [74] M. L. Robertson, K. Chang, W. M. Gramlich, M. A. Hillmyer 43 (2010) 1807.
- [75] Poly(lactic acid): Synthesis, Structures, Properties, Processing, and Applications R.A. Auras, L.T. Lim, S. E. M. Selke, H. Tsuji John Wiley & Sons, October 2010.
- [76] P. D. Santis, A. J. Kovacs, Molecular conformation of poly(S-lactic acid) Biopolymers, (1968) 6, 299-306.
- [77] H T Oyama, Polymer, (2009)50,747-751.
- [78] K. Enomoto, M. Ajioka and A. Yamaguchi, U. S. Patent, 310, 865 (1994).
- [79] T. Kashima, T. Kameoka, C. Higuchi, M. Ajioka and A. Yamaguchi. U.S Patent, 428, 126, (1995).
- [80] F. Ichikawa, M. Kobayashi, M. Ohta, Y. Yoshida, S. Obuchi and H. Itoh. U.S. Patent, 5,440, 008 (1995).
- [81] G. Schwach, J. Coudane, R. Engel and M. Vert, Polym. Bull., (1994) 32, 617-623.
- [82] R. Auras, B. Harte, S. Selke Macromol. Biosci., 4 (2004) 835.
- [83] Natureworks PLA injection molding guide for 3051D, Minnetonka, MN: Natureworks LLC; 2006 http://www.natureworkslc.com/~media/Technical_Resources/Processing_Guides/ProcessingGuide_Foam-Sheet-Extrusion_.pdf.
- [84] O. Martin, L Averouis, Poly (lactic acid): plasticization and properties of biodegradable multiphase systems Polymer 42 (2001) 6209.
- [85] Natureworks Sheet extrusion processing guide, Minnetonka, MN: Natureworks LLC; 2005. http://www.natureworkslc.com/~media/Technical_Resources/Processing_Guides/ProcessingGuide_Sheet-Extrusion_.pdf.

- [86] J. Wootthikanokkhan, P. Kasemwananimit, N. Sombatsompop, A. Kositchaiyong, S. Isarankurana, A. N. Kaabbuathong, *J. Appl. Polym. Sci.*, 126 (2012) 389.
- [87] Z. Kun-Yu, Xiang-hai, Z., Yu gang, Y Bin, D. Li-song, *Chem. Res. CHIN. Univ.*, 25, (2009). 748.
- [88] S. Zhang, X. Feng, S. Zhu, Q. Huan, K. Han, Y Ma, M yu, *Mater. Lett.*, 98(2013)., 238.
- [89] Z. Xiong, C. Li, S. Ma, J. Feng, Y. Yang, R. Zhang, J. Zhu, *Carbohydr Polym.* 95, (2013) 77.
- [90] H. Yao, F. Deng, K. Illai, Q. Wang, F. Zhang and Q. F. Chen *Express polymer letters*. 5 (2011) 937.
- [91] H. Zhang, N. Liu, X. Ran, C. Han, L. Han, Y. Zhuang and L. Dong, *J. Appl. Polym. Sci.*, 125 (2012) 550.
- [92] K. A. Afrifah and L. M. Matuana, *Macro. Mater. Eng.* 295 (2010) 802.
- [93] P. Ma, D.G. Bogaerds, J. G. P. Goossens, A. B Spoelstra, Y. Zhang , P. J. Lemstra, *Eur. Polym. J.* 48 (2012) 146.
- [94] Z. Su, Q. Li, Y. Liu, H. G-H, C. Wu, *Eur. Polym. J.* 45, (2009) 2428.
- [95] R. Taib, Z. A. Ghaleb and Z. A. M. Ishak, *J. App. Polym. Sci.*, 123 (2012) 2715.
- [96] Natureworks LLC Website. Technology Focus Report: Toughened PLA. Available at: http://www.natureworksllc.com/productandapplications/ingeobiopolymer/technicalpublications/_/media/Files/Toughened-PLA Technology-Focus.pdf.
- [97] H. Shimizu and Y. Li, *Eur. Polym. J.* 45(2009) 738.

- [98] R. Jaratrotkamjorn, C. Khaokong and V. Tanrattanakul, *J. App. Polym. Sci.*, 24 .(2012) 5027.
- [99] C. Zhang, C. Man, Y. Pan, W. Wang and L. J. Y. Dan *Polym. Int.* 60 (2011) 154.
- [100] W. C. V. Tanrattanakul, W. Chumeka, J. .Pilad, P. P. Pasetto, Effect of Poly(Vinyl Acetate) on Mechanical Properties and Characteristics of Poly(Lactic Acid)/Natural Rubber Blends, *J. Polym. Environ.* 21 (2013) 450.
- [101] J. Odent, J. M. Raquez, E. Duquesne and P. Dubois, *Euro. Polym. J.*, 48 (2012) 3331.
- [102] L. Wang, W. Ma, R. A. Gross and S.P. McCarthy, *Polym. Degrad. Stab.* 59 (1998) 161.
- [103] T. Semba, K. Kitagawa, U. S. Ishiaku and H. Hamada, *J. App. Polym.Sci.*, 101, (2006) 1816 .
- [104] M. Harada, K. Iida, K. Okamoto, H. Hayashi, K. Hirano, *Polym. Eng. Sci.*, 48 (2008) 1359.
- [105] R. U. Rao, K. Suman, V. K. Rao and K. Bhanukiran. *Int. J. Environ. Sci.Tech.* 3 (2011) 6259.
- [106] V. Vannaladsaysy, M. Todo, T. Takayama, M. Jaafar, Z. Ahad, K. J. Pasomsouk, *Mater. Sci.*, 44, (2009) 3006.
- [107] J. Lee, S. McCarthy, Proceedings of Annual Technical Conference of the Society of Plastics Engineers (ANTEC 2007), Cincinnati, Ohio, May 6 -11, 2007, 1569.
- [108] K. M. Schreck and M. A. Hillmyer, *J. Biotechnol.* 1132 (2007) 287.
- [109] L. Jiang, M. P. Wolcott, J. Zhang, *Biomacromol.* 7 (2006) 199.
- [110] B. Imre, K. Renner, B. Pukánszky, 8, (2014) 2.

- [111] P. Choudhary, S. Mohanty, S. K. Nayak, L. Unnikrishnan, J. Polym. Sci.121 (2011) 3223.
- [112] S. M. Lai , Y. C. Lan, J. Polym. Research, 20, (2013) 140.
- [113] Y. Li, H. Shimizu, Macromol. Biosci. 7(2007) 921.
- [114] NatureWorks LLC website .Technology Focus Report: Toughened PLA. Available at <http://www.natureworkslc.com/product-and-applications/ ingeo biopolymer/technical publications/media/files/ toughened -PLA focus>.
- [115] J.J. Han, H. X huang, J. Appl.Polym.Sci. 120 (2011). 3217.
- [116] F.Feng, L.Ye, J. App. Polym. Sci. 119 (2011), 2778.
- [117] R. M. Taib, S Ramarad, Z.A.M. Ishak, M. Todo, Polym. Composite. 31 (2010) 1213.
- [118] M. Garcia, I. Garmendia, and J. J. Garcia, J.App. Polym. Sci., 107, (2008) 2994.
- [119] S. Oza, H. Ning, I Ferguson, N. Lu, Composites: Part B. 67 (2014), 227.
- [120] Y. Song, J. Liu, S Chen, Y Zheng,, S. Ruan , Y. Bin, J. Polym. Environ. 21, (2013) 1117.
- [121] B. K. Goriparthi, K. N. S. Surnan, and N. M. Rao Composites Part A, 43 (2012), 1800 .
- [122] R. H. Hu, M.Y. Sun, J. K. Lim, Mater. Des., 31, (2010) 3167 .
- [123] V. Baheti, R. Mishra, J. Militky, B.K Behera, Fiber. Polym. 15 (2014), 1500.
- [124] H. Lee, S. Wang, Composites, 37, (2006) 80.
- [125] Y. Wang, Y. Weng, L. Wang. Polym.Test.) 36, (2014) 119.

- [126] M.R.N. Fazita, K Jayaraman, D Bhattacharya, MS Hossain. MKM Hafiz, A Khalil, *Polymers*, 7 (2015) 1476.
- [127] B. Ayana, S. Suin, B. B. Khatua, *Carbohydr. Polym.*, 110 (2014) 430.
- [128] N. Ogata, G. Jimenez., H. Kawai, T. Ogihara, *J. Polym. Sci., Part B: Polym. Phys.* 35(1997) 389.
- [129] M. Pluta, A. Galeski, M. Alexandre, M. A. Paul and P. Dubois, *J. App. Polym. Sci.* 86 (2002) 1497.
- [130] J. Y. Nam, S.S. Ray and M. Okamoto, *Macromolecules*, 36 (2003) 7126.
- [131] P. Maiti, K. Yamada, M .Okamoto, K. Ueda K. Okamoto, *Chem Mat*, 14, (2002) 4654.
- [132] H J Lee, T G Park, H S Park, D S Lee., Y K Lee, Sc Yoon, J Nam, *Biomaterials*, 24, (2003) 2773.
- [133] Y. Di, S. Iannace, E. D. Maio and L. Nicolais, *J. Polym. Sci., Part B: Polym. Phys.*, 43, (2005) 689.
- [134] V Krikorian, D.J. Pochan, *Chem. Mater.* 15 (2003), 4317.
- [135] M Pluta, *J. Polym.Part B: Polym. Physics*, 44(2006) 3392.
- [136] L Peterson, K. Oksman, *Compo.Sci Tech*, 66 (2006) 2187.
- [137] M. Pluta, J.K. Jeska, G. Boiteux, *Eur Polym J.* 43 (2007) 2819.
- [138] M. Farmahini-Farahani, Huining Xiao, Yi Zhao, *J. App. Polym. Sci.* 131 (2014) 40952.
- [139] K. Fukushima, A. Final, F. Geobaldo, A. Venturello, G. Camino, *eXPRESS Polymer Letters*, 142, (2012) 914.
- [140] J.H. Wu, M.S. Yen, M.C. Kuo, B.H. Chen., *Composites, Mater. Chem. Phys.* (2013) 726.

- [141] I.E. Yuzay, R. Auras, H.S. Valdez, S. Selke, *Polym. Degrad. Stab.* 95, (2010) 1769
- [142] M. K. M. Haafiz, A. Hassan Z. Zakaria, I.M. Inuwa, M.S. Islam, M. Jawaid, *Carbohydr. Polym.*, 95, (2013) 139.
- [143] A. P. Mathew, K Oksman, M Sain, *J. Appl. Polym. Sc.* 97 (2005) 2014.
- [144] P. Qu, Y. Gao, G. Wu, L Zhang, *Bioresourc*5 (2010) 1811.
- [145] L. Petereson, I. Kvien, K. Oksman, *Compo. Sci. Technol* 67(2007) 2535.
- [146] M.P. Arrieta, E. Fortunati, F. Dominici, E. Rayon, J. Lopez, J.M. Kenny, *Carbohydr. Polym.* 107 (2014) 16.
- [147] Z.Cao, Y.Lu, C.Zhang, Q.Zhang, A. Zhou, Y. Hu, D. Wu, G. Tao, F. Gong, W. Ma, C. Liu J., *Appl. Polym. Sci.* 134(2017) 44895.
- [148] <https://committee.iso.org/files/live/sites/tc61/files/The%20Plastic%20Industry%20Berlin%20Aug%202016%20-%20Copy.pdf>
- [149] J.Lunt, *Polym. Degrad. Stab.* 59 (1998) 145.
- [150] S. Lee, J. W. Lee, *KOREA AUST RHEOL J.* 17 (2005) 71.
- [151] L. Jiang, M.P. Wolcott, J. Zhang, *Biomacromolecules.* 7 (2006) 199.
- [152] M. Todo, S.D. Park, T. Takayama, K. Arakawa, *Eng.Frac.Mech* 74, (2007), 65.1872.
- [153] J.Lu, Z. Qiu, W. Yang, *Polymer* 48 (2007) 4196

.....✂.....

MATERIALS AND EXPERIMENTAL TECHNIQUES

Contents

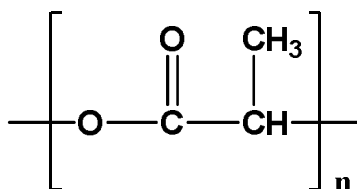
- 2.1 Materials
- 2.2 Methodology
- 2.3 Isolation of nanocellulose by steam explosion technique

This chapter gives a detailed description about the materials and experimental techniques used for the preparation of PLA blends and nanocomposites. The chapter also describes the isolation of nanofibrillated cellulose by steam explosion. The different characterization techniques employed are also described.

2.1 Materials

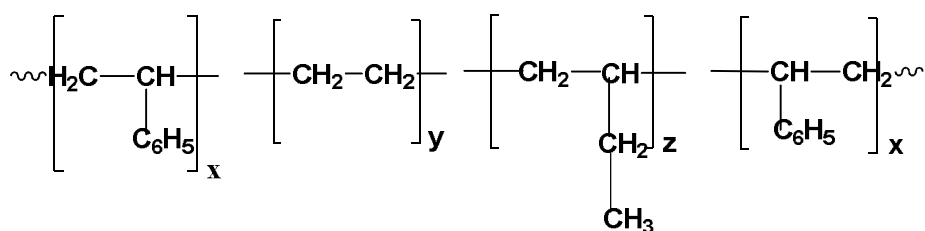
2.1.1 Polylactic Acid (PLA)

PLA (Ingeo™ Biopolymer 3001D) in the form of pellets with a density of 1.24 g/cm^3 and melt flow index of 22 g/10 min (at 210°C , 2.16 Kg load) was procured from Nature Works, USA. Ingeo Biopolymer 3001D (1.4% D isomer) has number average molecular weight and weight average molecular weight of 89141 g/mol and 158480 g/mol respectively and PDI of 1.7. Its relative solution viscosity is 3.1 ± 0.10 .



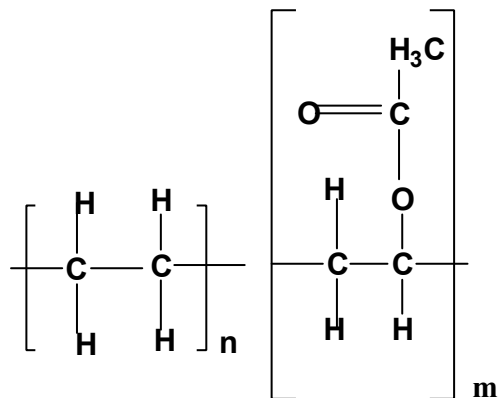
2.1.2 Styrene Ethylene Butylene Styrene (SEBS)

Styrene Ethylene Butylene Styrene (Taipol SEBS-6150) with a bound styrene content of 30.5% and specific gravity of 0.91 was purchased from Aquent Impex, Mumbai. It has a solution viscosity of 1900 cP at 25 °C.



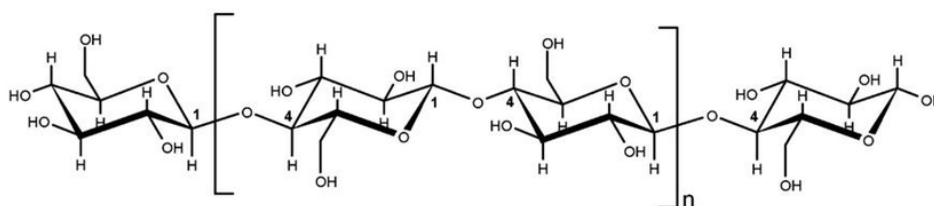
2.1.3 Ethylene vinyl acetate (EVA)

Ethylene vinyl acetate (EVA) with the commercial name “Levaprene 400” with specific gravity of 0.98, vinyl acetate content of 40% and Mooney viscosity of 20±4 MU was obtained from Lanxess India Pvt. Ltd.



2.1.4 Waste Cotton

Waste cotton for the isolation of nanocellulose was obtained from GRT, Alway. The structure of cellulose is shown below [1].



2.1.5 Other Chemicals

The various other chemicals used for the isolation of nanocellulose such as sodium hydroxide, oxalic acid and sodium hypochlorite (A.R. grade) were obtained from Nice chemicals, Cochin. For modification of SEBS chemicals such as maleic anhydride, dicumyl peroxide, and for modification of EVA, sodium hydroxide, potassium hydroxide, acetic anhydride, pyridine and tetrahydrofuran (THF) (AR grade) were procured from Merck India Pvt. Ltd.

2.2 Methodology

2.2.1 PLA Blends and Composite preparation

A corotating twin screw extruder (Specific ZV 20) equipped with a volumetric feeder and a strand pelletizer was employed to blend PLA with toughening agents. PLA was pre-dried at 80°C for 7 hrs in vacuum oven prior to melt blending technique. Twin screw extruder used for melt blending is shown in Figure 2.1



Figure 2.1 Twin screw extruder (Specific ZV 20)

2.2.1.1 Melt Blending

Extrusion is the most important technique used for melt processing of PLA. A typical screw consists of three sections namely 1. Feed zone which receives the polymer pellets and conveys the polymer into the screw and the channel depth is usually the same throughout the zone. 2. Transition zone (also called as compression or melting sections) where flight depth decreases gradually, compresses the pellets to improve the friction and contact with the barrel. 3. Metering zone is

characterized by a constant and shallow flight depth, which acts as a pump to meter accurately the required quantity of molten polymer. The L/D ratio (ratio of flight length of the screw to its outer diameter) determines the shear and residence time of the melt. Screws with large L/D ratio provides better mixing greater shear heating, and longer residence time in the extruder. Commercial grade PLA resins can be melt processed using a conventional extruder equipped with a general purpose screw of L/D ratio of 24–30. Another important screw parameter is the compression ratio, which is the ratio of the flight depth in the feed zone to the flight depth in the metering zone. The greater the compression ratio for a screw, the greater the shear heating it provides. The recommended compression ratio for PLA processing is in the range of 2–3 [2].

During the plasticizing process, PLA with toughening agent are fed from a hopper near the end of a barrel. The screw, driven by an electric or hydraulic motor, rotates and transports the material towards the other end of the barrel. The heat required for melting is provided by the heater bands wrapped around the barrel. As the screw rotates, the flights shear and push the polymer against the wall of the barrel which also provides frictional heat for melting the polymer. The combined thermal energy from the heater and frictional heat due to friction between the plastic and the screw and barrel, provide sufficient heat to raise the PLA polymer above its melting point (170–180 °C) by the time it reaches the end of the barrel. To ensure that all the crystalline phases are melted and to achieve an optimal melt viscosity for processing, the heater set point is usually set at 200–210 °C.

2.2.2 Preparation of test specimen

The extruded granules after drying were subjected to injection molding using Electronica Endura 90(Fig 2.2) in order to prepare the test specimen as per ASTM standard. The temperature and injection pressure used for injection molding process were maintained in the range of 175–190 °C and 110–120 bar, respectively. Dumb-bell shaped test specimens were used for the measurement of tensile properties. Figure 2.3 shows ASTM D 638 tensile test specimen. The thickness of the narrow portion was measured by a micrometer gauge. Stress – strain measurements were carried out using a Universal Testing Machine. Test was conducted in the standard laboratory atmosphere $23 \pm 2^\circ\text{C}$ and $50 \pm 5\%$ relative humidity for not less than 40 h prior to test in accordance of 25°C and 55 percent humidity [3]. Five samples have been taken for each analysis and the data reported are from the average of five and is statistically analysed by standard deviation method.



Figure 2.2 Injection molding machine (Electronica Endura 90)

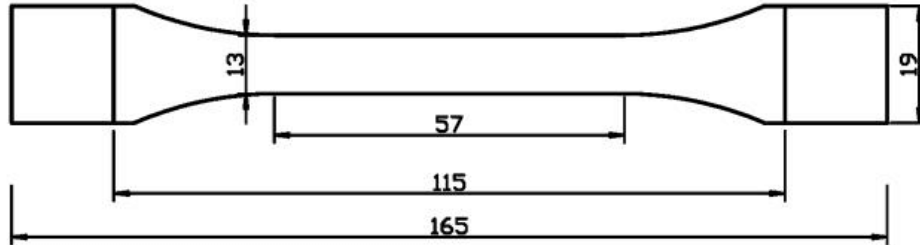


Figure 2.3 Dum-bell shaped test specimen for tensile strength [dimensions in mm] [4]

2.2.3 Characterization Techniques

2.2.3.1 Fourier Transform Infrared Spectroscopy (FTIR)

FTIR is mainly used for identification of different types of chemical bonds and functional groups present in various organic and inorganic compounds [5]. This technique also finds wide applicability in the field of polymers. All the samples of PLA based blends and nanocomposites were subjected to FTIR analysis (Model: Avatar 370 Make: Thermo Nicolet). The FTIR spectra for these samples were recorded in the wave number region ranging from 400 to 4000 cm^{-1} .

2.2.3.2 X ray diffraction (XRD)

The basic objective of x-ray diffraction is to study the arrangement of polymer molecules into crystalline and amorphous regions. It is a rapid analytical technique mainly used for phase identification of a crystalline material and can provide information on unit cell dimensions. X ray techniques are based on the interaction between x-ray radiation and the specimen. Depending on the angular regions of diffracted rays, XRD can be categorised into two. Wide angle X-ray Diffraction (WAXD)

is widely used which covers a broad range of Bragg's angle 2-theta from 2° up to 60°, while small angle diffraction experiments are carried out from a few seconds of arc upto a degree or so [6].

PLA samples were analyzed in a Bruker AXS D8 Advance X-Ray Powder Diffractometer with Cu K α radiation. The samples were scanned in the range of 3-80° at increment step of scanning 0.020° at a wave length of 1.5406 Å and Ni filter open at 30kV and 20mA.

2.2.3.3 Scanning Electron Microscopy (SEM)

SEM is one of the most versatile tools to analyse the morphology and microstructural characteristics of fractured surfaces. SEM observations reported in the present study were made on the fracture surface of the impact specimens. SEM of Impact fractured specimens was carried out using JEOL-6390LV (Germany). The fracture surface was coated with platinum before observation.

The isolated nanofibrillated cellulose was also subjected to SEM study.

2.2.3.4 Transmission Electron Microscopy (TEM)

TEM has become an important tool for micro structural characterisation of materials [7]. The images are made based on the intensity of electron emerging from the samples.

TEM analysis was conducted on JEOL JEM- 2100 Lab -6 (operating at 200 kV) to study the morphology of cellulose nano fibrils. 0.5 ml of 1 % solution of cellulose nano fibril was diluted to 100 times in distilled water. A drop of the solution was casted on to 300 mesh

Foamwar coated copper grids. TEM was also used to characterise the prepared nanocomposites.

2.2.3.5 Thermogravimetric analysis (TGA)

Thermogravimetric analysis (TGA), or simply thermogravimetry (TG), is a technique for measuring changes in the sample mass that occur while the sample temperature is varied in accord with a controlled temperature program [8].

TGA provides information about physical phenomena such as second order phase transitions including vapourisation, sublimation, absorption and desorption. It can also give information about chemical phenomena including chemisorptions, desolvation (mainly dehydration), decomposition and solid-gas reactions.(oxidation or reduction). It is commonly used to determine selected characteristics of materials that exhibit either mass loss or gain due to decomposition, oxidation, or loss of volatiles (such as moisture). Common applications of TGA include material characterization through analysis of decomposition patterns, studies of degradation mechanisms and reaction kinetics, determination of organic content and inorganic (e.g. ash) content in a sample, which may be useful for corroborating predicted material structures or simply for chemical analysis. It is an especially useful technique for the study of polymeric materials including thermoplastics, thermosets, elastomers, composites, plastic films, fibers, coatings and paints. studies of degradation mechanisms and reaction kinetics, determination of organic content in a sample, and determination of inorganic (e.g. ash) content in a

sample, which may be useful for corroborating predicted material structures or simply used as a chemical analysis.

The sample was placed in a temperature programmed furnace. Thermal stability was analyzed using TGA Q-50 of TA instruments under N₂ atmosphere. The samples weight of about 10-15 mg was heated at a rate of 10°C/min from ambient temperature to 600°C. The corresponding weight changes are noted with the help of an ultra-sensitive microbalance. The data of weight loss versus temperature and time is recorded online in the TA Instrument's Q series Explorer software. The analysis of the thermogravimetric (TG) and derivative thermogravimetric (DTG) curves are done using TA Instrument's Universal Analysis 2000 software version 3.38 [8].

2.2.3.6 Differential Scanning Calorimetry (DSC)

DSC is a thermo-analytical technique in which the difference in the amount of heat required to increase the temperature of a sample and reference is measured as a function of temperature. It is used to investigate thermal transitions, such as phase changes, crystallization, melting, glass transitions of a material as a function of temperature [9].

When the sample undergoes a physical transformation such as phase transitions, more or less heat will need to flow to it than the reference to maintain both at the same temperature. Whether less or more heat must flow to the sample depends on whether the process is exothermic or endothermic. Heat flow i.e. heat absorption (endothermic) or heat emission (exothermic), is measured as a function of time or

temperature of the sample and the result is compared with that of a thermally inert reference. The materials, as they undergo changes in chemical and physical properties, which are detected by transducers, which changes into electrical signals that are collected and analyzed to give thermograms. The melting and crystallization parameter, such as melting point (T_m), Heat of fusion (ΔH_f), temperature of crystallization (T_c), and Heat of crystallization (ΔH_c) were used for the comparison of blends and composites.

Thermal characterisation of all the blends and composites were performed by DSC analysis using Q20 model TA instruments, Walters with a double cycle of heating from 30 to 210°C at 10°C/min separated by a single cooling cycle at 10°C/min kept at isothermal for 5 min.

Glass transition temperature, crystallisation temperature, melting point, crystallisation enthalpy, and melting enthalpy were determined by heating and cooling scans. The percentage crystallinity of PLA blends were determined using the equation (1)

$$\chi_c = \frac{\Delta H_m}{\Delta H_o} * 100 \dots\dots\dots (2.1)$$

where ΔH_m is the enthalpy of melting and ΔH_o is the enthalpy of crystallisation of 100% crystalline PLA (93.7 J/g)[10].

2.2.3.7 Mechanical properties

a) Tensile Tests

Tensile properties of different compositions were examined by using universal testing machine. The tensile machine of a constant rate of

crosshead movement was used for the determination of tensile properties. It has a fixed or essentially stationary member carrying one grip, and a movable member carrying second grip. Self aligning grips are employed for holding the test specimen between the fixed member and the movable member prevents alignment problems. A controlled velocity drive mechanism was used. A load indicating mechanism capable of indicating total tensile load with an accuracy of (1% of the indicted value) was used.



Figure 2.4 Universal testing machine

An extension indicator, commonly known as extensometer, is used to determine the distance between two designated points located within the gauge length of the test specimen as the specimen is stretched. Stress, elongation, modulus, energy, and statistical calculations are performed automatically and presented on a visual display or hard copy-print out at

the end of the test. Figure 2.4 represents the universal testing machine (UTM).

b) Test Specimen and Conditioning

Test specimen

Test specimens for tensile tests were injection molded and the tensile tests were conducted according to the ASTM D 638.

i). Tensile Strength

The test specimen was positioned vertically in the grips of the testing machine. The grips were tightened evenly and firmly to prevent any slippage. The speed of testing was set at the proper rate and the machine was started. As the specimen elongates the resistance of the specimen increases and was detected by a load cell. This load value (force) was recorded by the instrument. The elongation of the specimen was continued until a rupture of the specimen was observed. Load value at break was also recorded. The tensile strength at yield and at break (ultimate tensile strength) was calculated. The tensile strength, modulus was calculated by using the equation,

$$\text{Tensile strength (MPa)} = \frac{\text{Ultimate load(N)}}{\text{Cross sectional area (mm}^2\text{)}}$$

ii). Tensile Modulus

An extensometer was attached to the specimen. The extensometer is a strain gauge type of device that magnifies the actual stretch of the specimen. The simultaneous stress strain curve is plotted on graph.

$$\text{Tensile modulus (MPa)} = \frac{\text{Difference in stress}}{\text{Difference in corresponding strain}}$$

iii). Elongation at yield

The elongation produced in the gauge length of the test piece upto the yield point original length (gauge length)

$$\text{Elongation at Yield} = \frac{\text{Change in length (elongation)}}{\text{Original length (gauge length)}}$$

iv). Percentage elongation at Break

The elongation at break, or at maximum extension, produced in the gauge length of the test piece is generally expressed as a percentage of gauge length.

$$\text{Percentage of elongation} = \epsilon \times 100$$

where ϵ is the ratio of elongation (ΔL) to the gauge length (L_0)

c) Flexural Tests

Determination of flexural properties of plastics involves three-point loading system utilizing center loading on a simple supported beam. A bar of rectangular cross section rests on two supports and is loaded by means of a loading nose midway between the supports. The maximum axial fiber stresses occur on a line under the loading nose. A close up of a specimen under flexural test is shown in Figure 2.5.



Figure 2.5 Universal testing machine under flexural tests

The machine used for tensile testing is also used for flexural testing (Tinius Olsen Universal Tester). The upper portion of the movable cross head was used for flexural testing.

The machine operated at a constant rate of cross head motion over the entire range. The loading nose and support had cylindrical surfaces. The radius of the nose and the nose support was 1/8 in. A strain-gauge type of mechanism called a deflectometer was used to measure deflection in the specimen.

d) Test specimen and conditioning: ASTM D 790

The specimen used for flexural testing was bars of uniformly rectangular cross section according to ASTM D 790 standard [11]. The test specimen of size 1/8×1/2×4 in. are used.

Test procedure

The test was initiated by applying the load to the specimen at the specified cross head rate. The specimen lies on a support span and the load was applied to the center by the loading nose produced three point bending at a specified rate. The load is the sample material's flexural strength. The deflection was measured by a gauge under the specimen in contact with it in the center of the support span. The test was stopped when the specimen reaches 5% deflection.

The test material under was deformed significantly but did not break, the load at yield, measured at 5% deformation/strain of the outer surface, is reported as the flexural strength or flexural yield strength. Figure 2.6 shows the forces involved in bending a simple beam.

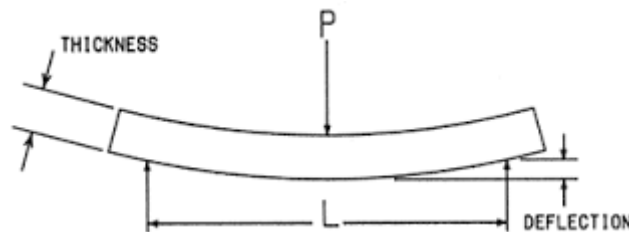


Figure 2.6 Forces involved in bending a simple beam [11]

e) Impact Tests

The impact strength describes the ability of a material to absorb shock and impact energy without breaking. The impact strength is calculated as the ratio of impact absorption to test specimen cross-section. Toughness is dependent upon temperature and the shape of the test specimen. The area under the stress-strain curve is directly proportional

to the toughness of the material. Higher the impact strength of the material, higher will be the toughness and vice versa. Figure 2.7 shows the impact tester. The Izod impact strength of the injection molded samples was determined as per ASTM D 256 [12]. The test was carried out machine with a pendulum of 2.7798 J and striking velocity of 3.46 m/s. Sample is clamped vertically in the base of the machine. A pendulum swings on its track and strikes the sample. The energy lost as the pendulum continues on its path is measured from the distance of follow through. The impact energy is directly read from the machine.

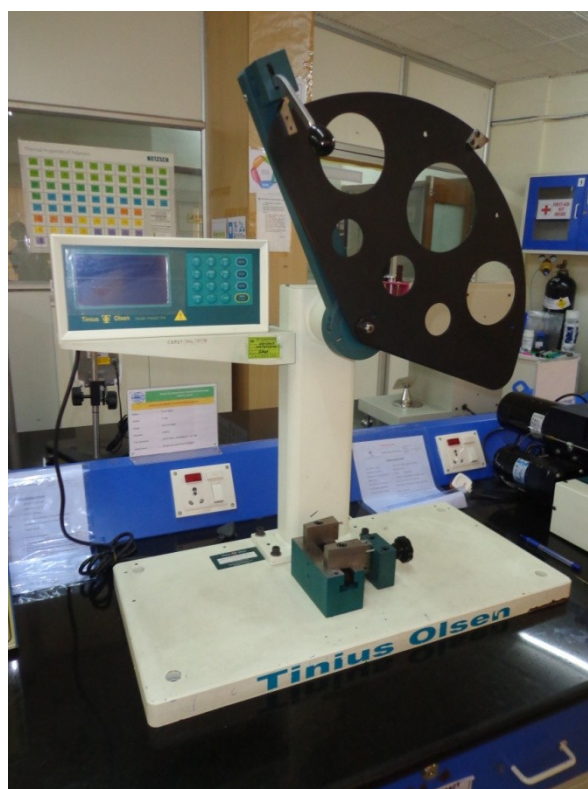


Figure 2.7 Impact Tester

2.3 Isolation of nanocellulose by steam explosion technique

Steam explosion is a pre-treatment process that helps in the extraction of cellulose fibers from plant biomass, which can be used either alone or in combination with high-pressure disintegration. This method involves short term cooking under steam at high pressure (1-3.5 MPa) and at high temperature (120-210 °C) in an autoclave. The pretreatment with the compressed steam is followed by an explosive decompression, during which the flash evaporation of water exerts a high shear force and causes the material to rupture which results in substantial breakdown of the plant material structure, viz, hemicelluloses, degradation of lignin, and defibrillation etc. The addition of sodium hydroxide enhances the pretreatment efficiency [13,14]. Steam explosion has been employed for the extraction of fibers from flax [15], cotton [16], wheat straw[17], bamboo[18], pineapple leaf fibres [19] etc. The cellulose nanofibrils extracted by this method have higher aspect ratio than those isolated with other methods. The major advantages of steam explosion include low energy and chemical consumption, environment friendly and low capital investment. However, this process should be repeated several times to release the fibrillated material efficiently. The autoclave employed for the present study to isolate cellulose nanofibers from cotton waste is shown in Figure 2.8



Figure 2.8 Autoclave (Jiotech ST-85 G)

2.3.1 Characterisation of cellulose nanofibers

2.3.1.1 FTIR

FTIR spectra for raw cotton, bleached cotton and nanocellulose were recorded using an infrared spectrophotometer (Make: Thermo Nicolet and Model: Avatar 370). The measurements were made in the wave number region ranging from 4000 and 400 cm^{-1} with a resolution of 4 cm^{-1} . A total of 100 scans were used for obtaining the spectra. About 2 mg of fibre was crushed into small particles in liquid nitrogen. The fibre particles were then mixed with KBr and pressed into a small disc about 1 mm thick.

2.3.1.2 X- ray Diffraction (XRD)

Isolated nanofibrillated cellulose was analysed using Bruker AXSD8 Advance powder X-ray diffractometer. The X-ray diffraction pattern was recorded in a range of 0 to 80 with a step of 0.020 and step time 65.6s. The wavelength of the Cu/K α rod source was 0.15406 nm and the spectra were obtained at 35Ma with an accerlerating voltage of 40kV.

2.3.1.3 Scanning Electron Microscopy

SEM of isolated nanocellulose fibrils dispersion was carried out using JEOL-6390LV (Germany). Also the surface of raw cotton and bleached cotton was studied using SEM.

2.3.1.4 Transmission Electron Microscopy

TEM was used to study the morphology of cellulose nano fibrils. TEM analysis was conducted on JEOL JEM- 2100 Lab -6 operating at 200 kV. 0.5 ml of % solution of cellulose nano fibril was diluted to 100 times in distilled water. A drop of the solution was casted on to 300 meshes Foamwar coated copper grids and allowed to dry at room temperature.

2.3.1.5 Thermo-gravimetric Analysis (TGA)

The thermal stability of the samples were investigated with Q50, TA instruments, Walters, USA under nitrogen atmosphere from room temperature to 600 °C at a heating rate of 10 °C /min.

References

- [1] Mechanisms affecting the structure and properties of heat-treated and high-temperature dried Norway spruce (*Picea abies*) wood. November 2011.
- [2] Natureworks polymer technical data sheets—PLA polymer 7032D. Minnetonka, MN: Natureworks LLC; 2005
- [3] Handbook of Plastics Testing and Failure Analysis, 3rd Edition Vishu Shah John Wiley & Sons, 1998.
- [4] <http://www.astm.org/standards/D638.htm>
- [5] S.A. Liebman, D.H. Ahlstrom, P.R. Griffiths, *Appl. Spectrosc.* 30(1976) 355.
- [6] L. E. Alexander, *X-ray Diffraction Methods in Polymer Science*, Wiley-Interscience, New John Wiley, New York (1979).
- [7] D.B. Williams, C.B. Carter, *Transmission Electron Microscopy- A Textbook for Materials Science*, Springer 2009. L. E. Alexander, *X-ray Diffraction Methods in Polymer Science*, Wiley-Interscience, New John Wiley, New York (1979).
- [8] www.tainstruments.com
- [9] A.W. Salamon, J. Kenneth *Practical Uses of Differential Scanning Calorimetry for Plastics*, Marcel Dekker New York, 2003.
- [10] E.Hassan, Y.Wei, H.Jiao, Y.Muhuo, *Journal of Fiber Bioengineering and Informatics*, 2013, 6, 85-94
- [11] <https://www.astm.org/Standards/D790.htm>
- [12] <https://www.astm.org/Standards/D256.htm>
- [13] C. Cristóbal, R. Encarnación, B. Mercedes, M. Paloma, M. N. José, C. Eulogio, *Fuel*, 2008, 87, 692–700.

- [14] B. Deepa, E. Abraham, B.M.Cherian, A. Bismarck, , J. J. Blaker, L.A. Pothan, A.L. Leão, S.F. de Souza, M. Kottaisamy, *Bioresour Technol.*, 102 (2011) 1988.
- [15] R. Kessler, U. Becker, R. Kohler, B. Goth, *Biomass Bioenergy*. 14 (1998) 237.
- [16] T. Jeoh, F. Agblevor, *Biomass Bioenergy*, 21 (2001) 109.
- [17] A. Kaushik, M. Singh, G. Verma, *Carbohydr Polym.* 82(2010) 337.
- [18] S. Shao, G. Wen, Z. Jin, *Wood Sci. Technol.* 42 (2008) 439.
- [19] B.M. Cherian, A.L. Leão, S. F. de Souza, S. Thomas, L.A. Pothan, M. Kottaisamy, *Carbohydr Polym.* 81 (2010) 720.

.....✪✪.....

POLYLACTIC ACID (PLA) /STYRENE ETHYLENE BUTYLENE STYRENE (SEBS) AND PLA /MA-g-SEBS BLENDS

- 3.1 Introduction
- 3.2 Experimental
- 3.3 Analysis and Characterisation
- 3.4 Results and discussions
- 3.5 Thermal Properties
- 3.6 Thermo-gravimetric Analysis
- 3.7 Conclusion

This chapter deals with chemical modification of Styrene Ethylene Butylene Styrene (SEBS) by melt grafting technique using maleic anhydride and dicumyl peroxide. Styrene Ethylene Butylene Styrene and maleic anhydride grafted SEBS are used as toughening agents to study their effect for its toughness, high strength and heat resistance on PLA. PLA/SEBS and PLA /Maleic Anhydride grafted SEBS (MA-g-SEBS) blends were prepared under four different compositions by melt mixing technique using a co-rotating twin-screw extruder after optimising the mixing conditions. The mechanical properties of the blends such as tensile, flexural and impact strengths were investigated using specimens prepared by injection moulding process. The percentage elongation and impact strength of PLA/MA-g-SEBS blends were found to be increased significantly by 540 % and 134% respectively in comparison with virgin PLA and PLA/SEBS blends. However, tensile strength and modulus of PLA/SEBS and PLA/MA-g-SEBS blends decreased compared to pristine PLA. SEM behaviour supported the higher impact property of polylactic acid with the incorporation of modified SEBS via multiple crazing and cavitation mechanisms. DSC study also supported greater compatibility between maleated SEBS and PLA.

3.1 Introduction

The emerging concern over persistent problem of plastic waste disposal has created much interest in the use of biodegradable plastics. PLA is a biopolymer with excellent biodegradability, derived from renewable resources such as corn starch, making it a sustainable alternative to petrochemical-based plastic products. However, with low glass transition temperature (55 - 65 °C), its inherent brittleness and low toughness severely limit its range of applications. In such a scenario, several strategies have been put forward to improve its material properties. A number of modifications, such as copolymerization, plasticization, and blending with other polymers have been in use to improve the flexibility of PLA. Blending PLA with other polymers is the most viable methodology for toughening PLA [1]. A number of studies has already been reported on blends of PLA with various biopolymers for its property improvement including poly(hydroxyalkanoate)s (PHAs) poly(caprolactone)(PCL) poly(butylene succinate) (PBS), poly(butylene adipate-co-terephthalate) (PBAT), and also copolymers like poly(ethylene-co-glycidyl methacrylate) (EGMA) and poly(ethylene-co-octene).

Noda et al. [2] reported that the toughness of PLA was substantially increased without a reduction in the optical clarity of PLA/PHA copolymer blend. There occurred a reduction in crystallisation of PHA copolymer finely dispersed in PLA matrix. Broz et al. [3] investigated the mechanical and structural properties of PDLA and poly (epsilon-caprolactone). SEM studies revealed the poor adhesion between the blend constituents. Semba et al. [4] made an attempt to reduce the brittle

behaviour of PLA by blending it with polycaprolactone. Dicumyl peroxide (DCP) was added to improve ultimate tensile strain. DCP enhanced the viscous property which agreed with ductility and impact property. Wang et al.[5] prepared biodegradable polymer blends consisting of PLLA and poly(butylene succinate) (PBS) in the presence of dicumyl peroxide (DCP). The degree of crystallinity of PBS and the cold crystallization ability of PLLA gradually reduced with increasing DCP content. The addition of DCP induced an increase in viscosity of the blends at low frequencies and also resulted in finer dispersion of PBS particles and better interfacial adhesion between PLLA and PBS. The thermal studies of Yokohara et al. [6] found that PBS could enhance the crystallisation of PLA. Jiang et al. [7] found that with the increase in PBAT content (5-20 wt %), PLA-PBAT blend showed decreased tensile strength and modulus whereas elongation and toughness were dramatically increased. Zhang et al. [8] melt blended polylactic acid and poly (butylene adipate-co-terephthalate) in presence of glycidyl methacrylate. Oyama et al. [9] found a dramatic improvement in mechanical property of polylactic acid by blending PLA with poly(ethylene -glycidyl methacrylate). Li et al. [10] prepared Polylactide (PLA)/poly(ethylene-co-octene) (POE) blends via melt blending using ethylene-glycidyl methacrylate copolymer (EGMA) as a compatibilizer. One of the approaches used to toughen PLA is by blending it with an elastomeric component. Tanrattanakul et al. [11] toughened PLA by blending with natural rubber (NR), epoxidized natural rubber (ENR) and natural rubber grafted with poly (methyl methacrylate). Flexural modulus, flexural strength, and flexural strain of these blends were much lower than PLA. NR was found to be the best

toughening agent compared with NR-g-PMMA and ENR. NatureWorks [12] recently identified toughening agent called Blendex™ 338, for PLA. It is an ABS resin containing 70% butadiene rubber, which acts as an effective toughener among various impact modifiers. The impact strength and elongation was increased to 20% with the use of Blendex™ 338 compared to neat PLA whereas the tensile yield strength of the blend was decreased compared to neat PLA. Yao et al. [13] studied blends of PLA/poly(propylenecarbonate) (PPC) using maleic anhydride (MA) to modify its properties. The toughness was improved while the strength remained same by addition of very low content (as low as 0.9%) of MA into the blends. Zhang et al. [14] prepared PLA/MBS (Methyl Methacrylate-Butadiene-Styrene) blends via melt mixing. The addition of MBS changed the tensile behaviour of the PLA significantly. The impact strength was increased from 4.7 kJ/m² for neat PLA to 97.2 kJ/m² for PLA/MBS (75/25) blend. Glycidyl Methacrylate (GMA)-grafted POE (mPOE) as a toughening agent was reported for PLA by Su et al [15].

To enhance the compatibility between PLA and ABS, Shimizu et al. [16] introduced styrene acrylonitrile GMA copolymer (SAN-GMA) as a reactive compatibilizer and ethyltriphenylphosphonium bromide (ETPB) as a catalyst during melt blending. The compatibilized PLLA/ABS blends exhibited improved impact strength and elongation but showed slight reductions in modulus and tensile strength.

In recent times, maleated rubbers like maleic anhydride grafted styrene ethylene butylenes styrene (MA-g-SEBS) maleic anhydride grafted ethylene propylene rubber (MA g-EPM) etc were found to serve

well as toughening agent for polymer blends and nano composites. Wilkinson et al. [17] studied the effects of SEBS-g-maleic anhydride on polypropylene/PA6/SEBS ternary blends. Mechanical tests showed that these blends to exhibit inferior low-strain tensile properties, but superior ultimate tensile properties and impact strength compared to the matrix PP. Sharma and co-workers [18] studied the effects of crystallinity of PP and flexibility of SEBS-g-MA copolymer on the mechanical properties of PP/SEBS-g-MA blend. It was found that the tensile modulus and strength decreased but tensile elongation and impact strength enhanced. Morphological studies showed good dispersion of SEBS-g-MA in polypropylene with a weak level of interaction between the phases. Impact strength and ductility of polyamide 6/polypropylene was significantly improved by the addition of styrene-ethylene butylene styrene copolymers [19]. The flexural yield displacement of PLA/nano clay composite was increased by the presence of maleic anhydride grafted ethylene –propylene rubber [20].

In the present study, SEBS and MA-g-SEBS are used as toughening agents for PLA owing to their high impact strength and superior heat resistance in comparison with other elastomeric toughening agents. PLA melt blended with SEBS and MA-g-SEBS at different compositions and its properties were evaluated. The physico-mechanical, thermal and morphological properties of the above blends were investigated and the properties were compared with virgin PLA.

3.2 Experimental

3.2.1 Materials

The details of the polymers and chemicals used for the study are discussed in **Chapter 2** (section 2.1)

3.2.2 Grafting of maleic anhydride on SEBS

The melt grafting reactions were carried out in a twin screw extruder (Specific ZV 20) using Styrene Ethylene Butylene Styrene (SEBS) (94.5%), maleic anhydride (5%) and dicumyl peroxide (0.5%). SEBS pellets and powders of maleic anhydride and dicumyl peroxide was fed into hopper. The temperatures from hopper to die at six different zones were 150, 160, 170, 180, 190, 195 °C, respectively, and the screw speed was fixed at 72 rpm. The extrudate (yield of 85%) were chopped into 3 mm length and dried it well which was used for test specimen preparation by injection molding.

3.2.2.1 Melt Blending

A corotating twin screw extruder (Specific ZV 20) equipped with a volumetric feeder and a strand pelletizer was employed to blend PLA with SEBS and also PLA with MA-g-SEBS. PLA was pre-dried at 80°C for 7 hrs in vacuum oven prior to melt blending technique. PLA / SEBS and PLA / Maleic Anhydride grafted SEBS (MA-g-SEBS) blends were prepared under four different compositions (SEBS and MA-g-SEBS were of 5, 10, 15 and 20 wt% each) by melt mixing technique with a co-rotating twin –screw extruder (Specific ZV 20) with a temperature zone set at (155-195 °C). The screw speed was set at 60 rpm. The extruded granules

were injection moulded (Electronica Endura 90) to carry out different mechanical tests.

3.3 Analysis and Characterisation

3.3.1 Analysis of Maleated SEBS

a). Grafting Degree (Gd)

The grafting degree (Gd) was analysed according to Zhou et al. [21]. Approximately 0.2 g of MA -g- SEBS was dissolved in 50 ml toluene under reflux for 30 min. Then, 100 ml of hydrochloric acid (0.1 M) was added to the solution prior to titration with 0.1 M KOH using phenolphthalein as the indicator. A blank titration was done using the same method.

$$Gd = \frac{N(V_0 - V)98.06}{2XWX100}$$

Where W - weight of sample (g)

N - normality of KOH

V - volume of KOH (ml) for blank titration

V₀ - volume of KOH (ml) for MA-g-SEBS titration

b). Acid number

The acid number of MA - g- SEBS was determined by titration method [22]. A sample of 0.1 g was placed in a volumetric flask with 10 ml acetone, 10 ml hydrochloric acid (0.1 M) and 100 ml water. The solution was then titrated with 0.1 M KOH using phenolphthalein as indicator. A blank titration was also done. Acid number was derived as follows:

$$A \text{ (eq/kg)} = \frac{V' - H}{WXf}$$

Where W - weight of the sample

V' - volume of KOH (ml) for sample titration

H - volume of KOH (ml) for blank titration

f - factor value of KOH solution (0.1 M) = concentration of KOH (M) solution

3.3.2 Thermal Characterisation

a). DSC Analysis

Thermal characterisation of all the blends were performed by DSC analysis using Q20 model TA instruments, Walters, USA with a double cycle of heating from 0 to 210 °C at 10 °C/min separated by a single cooling cycle at 10 °C/min kept at isothermal for 5 minutes at 210 and 0 °C. Glass transition temperature, crystallisation temperature, melting point, crystallisation enthalpy and melting enthalpy were determined by heating and cooling scans. The percentage crystallinity of PLA PLA/SEBS, PLA/MA-g-SEBS blend was determined using equation 3.1.

$$\chi_c = \frac{\Delta H_m}{\Delta H_o} * 100 \dots\dots\dots (3.1)$$

Where ΔH_m is the enthalpy of melting and ΔH_o is the enthalpy of crystallisation of 100% crystalline PLA (93.7 J /g)

b). Thermo-gravimetric Analysis

The thermal stability of the samples were investigated by Thermogravimetric analysis (TGA) using TA instruments Q50, Walters,

USA under nitrogen atmosphere from room temperature to 600 °C at a heating rate of 10 °C /min.

3.3.3 Scanning Electron Microscopy

The SEM of Impact fractured specimens was carried out using JEOL-6390LV (Germany). The fracture surface was coated with platinum before analysis.

3.3.4 Fourier Transform Infrared Spectroscopy

FTIR studies were performed using Thermo Nicolet, Avatar 370 at a resolution of 4 cm⁻¹ in the frequency range from 4000-400 cm⁻¹.

3.3.5 Mechanical Properties

The tensile properties of all the blends were performed as per ASTM D-638 (Shimadzu Autograph model AG-IS 50KN) using five injection molded dumb bell-shaped specimens (165 mm × 13mm × 3.2 mm) with a cross-head speed of 50 mm/min.

The flexural properties were also determined by three-point bending test in accordance with ASTM D790. The span length was set at 96 mm at the speed of 3 mm/min.

The Izod impact strength tests of all blends were carried out according to ASTM D-256 using Tinius Olsen IT 504 impact tester, USA with specimen dimensions of 63.5 mm × 12.7 mm (notch depth of 2.54 mm and notch angle of 45°).

3.4 Results and discussions

3.4.1 Chemical structure characterisation of MA-g-SEBS

The grafting efficiency and acid value of MA-g-SEBS was found to be 1.87 and 0.14 respectively by titration method.

FTIR is used to investigate the molecule structure of polymer, especially for grafting systems. Figure 3.1 represents the FTIR spectra of MA-g-SEBS compared with SEBS and MA. The absorption band at 1728 cm^{-1} due to the C=O stretching of cyclic anhydride indicates that maleic anhydride is grafted on SEBS. The compatibilised blends have exhibited additional stretching frequency corresponding to carbonyl functional groups from MA at 1706 cm^{-1} . FTIR spectrum of MAH has been given the stretching frequency for carbonyl group at around $1,706\text{ cm}^{-1}$ and the peak has been displaced to lower vibrational region (1728 cm^{-1}) in the compatibilized blend. This may be due to the restriction in the molecular vibration in carbonyl functionality due to the effective dipole-dipole interaction between polar groups of PLA and anhydride group of MA [23].

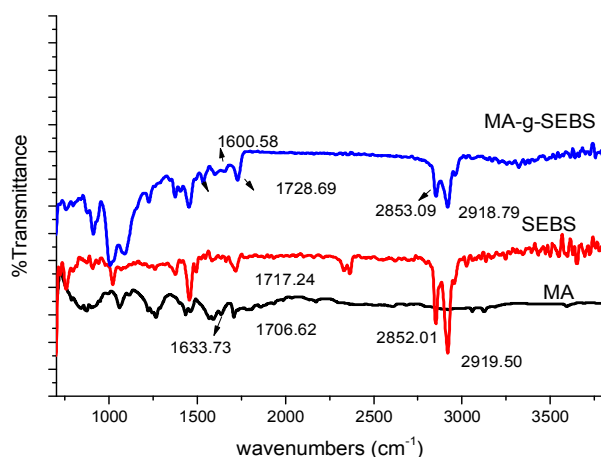


Figure 3.1 FTIR spectra of MA-g-SEBS, SEBS and MA

3.4.2 Mechanical Properties

Variations in tensile strength, modulus, and elongation at break, flexural strength and flexural modulus of various blends of PLA are shown in Table 3.1. PLA/SEBS and PLA/MA-g-SEBS blends shows higher percentage elongation compared to neat PLA. PLA/MA-g-SEBS blends in all compositions show higher impact strength in comparison with PLA/SEBS and neat PLA. Tensile strength and modulus of PLA/SEBS and PLA/SEBS-g-MA blends were decreased compared to pristine PLA. This is attributed to the lower modulus and elastomeric nature of SEBS/maleated SEBS [22]. Flexural strength and modulus also gradually decreased with increase in concentration of maleated SEBS. The percentage elongation of PLA/SEBS was found to be higher than that of virgin PLA which indicates the plasticisation effect of SEBS on PLA. The percentage elongation of PLA/MA-g -SEBS (80:20) blend increased significantly in comparison with neat PLA and PLA/SEBS which indicates the change of mode from brittle to ductile [23].

Table 3.1 Mechanical properties of virgin PLA, PLA/SEBS, and PLA/MA-g-SEBS

Material designation	Tensile strength (MPa)	Tensile modulus (MPa)	Elongation at break (%)	Flexural strength (MPa)	Flexural modulus (MPa)	Impact strength (kJ/m ²)
PLA	62.85±0.5	2883.7±0.5	3.50±0.20	63.54±0.45	2834.80±0.35	3.10±0.2
PLSE-5	42.68±0.45	2553.3±0.57	17.89±0.80	67.30±0.2	2673.30±0.34	4.10±0.1
PLSE-10	43.78±0.2	2560.90±0.35	17.40±0.54	64.56±0.54	2680.54±0.76	4.21±.02
PLSE-15	41.41±0.43	2552.30±0.40	23.82±0.30	66.45±0.4	2650.20±0.13	4.24±.04
PLSE-20	38.47±0.20	2420.30±0.67	21.54±0.44	65.20±0.1	2548.70±0.52	4.29±.1
PLSEG-5	42.19±0.24	2583.76±0.70	9.37±0.45	67.40±0.32	2656.20±0.55	5.45±.05
PLSEG-10	39.84±0.35	2435.77±0.35	15.89±0.9	61.83±0.25	2390.90±0.9	7.21±.04
PLSEG-15	33.33±0.50	2220.08±0.32	19.52±0.56	51.30±0.1	2441.01±0.24	7.23±.01
PLSEG-20	30.86±0.13	2011.27±0.79	22.41±0.36	44.11±0.1	2191.40±0.12	7.28±.03

PLSE-PLA/SEBS

PLASEG-PLA/MA-g-SEBS

The impact strength of neat PLA was only 3.1 kJ/ m², and the samples fractured clearly in a brittle manner. The impact strength of all the compositions of PLA/SEBS and PLA/MA-g-SEBS blends were higher than that of neat PLA. The addition of MA-g-SEBS resulted in greater toughness and the brittle-ductile transition was achieved at 10—20 wt % of MA-g-SEBS. For the blend with 20 wt% of maleated SEBS elastomer, the impact strength was increased to 7.28 kJ/m² (134 %) which was more than double compared to virgin PLA (3.1 kJ/m²). This may be due to the strong interfacial adhesion between the PLA matrix and grafted elastomer resulting in brittle to ductile transition. The elastomeric nature of maleated SEBS enabled to absorb impact energy that led to better toughness for PLA/MA-g-SEBS blends (80:20) [24].

3.4.3 Blend morphology

Figure 3.2 represents the SEM micrographs of impact fractured surfaces of PLA, PLA / SEBS (80:20) PLA / MA-g-SEBS blends (80:20). For virgin PLA, the fracture surface was found to be relatively smooth and homogeneous whereas the blends of PLA with SEBS showed a clear stress-whitening surface (Figure 3.2 a). However, the impact fractured surfaces of blends became increasingly rough with the increase in concentration of maleated SEBS (10-20 wt %) which may lead to higher impact strength in comparison with PLA and PLA/SEBS.

PLA / SEBS and PLA / MA-g-SEBS blends show oval cavities around the matrix that underwent some deformation. The dispersed elastomeric phases cavitate and debond on the application of load. Particulate cavitation and void formation generate new stress whitening that facilitates the deformation of matrix. The plastic deformation can effectively help in the energy dissipation and high impact strength of the matrix. [25]

Figure 3.2(b) shows that there is a poor interfacial adhesion between rubber particles and PLA matrix resulting in more number of small voids. This is because SEBS is non polar and forms an immiscible blend with PLA. SEBS could only add on plasticising effect on polylactic acid. In the case of MA-g-SEBS (Figure 3.2c), the number of voids are less due to the fact that the maleic anhydride grafting on to SEBS increased the compatibility between PLA and SEBS. On the other hand, the maleic anhydride groups, grafted with backbone of MA-g-SEBS have good compatibility with polylactic acid. MA-g-SEBS imparts both plasticising and wetting characteristics to PLA / MA-g-SEBS, which causes an enhancement in impact property in binary blends via multiple crazing and cavitations toughening mechanisms. The dispersed MA-g-SEBS phase in small average particle size observed in these micrographs aids for stress transfer across the interface to matrix. The addition of MA-g-SEBS increased the rate of crystallisation and thereby toughened the matrix system.

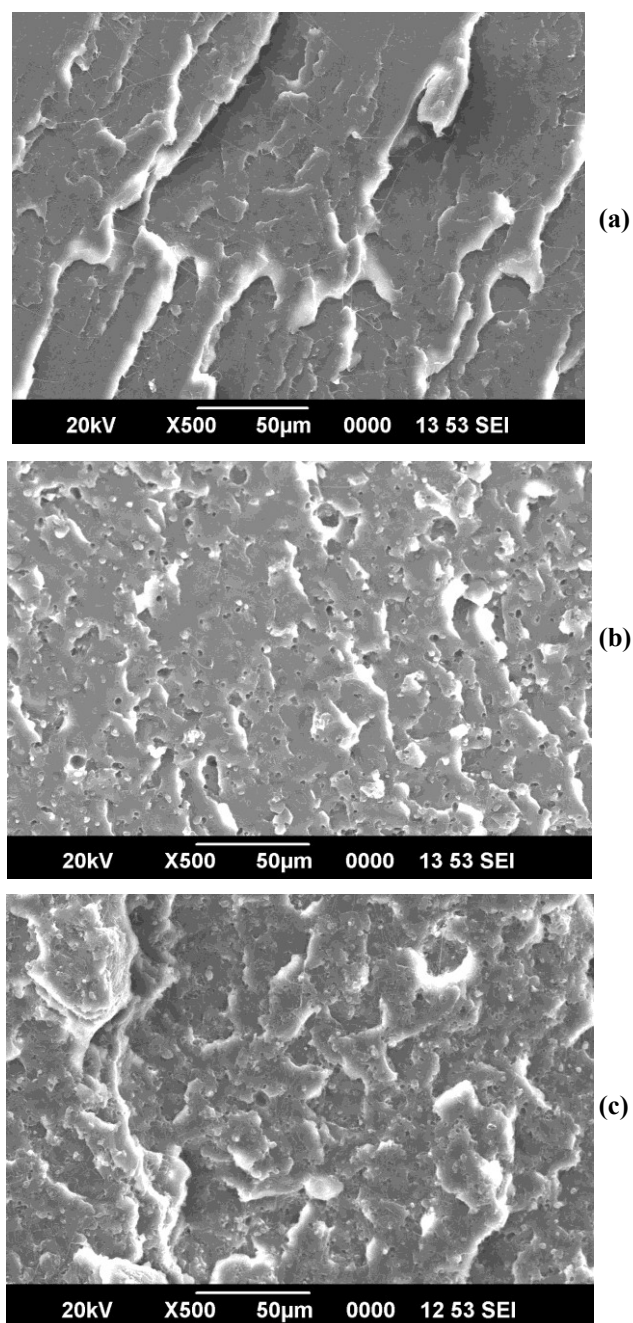


Figure 3.2 SEM images of (a) Virgin PLA (b) PLA/SEBS (10 wt %) (c) PLA/MA-g-SEBS (10 wt %)

3.4.4 Thermal Properties

A) Differential Scanning Calorimetry (DSC):

DSC thermograms of virgin PLA and its blends are shown in Figure 3.5. The thermal characteristics such as glass transition temperature (T_g), Crystallisation temperature (T_c), melt temperature (T_m), enthalpy of crystallisation (ΔH_c), enthalpy of melting (ΔH_m) and Percentatge crystallinity (χ_c) of PLA blends are summarised in Table 3.2.

Table 3.2 Thermal Characteristics of PLA, PLA/SEBS and PLA/MA-g-SEBS

Thermal characteristics						
Materials designation	T _c (°C)	T _g (°C)	T _m (°C)	ΔH_c ($\frac{j}{g}$)	ΔH_m ($\frac{j}{g}$)	χ_c (%)
PLA	105.55	62.38	169.56	23.63	32.63	34.86
PLSE-5	99.63	61.29	168.46	14.94	63.04	67.35
PLSE-10	99.72	59.29	166.95	10.59	44.67	47.72
PLSE-15	104.56	60.60	168.14	21.59	41.11	43.90
PLSE-20	109.26	62.30	169.78	31.27	46.89	50.09
PLSEG-5	106.27	61.85	169.50	20.75	29.78	31.82
PLSEG-10	108.80	62.24	169.93	27.81	36.50	39.00
PLSEG-15	109.67	62.22	170.99	25.41	32.81	35.06
PLSEG-20	110.96	62.40	171.28	24.31	31.76	33.94

PLSE-PLA/SEBS

PLASEG-PLA/MA-g-SEBS

T_g of PLA/SEBS blends was slightly shifted to lower temperature when compared to that of neat PLA due to the plasticization effect of runbber component without any interaction between the constituents. However, T_g of PLA/MA-g-SEBS blends (5-20 wt %) was found to be slightly shifted to higher temperature or the same when compared with PLA (62.38) which confirms better compatibility between carbonyl group of PLA and anhydride part of MA-g-SEBS.

It can be seen that the crystallinity of pure PLA is 34.86 %. In the case of PLA /SEBS blends the crystallinity increased in comparison with virgin PLA. This may be due to the presence of SEBS promoted heterogeneous nucleation and it enhanced the rate of crystallisation. It can also be observed an increase in the rate of crystallisation from 34.86 % in pure PLA to 50.09 % for higher percentage composition of SEBS.

The crystallinity was reduced in the case of PLA/maleated SEBS indicating the interaction between maleic anhydride moiety of SEBS and PLA. Hence, the impact strength of PLA/ MA-g-SEBS blends was also increased in comparison with PLA/SEBS and neat PLA.

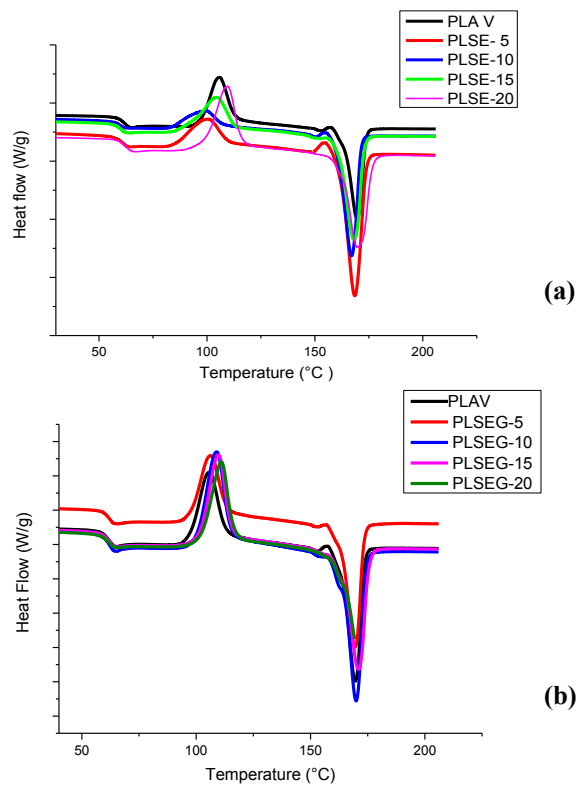


**Figure 3.5 DSC curves of a) PLA/SEBS (PLSE)
b) PLA /MA-g- SEBS(PLSEG)**

B) Thermo-gravimetric Analysis (TGA):

The TGA curves of neat PLA, PLA/SEBS and PLA/MA-g-SEBS are shown in Fig 3.6 (a) and (b). TGA results are tabulated in Table 3.2. As evident from Table 3.3, SEBS is thermally stable than PLA with an onset degradation temperature of 419 °C. The temperature at 5 % weight loss (T₅) of all PLA/SEBS and PLA/MA-g-SEBS blends were found to be higher than virgin PLA which indicates that SEBS has stabilised PLA initially. However, at T_{onset}, T₅₀ and T₉₅, the thermal stability was lowered compared to neat PLA. At higher temperature (Tonset), the rubber component may have catalysed the thermal degradation of PLA/SEBS and PLA/ MA- g- SEBS blends.

Table 3.3 Thermo gravimetric data of PLA, SEBS, PLA/SEBS and PLA /MA-g- SEBS

Materials designation	T ₅ (°C)	Thermal characteristics			
		T ₅₀ (°C)	T ₉₅ (°C)	T _{onset} (°C)	T _{peak} (°C)
PLA V	383.66	365.14	392.21	347.64	371.18
SEBS	383.85	442.46	469.63	419.84	453.99
PLSE-5	393.87	334.31	294.04	316.58	340.55
PLSE-10	415.99	327.51	282.70	307.39	330.34
PLSE-15	431.06	334.17	286.90	313.74	339.37
PLSE-20	427.33	332.05	290.64	308.61	334.31
PLSEG-5	412.02	343.96	304.82	324.52	348.82
PLSEG-10	426.20	346.96	307.66	325.09	347.93
PLSEG-15	438.11	346.79	305.96	324.06	347.93
PLSEG-20	443.21	342.782	303.12	318.78	344.52

T_{onset}-Onsetdegradation temperature
 T_{peak}-Peak degradation temperature
 T₅-Tempearture at 5% weight loss
 T₅₀ Tempearture at 50% weight loss
 T₉₅ Tempearture at 95% weight loss

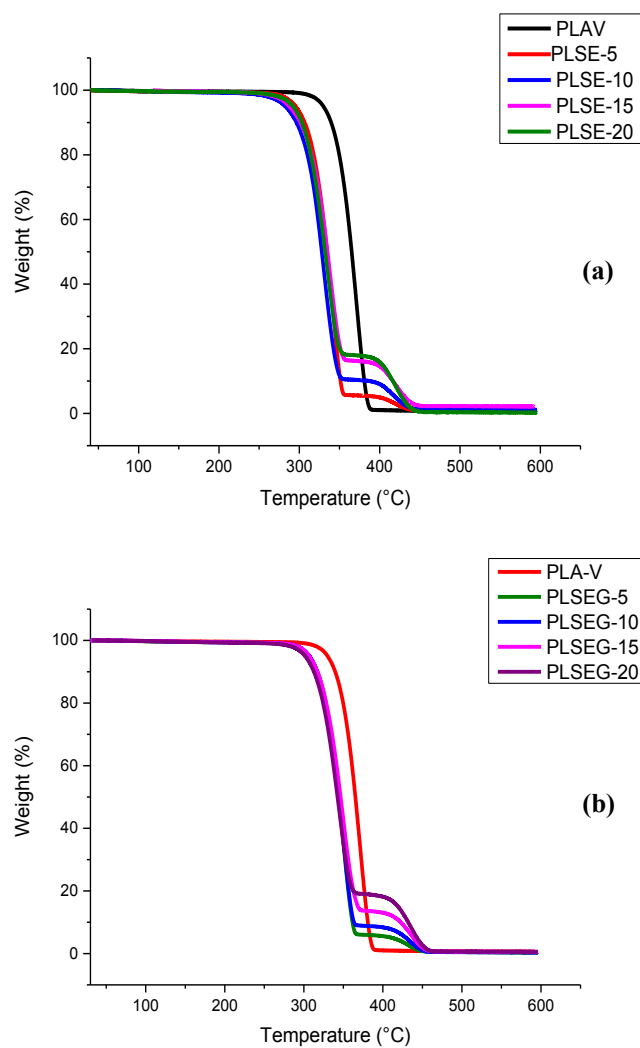


**Figure 3.6 TGA curves of a) PLA/SEBS (PLSE)
b) PLA/MA-g-SEBS(PLSEG)**

3.5 Conclusion

SEBS and MA-g-SEBS at various compositions were used as toughening agents for modification of PLA. For PLA with 20 wt% of maleated SEBS elastomer, the impact strength increased to 7.28 kJ/m² which was more than double (134 %) compared to virgin PLA (3.1 kJ/m²). SEM study revealed that MA-g-SEBS imparted both plasticising and wetting characteristics to PLA which resulted in better impact property via multiple crazing and cavitations toughening mechanisms. The percentage elongation of PLA/ MA-g -SEBS (80:20) blend increased significantly in comparison with neat PLA which revealed the change of mode from brittle to ductile. Thermal stability of PLA/MA-g-SEBS was marginally reduced with the addition of maleic anhydride grafted SEBS in comparison with virgin PLA. DSC study also supported greater compatibility between maleated SEBS and PLA.

The work included in this chapter has been published:

“Toughening of Poly(lactic Acid (PLA) Using Styrene Ethylene Butylene Styrene (SEBS) By Melt Blending: Mechanical, Thermal and Morphological studies”
VH Sangeetha, TO Varghese, SK Nayak, Polymer Engineering & Science, 2016, 56 (6), 669-675.

References

- [1] K. S. Anderson, K.M Shreck, and A.M. Hilmyer, Polym. Rev. 48 (2008) 85.
- [2] I. Noda, M.M. Satkowski, A.E. Dowrey, and Marcott C Macromol. Biosci. 4(2004) 269.
- [3] M.E. Broz, D.L. Vander Hart, and N.R. Washburn Biomaterials 24(2003) 4181.
- [4] T. Semba, K. Kitagawa, U.S. Ishiaku, and H. Hamada J.Appl. Polym. Sci. 101 (2006) 1816.
- [5] R. Wang, S .Wang, Y. Zhang, C. Wan and P. Ma Polym Eng. Sci.49 (2009) 26.
- [6] T. Yokohara, and M. Yamaguchi Eur. Polym. J. 44 (2008) 677.
- [7] L. Jiang, M.P. Wolcott, and J. Zhang Biomacromolecules 7(2006) 199.
- [8] N. Zhang, Q. Wang, J. Ren, and L. Wang J. Mater. Sci. 44 (2009) 250.
- [9] H.T. Oyama, Polymer 50, (2009) 747.
- [10] D. Li, B. Shentu, and X. Weng J. Macromol.Sci. 50(2011) 2050.
- [11] W. Chumeka, W.C.V. Tanrattanakul, J. Franc and P. P. Pasetto, J. Polym. Environ. 21, (2013) 450.
- [12] Natureworks LLC Website. Technology Focus Rep0rt: Toughened PLA. Available at: http://www.natureworksllc.com/productandapplications/ingeobiopolymer/technicalpublications/___/media/Files/Toughened-PLAT echnology-Focuspdf.ashx
- [13] H. Yao, F. Deng, K. Illai, Q. Wang, Zhang and Q.F. Chen Expresspolymlett. 5, (2011) 937.

- [14] H. Zhang, N. Liu, X. Ran, Han, C. L Han, Y. Zhuang, and L. Dong J. Appl. Polym. Sci. 125 (2012) 550.
- [15] Z. Su, Q. Li, Y. Liu, G. H. Hu, and C. Wu, Eur. Polym. J 45, (2009) 2428.
- [16] H. Shimizu, and Y. Li, Eur. Polym. J., 45 (2009) 738.
- [17] A.N. Wilkinson, M.L Clemens, and V.M Harding, Polymer, 45, (2004) 5239.
- [18] R. Sharma, and S. N. Maiti, Polym. Plast. Technol. Eng. 45(2014) 229.
- [19] Kusmono, Z.A.M. Ishak, W.S. Chow, T. Takeichi, and Rochmadi Eur. Polym. J. 44 (2008) 1023,.
- [20] Z.A. Kusmono, M. Ishak, W.S. Chow, T. Takeichi, and Rochmadi Composites Part A, 95, (2008) 627.
- [21] X. Zhou, G. Dai, W. Guo, Qunfang, and Lin J. Appl. Polym. Sci. 76 (2000) 1359.
- [22] H. Matsuda, M. Ueda, and H. Mori, Wood Sci. Tech. 22, (1998)
- [23] S. Bonda, S. Mohanty, and S.K. Nayak, Iran Polym J (2014) 23:415–425
- [24] Y.Y. Leu, Z. A. M. Ishak, and W. S. Chow, J. Appl. Polym. Sc. 124, (2012) 1200.
- [25] P. Choudhary, S. Mohanty, S.K. Nayak, and L. Unnikrishnan, J. Appl. Polym. Sci. 121 (2011) 3223.

.....✂.....

Chapter 4

ISOLATION AND CHARACTERISATION OF NANOFIBRILLATED CELLULOSE FROM WASTE COTTON USING STEAM EXPLOSION PROCESS

Contents	4.1 Introduction
	4.2 Materials
	4.3 Analysis and Characterisation
	4.4 Results and discussions
	4.5 Conclusion

Waste management is a major challenge faced by human beings in domestic life and industrially. Garment industry has abundant waste of cotton rags and cuttings during its manufacture. As cotton is the largest source of cellulose with a cellulose content of 87 to 96%, its waste can be effectively utilised for the production of value added products like nanofibrillated cellulose for use as reinforcements in polymers. This chapter deals with the isolation of nanofibrillated cellulose from waste cotton using Steam explosion process, a thermomechanical process employed to disrupt the structural components of cellulose. Steam at high pressure penetrates through the lignocellulosic biomass through diffusion. Shear force generated by the immediate release of pressure hydrolyses the glycosidic bond and hydrogen bonds between the glucose chains, leads to the formation of nanofibers. Steam explosion followed by mild acid treatment was used for nanocellulose isolation. Nanocellulose was characterised by different techniques like TEM, SEM, and XRD.

4.1 Introduction

In the present scenario, reducing the consumption of petroleum feed stocks and increasing the use of sustainable and renewable resources is a major challenging task. Cellulose and cellulosic derivatives are used as sustainable replacement of petroleum based polymers. Cellulose possesses good mechanical properties and is renewable, biodegradable as well as non toxic. Wood and other lignocellulosic fibers provide excellent mechanical strength and high strength to weight ratio so that there is a wide demand for such renewable materials. Nanomaterials can be isolated from the cellulosic sources owing to its semicrystalline nature and hierarchical structure [1]. The nanomaterial landscape is vast, with the power to drive polymer mechanical properties to extreme values. The production of nanocellulose is being carried out by different methods, such as acid hydrolysis [3] ball milling [4] etc.

Nanocellulose can be of two types: cellulose nanocrystals and nanofibrillated cellulose. Nanofibrillated cellulose refers to material with fibril length in several micrometers whereas width in nanometer range. Nanofibrils contain both amorphous and crystalline region. Different mechanical treatments are adopted to isolate nanofibrils which include high pressure homogenisation or grinding [5]. However this production method is affected by high energy consumption for fiber delamination. [6-8]. Nanocrystals are produced by chemical methods like acid hydrolysis. CNFs can be prepared via high shearing followed by homogenisation at high pressure. High pressure homogenisers, autoclaves, grinders, cryocrushers are generally employed for its isolation. Reduction

of energy consumption has already been a leading edge in the isolation of nanofibrillated cellulose. Cherian et al has isolated nanocellulose from pineapple leaf fibres via steam explosion [9]. Saelee et al. [10] also extracted cellulose from sugarcane bagasse using steam explosion method. Abraham et al. [11] employed three different sources namely pineapple leaf, banana and jute fiber to extract micro fibrils. In the earlier work nanocellulose has also been prepared from coir fiber, cotton linters etc [12]. Steam explosion was found to be an effective method for the extraction of nanocellulose from biomass. Deepa et al. [13] extracted cellulose nanofibers from banana fibers by steam explosion technique and also studied the degradation characteristics of the chemically treated fibers with untreated fiber.

The present study focuses on the isolation of nanofibrillated cellulose from waste cotton using steam explosion process, a thermo mechanical process which breaks the structural components of natural fiber. Steam at high pressure penetrates through the lignocellulosic biomass through diffusion process. The sudden release of pressure generates shear force that hydrolyses the glycosidic bond, inter and intra molecular hydrogen bonds between the glucose chains, leading to the formation of nanofibers.

4.2 Materials

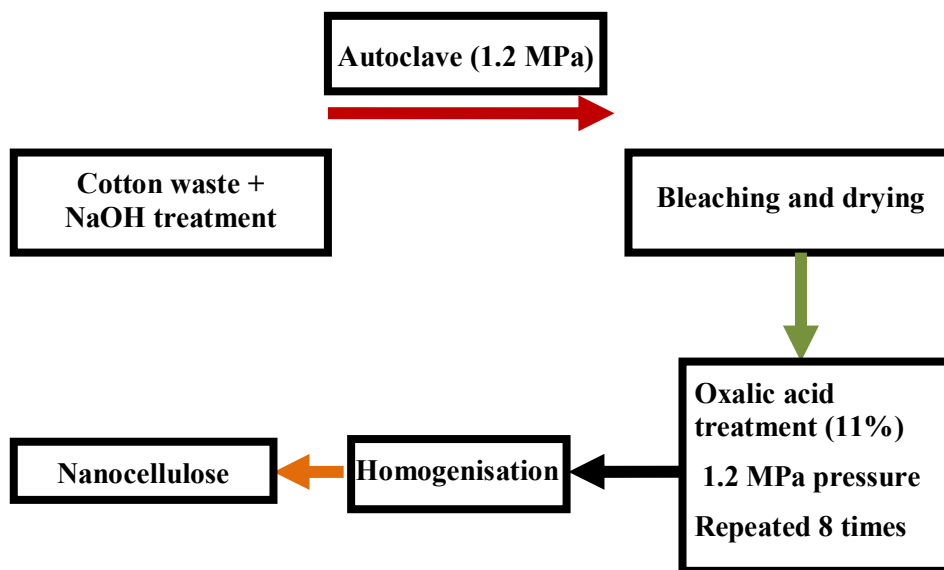
Waste cotton which is the principal source of cellulose was obtained from GRT, Alwaye. The various chemicals used for the extraction such as NaOH, Oxalic acid and sodium hypochlorite (A.R. grade) were obtained from Nice chemicals, Cochin.

4.2.1 Isolation of nano fibrillated cellulose from cotton waste using steam explosion

Steam explosion is a process in which biomass is treated with hot steam at high temperature (180 to 240 °C) under high pressure (1 to 3.5 MPa) followed by an explosive decompression of the biomass that results in a rupture of the biomass fiber rigid structure. The sudden release of pressure defibrillates the cellulose bundles and results in a better accessibility of the cellulose for subsequent. The different steps used for the isolation of nano fibrillated cellulose are shown in scheme 4.1 [14].

50 g of Waste cotton, chopped to ~ 1 cm length which was treated with 2% NaOH (fibre to liquor ratio of 1:10) and then steam exploded in an autoclave under 1.2 MPa pressure at 120 °C for a period of one hour. The pressure was removed immediately and was washed with distilled water until it gets rid of alkali. The steam exploded fibers were bleached using a mixture of NaOH (27 g) and acetic acid (78.8g) and a mixture of 1:3 sodium hypochlorite solutions for six times. After bleaching, the fibers were washed thoroughly in distilled water and dried. The steam exploded fibers were treated with oxalic acid (11%) in an autoclave under 1.2 MPa pressure at 120 °C again for one hour. The pressure was released immediately. The pressure was again raised to 1.2 MPa and cotton fibers were kept under pressure for twenty minutes. Again pressure was released. The above raise and release of pressure was repeated eight times. The suspension obtained was washed with water until the washings have no effect on KMnO_4 , The acid free suspension was

stirred using a mechanical stirrer until the fibers disperse uniformly. The obtained nano cellulose was designated as NFC.



Scheme 4.1 Isolation of nanocellulose by steam explosion

4.3 Analysis and Characterisation

4.3.1 Fourier Transform Infra Red Spectroscopy (FTIR)

FTIR spectra for raw cotton, bleached cotton and nanocellulose were recorded using an infrared spectrophotometer (Make: Thermo Nicolet and Model: Avatar 370). The measurements were made in the wave number region ranging from 4000 and 400 cm^{-1} with a resolution of 4 cm^{-1} .

4.3.2 X- ray Diffraction (XRD)

The synthesised nanofibrillated cellulose was analysed using Bruker AXSD8 Advance powder X-ray diffractometer. The X-ray diffraction pattern was recorded in a range of 0 to 80 with a step of 0.020 and step time 65.6s. The wavelength of the Cu/K α rod source was 0.15406 nm and the spectra were obtained at 35mA with an accelerating voltage of 40kV.

4.3.3 Scanning Electron Microscopy (SEM)

The SEM of Impact fractured specimens was carried out using JEOL-6390LV (Germany). The fracture surface was coated with platinum before observation.

4.3.4 Transmission Electron Microscopy (TEM)

TEM was used to study the morphology of cellulose nano fibrils. TEM analysis was conducted on JEOL JEM- 2100 Lab -6 operating at 200 kV. 0.5 ml of % solution of cellulose nano fibril was diluted to 100 times in distilled water. A drop of the solution was casted on to 300 mesh Foamwar coated copper grids and allowed to dry at room temperature.

4.3.5 Thermo-gravimetric Analysis (TGA)

The thermal stability of the samples were investigated with Q50 , TA instruments, Walters, USA under nitrogen atmosphere from room temperature to 600 °C at a heating rate of 10 °C /min.

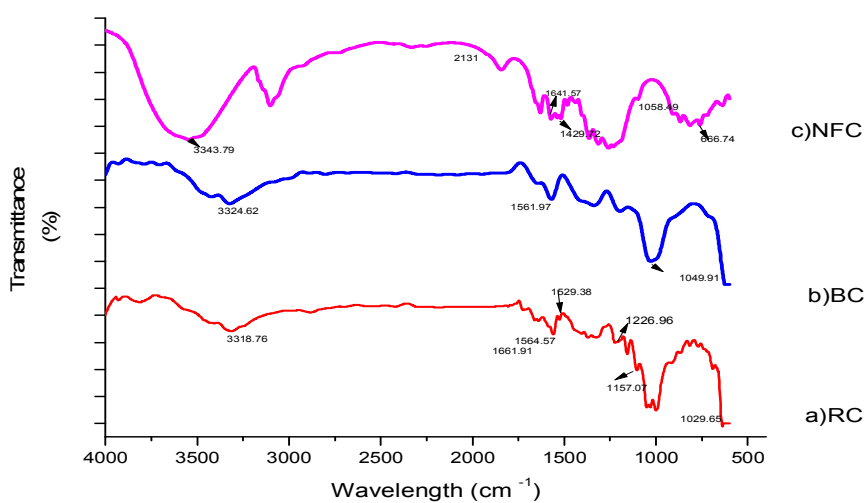
4.4 Results and Discussions

4.4.1 FTIR Analysis of treated and untreated waste cotton and nano cellulose

Fig. 4.1 gives the FTIR spectrum of cotton fiber isolated at different stages. It was found that the alkali treatment reduces the hydrogen bonding due to removal of the hydroxyl groups which shows decrease in the intensity of the peak between 3200 and 3400 cm^{-1} compared to the untreated fiber [15, 16]. For raw cotton, the absorption peak at 1529 cm^{-1} corresponds to lignin. The peak at 1226 cm^{-1} corresponds to CO stretching of aryl group in lignin. However, this peak disappeared upon bleaching due to the removal of lignin on bleaching. Also the absorption at 1157 cm^{-1} represents the anti-symmetric deformation of C-O-C bond. All raw and bleached fibers exhibited peak at 1050 and 893 cm^{-1} due to traces of lignin and hemicelluloses. In the case of nano cellulose at 3343 cm^{-1} absorption is due to increase in free OH groups exposed in cellulose structure after subsequent treatments [11] and also may be due to the moisture adsorbed from the environment. Also the peak at 1641 cm^{-1} corresponds to OH groups from water vapour adsorbed from the atmosphere [17-19]. The peak observed in the spectra of nanocellulose at 1163 cm^{-1} range is due to the C-O-C pyranose ring (antisymmetric in phase ring) stretching vibration. The main absorption peaks of the sample at different stages are shown in Table 4.1.

Table 4.1 Main absorption peak of waste cotton at different stages

Raw Coton	Bleached Cotton	Nanofibrillated Cellulose	Involved groups
3318 cm ⁻¹	3324 cm ⁻¹	3343.79 cm ⁻¹	OH stretching
		2131.98 cm ⁻¹	C-H stretching
1529.38 cm ⁻¹	-	-	Aromatic C = C stretching in lignin
1029.65 cm ⁻¹	1049.91 cm ⁻¹	1058.49 cm ⁻¹	C-O, C-C stretching or C-OH bending
653.042.669.62, 688.67 cm ⁻¹	684.53 cm ⁻¹	666.74,614.26 cm ⁻¹	C-OH out-of-plane bending

**Figure 4.1 FTIR of a) Raw cotton (RC) b) Bleached cotton (BC) and c) Nanocellulose (NC)**

4.4.2 X-ray diffraction analysis of nanocellulose

Fig. 4.2 shows the XRD pattern of Raw cotton and nano fibrillated cellulose from waste cotton. The major diffraction peak for raw cotton was found at $2\theta = 22.54$ assigned to crystalline planes with miller indices 200 indicating the presence of cellulose I structure [20] whereas nanocellulose showed prominent peak with an intensity of $2\theta = 22.60, 20.62, 18.21, 16.389, 26.7, 21$ respectively. The crystallinity index of nano cellulose was found to be 66 percent based on Segal's empirical method [21].

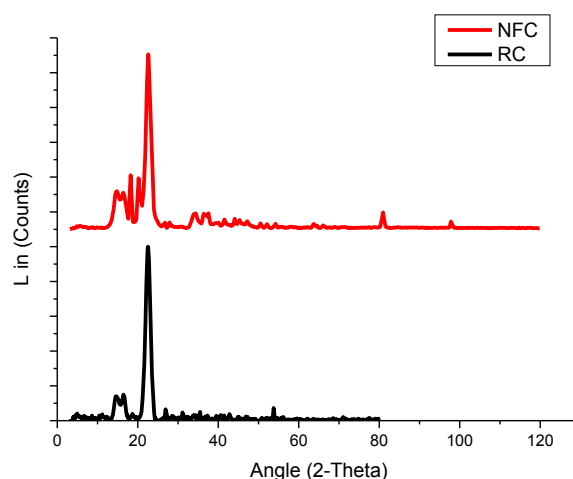


Figure 4.2 XRD of Raw cotton (RC) and Nanofibrillated cellulose (NFC)

4.4.3 SEM Analysis of treated and untreated waste cotton, nano cellulose and its nanocomposites

Waste cotton fibers in Fig. 4.3 (a) showed a twisted ribbon like shape and they had a relatively smooth surface, primarily due to wax coating on the fiber surface. Also, due to the removal of binding material, the

fibers were separated into individual form. Partial removal of binding constituents and defibrillation are important in the point of bleaching (Fig 4.3 b) and subsequent steps of nano cellulose isolation. Acid treatment together with steam explosion after bleaching helps in the total disintegration of fibrils to form nano fibrils via acid treatment and homogenisation as shown. Fig. 4.3 (c) and 4.3 (d) displays highly entangled nano fibrils with diameters ranging from 67-70 nm which signifies the resistance to flow and gel like character.

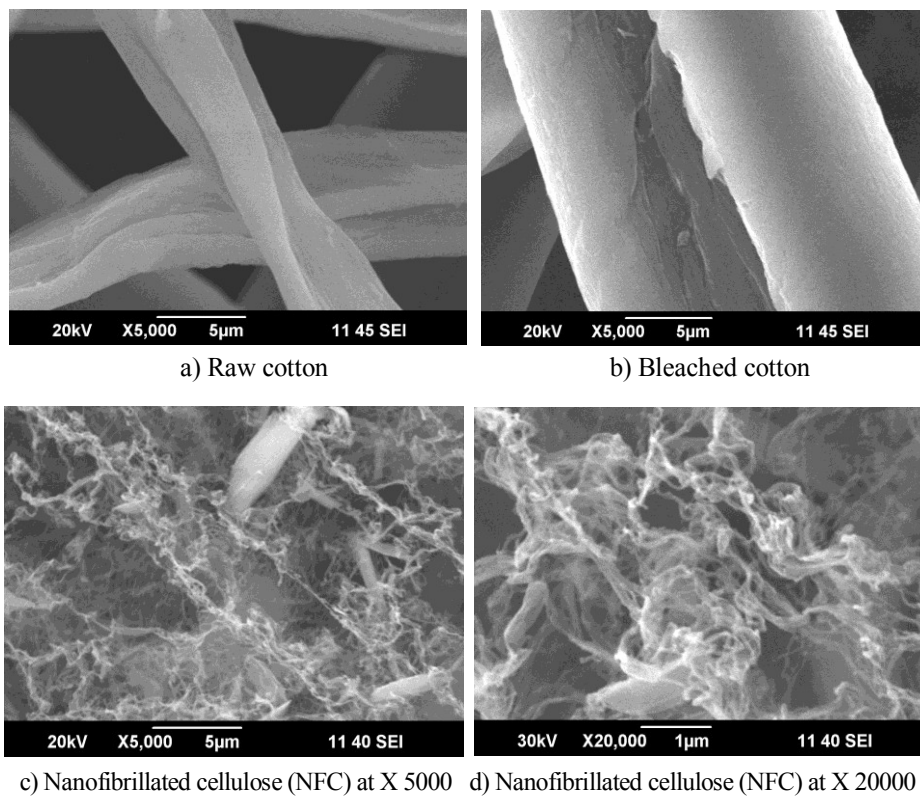
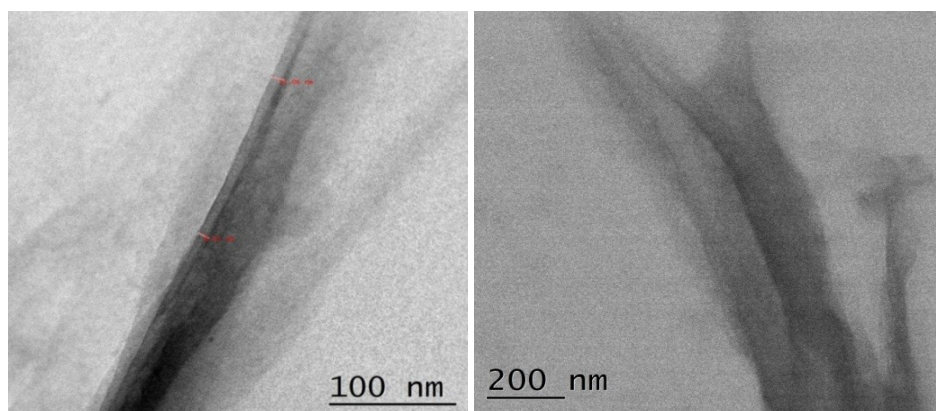


Figure 4.3 SEM of a) Raw cotton b) Bleached cotton c) Nanofibrillated cellulose (NFC) at X 5000 d) Nanofibrillated cellulose (NFC) at X 20000

4.4.4 Transmission Electron Microscope Analysis

TEM micrographs, Fig. 4.4 (a) and b) supported the effectiveness of steam explosion followed by acid treatment in the isolation of nano fibrils. The acid treatment could cleave the amorphous region and thereby keep the crystalline domains intact and was able to reduce the size of fiber from micron to nanometric dimensions [22].



a) Nanofibrillated cellulose (NFC) at 100 nm b) Nanofibrillated cellulose (NFC) at 200 nm

**Figure 4.4 TEM of a) Nanofibrillated cellulose (NFC) at 100 nm
b) Nanofibrillated cellulose (NFC) at 200 nm**

4.4.5 Thermogravimetric Analysis (TGA)

Figure 4.5 represents the thermogravimetric curves of raw cotton and nanofibrillated cellulose. The initial weight loss in the region up to 110 °C is mainly due to the vaporisation of water from the cellulose samples. There is a major change in the onset degradation of raw cotton to isolated nanofibrillated cellulose. The onset degradation point of raw cotton and nano fibrillated cellulose was found to be 287°C and 316 °C respectively. Nano fibrillated cellulose formed via steam explosion and

mild acid treatment enhanced the thermal stability of nanocellulose which may be probably due to the partial destruction of crystalline region.

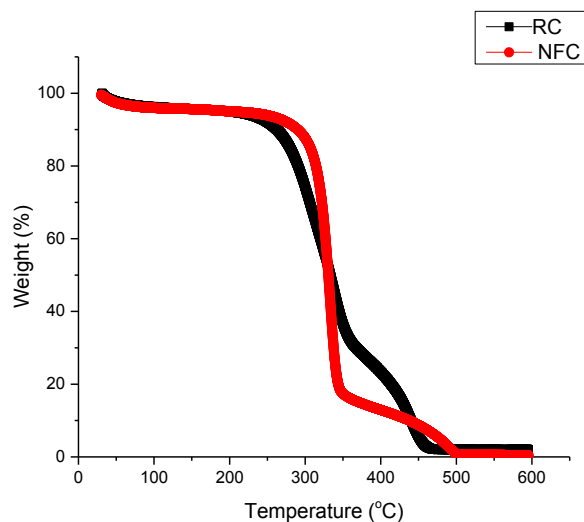


Figure 4.5 TGA of Nanofibrillated cellulose (NFC) and raw cotton (RC)

4.5 Conclusion

Nanofibrillated cellulose was isolated from waste cotton and was confirmed by different analysis like SEM, TEM and XRD. The crystallinity index of nanofibrillated cellulose was found to be 66 percent based on Seigel's empirical method. SEM images showed highly entangled nano fibrils with diameters ranging from 67-70 nm. TEM results revealed reduction in the size of fiber from micro to nano upon mild acid treatment along with steam explosion.

References

- [1] C.J. Gao, L.G. Tang, Cellulosic science (Chinese), Science Press, Beijing,1996,1-12
- [2] D. Klemm, B. Heublein, H. P. Fink, A. Bohn, Angewandte Chemie International Edition, 44 (2005)3358.
- [3] E. H. Qua, P. R. Hornsby, H. S. S. Sharma, G Lyons, J. Mater. Sci., 46(2011) 6029.
- [4] V. K. Baheti, R. Abbasi, J. Militky, WJET. 9 (2012) 45.
- [5] A. Dufresne, Nanocellulose: From Nature to High Performance Tailored Materials, Walter de Gruyter GmbH & Co. KG, 2012
- [6] A. N. Nakagaito, H Yano, Appl Phys A Mater Sci Process,78 (2004) 547.
- [7] Ø Eriksen, K Syverud, Ø Gregersen, NORD PULP PAP RES J 23 (2008) 299.
- [8] T. Zimmermann, N. Bordeanu, E. Strub, Carbohydr. Polym. 79(2010) 1086.
- [9] B.M. Cherian, A. L. Leão, S. F. de Souza, S. Thomas, L. A. Pothan, M. Kottaisamy Carbohydr. Polym. 81 (2010)720.
- [10] K. Saelee, N, Yingkamhaeng, T. Nimchua, P. Sukyai, The 26th Annual Meeting of the Thai Society for Biotechnology and International Conference, 2014.
- [11] E. Abraham, B. Deepa, L. A. Pothan, M. Jacob, S. Thomas, R. Anandjiwala, Carbohydr. Polym. 86(2011)1468.
- [12] P. S. Morais , M. D. F. Rosa, M. M. Filho, L.D. Nascimento, D. M. Nascimento, A . R. Cassales 91(2013) 229.
- [13] E. Abraham,, B. Deepa,, L.A. Pothan, J. Cintil, S. Thomas, M.J. John, R., Anandjiwala S.S. Narine, Carbohydr. Polym. 92 (2013)1477.

- [14] B.M. Cherian, A. Leao, S. F. Souza, S. Thomas, L. A. Pothan, M. Kottaisamy, *Carbohydr. Polym.* 81 (2010) 720.
- [15] N. Reddy, & Y. Yang, *Polymer*. 46 (2005) 5494.
- [16] J. Lojewska, P. Miskowicz, T. Lojewski, L. M. Pronienwicz, *Polym. Degrad. Stab.* 88 (2005) 512.
- [17] J.X. Sun, F. Xu, X.F. Sun, B. Xiao, R.C. Sun, *Polym. Degrad. Stab.* 88 (2005) 521.
- [18] Z. P. Yang, S.W. Xu, X.L. Ma, S.Y. Wang, *Wood Sci. Technol.* 42 (2008) 621.
- [19] M.F. Rosa, E.S. Medeiros, J.A. Malmonge, K.S. Gregorski, D.F. Wood, L.H.C. Mattoso, G. Glenn, W.J. Orts, S.H. Imam, *Carbohydr. Polym.* 81 (2010) 83–92.
- [20] Y.P. Liu, H. Hu, *Polym.* 9 (2008) 735.
- [21] L. C. Segal, J. Jr Creely, A.E.J. Martin, C. M. Conrad, *Text. Res. J.* 29 (1959) 786.
- [22] C. J. Chirayil, J. Joy, L. Mathew, M. Mozetic, J. Koetz, S. Thomas, *Ind Crops Prod* 59(2014)27.

.....✎.....

Chapter 5

EFFECT OF NANOCELLULOSE ON MA-g-SEBS TOUGHENED PLA SYSTEM

Contents	5.1 Introduction
	5.2 Experimental
	5.3 Results and discussion
	5.4 Conclusion

Bionanocomposites of maleated Styrene Ethylene Butylene Styrene toughened PLA reinforced with nano cellulose were fabricated by twin screw extruder and tested for thermo-mechanical behaviour using injection molded specimen. Mechanical property evaluation showed that the composites containing nanocellulose exhibited higher modulus compared to virgin PLA and PLA binary blend system containing SEBS or MA-g-SEBS. The elongation of bionanocomposites was substantially increased, possibly due to good dispersion of the nanocellulose and plasticising effect of maleated SEBS. Morphological studies were also carried out to investigate the effect of nanocellulose on toughened PLA. The impact strength was also found to be higher compared to virgin PLA by the incorporation of nano cellulose to SEBS toughened PLA. Differential Scanning Calorimetry (DSC) measurements observed an increase in crystallization of PLA by heterogeneous nucleation effect of NFC.

5.1 Introduction

Renewable resource based materials are increasingly used as a potential source to produce biopolymers due to less energy consumption and liberating smaller amount of toxic pollutants over their life cycle than products from fossil fuels. PLA is one of the most resourceful and sustainable aliphatic thermoplastic polyester derived from 100% renewable sources like corn. PLA is now widely used for a myriad of different applications owing to its bio-compatibility, bio-degradability, less toxicity, vast range of mechanical properties. It has the ability to mold into different shapes and comparable performance to petroleum based plastics. Its increasing popularity in terms of biodegradability and compostability has extended its use from packaging to medical, textile, automotive, cosmetic and household applications. However, poor toughness (very brittle), thermal stability and less reactive side group of PLA restricts its use in both common and high end applications.

Many different approaches and research works are reported to overcome the short comings of PLA, which include chemical or physical modification, melt blending use of reinforcing agents like natural fibers, incorporation of nano fillers etc. The slow crystallisation rate of PLA hampers its widespread applications in the commercial point of view. Lower crystallinity in turn results in poor mechanical properties, poor thermal stability and even poor barrier properties. One of the methods to improve the crystallisation rate of PLA is by the incorporation of nano fillers. The inclusion of heterogeneous nucleating agents with high nucleation density enhances the faster crystallisation [1-2]. Nanocellulose

has the credibility to enhance the mechanical thermal and barrier properties of Polylactic acid due to their inherent mechanical strength, high aspect ratio, renewability and biodegradability [3 -6].

Nanofibrillated Cellulose (NFC) are cellulose fibers with diameter nano range and length of several micrometers. Different non-wood sources such as sugar beet pulp [7,8], wheat straw and soy hulls [9], sisal [10], bagasse [11], palm trees [12], carrots [13], luffa cylindrica [14], cotton [15] etc are already used to isolate nano cellulose. The first successful isolation of cellulose microfibrils was reported in 1983 by Turbak et al. and Herrick et al. [16, 17] using a Gaulin laboratory homogenizer but only after 20 years later only the prominent use of these materials were started.

In the last few years, research on nanocomposites containing NFC has been noticeably intensified which is reflected by a number of detailed reviews, providing a detailed description on this advanced research topic [18, 19]. Sanna Virtanen [20] et al. prepared chemically surface-modified nanofibrillated cellulose (NFC) and incorporated at low levels (0.5 to 3 wt%) as reinforcement in a polyvinyl alcohol (PVA) matrix. The modified NFC–PVA films prepared by solution casting showed improved mechanical performance and good optical properties. 1 wt. % addition of surface-functionalized NFC to PVA matrix increased the modulus and tensile strength of PVA by 474% and 224%, respectively. Yottha Srithep [21] prepared biodegradable nanocomposites using nanofibrillated cellulose (NFC) as reinforcement and poly (3-hydroxybutyrate-co-3-hydroxyvalerate, PHBV) as polymer matrix.

NFC increased the modulus of PHBV, whereas toughness decreased as the amount of NFC increased. The addition of NFC to PHBV increased the crystallization and glass transition temperatures, but caused the thermal degradation of PHBV due to residual moisture and hydroxyl group in the NFC.

Also, K. Larsson et al. [22], successfully made bionanocomposite material using PLA latex and NFC. NFC with high aspect ratio was produced by homogenization of enzymatic pre-treated wood pulp. Tensile strength, Young's modulus, and strain at break were all linearly increased with increasing NFC reinforcement.

Bulota et al. [23] fabricated composites from PLA and acetylated microfibrillated cellulose (MFC) via solvent casting. Mechanical testing showed that Young's modulus increased by approximately 70% and the tensile strength increased by approximately 60% at a fiber weight fraction of 20%. To overcome the drawbacks of natural fiber reinforced PLA composites, reinforcement with cellulose nanowhiskers or microcrystalline cellulose has been studied by melt extrusion compounding using twin screw extruders [24, 25]. However, as the kneading process resulted in the agglomeration of nano crystalline cellulose and whiskers as well as deterioration of the PLA, composites exhibiting higher strength than neat PLA could not be obtained.

In this chapter, the isolated nanofibrillated cellulose was added to SEBS toughened PLA, to investigate its effect on thermal and mechanical properties making it viable for automotive, semi-structural and electronic applications.

5.2 Experimental

5.2.1 Materials

The details of the polymers and chemicals used for the study are discussed in Chapter 2 (section 2.1)

5.2.2 Fabrication of Toughened PLA Nanocomposite

Maleic anhydride grafted SEBS (10 wt. %) was used as toughening agents to study their effect for its toughness on PLA. PLA and nano cellulose were predried at 80°C for 6 hrs to remove the moisture content if any before extrusion. Maleated SEBS, nano cellulose and PLA were pre-mixed in a zip lock bag and then later were melt mixed in a corotating twin screw extruder (Specific ZV 20) equipped with a volumetric feeder and a strand pelletizer. The temperature was set at 165-195 °C and the screw speed was set at 14 rpm. PLA bio nanocomposites were prepared by the addition of 1, 2 and 3 wt % nanocellulose to PLA toughened by using maleated SEBS. The different percentage compositions are given in Table 5.1.

Table 5.1 Percentage composition of the samples

Sample code	PLA (wt%)	MA-g-SEBS (wt%)	Nanocellulose (NFC) (wt%)
PLA	100	-	-
PLSEGNC-1	90	10	1
PLSEGNC-2	90	10	2
PLSEGNC-3	90	10	3

5.2.3 Analysis and Characterisation

5.2.3.1 X ray Diffraction (XRD)

Prepared bionanocomposites were analysed using Bruker AXSD8 Advance powder X-ray diffractometer. The X-ray diffraction pattern was recorded in a range of 0 to 80° with a step of 0.020 and step time 65.6s. The wavelength of the Cu/K α rod source was 0.15406 nm and the spectra were obtained at 35mA with an accelerating voltage of 40kV.

5.2.3.2 Scanning Electron Microscopy (SEM)

The SEM of impact fractured specimens was carried out using JEOL-6390LV (Germany). The fractured surface of the specimen was coated with platinum before SEM study.

5.2.3.3 Transmission Electron Microscopy (TEM)

The structure of nanocomposites and nano fibrillated dispersion was visually observed using transmission electron microscopy (TEM). The electron microscope JEOL JEM- 2100 Lab -6 was operated at 200 kV. The ultrathin size samples of less than 100 nm for the imaging have been prepared using a Cryo Leica EM UC6 instrument (Leica Microsystems, Switzerland) with diamond knife and viewed without staining.

5.2.3.4 Thermal Characterisation

DSC Analysis:

Thermal characterisation of all the composites were performed by DSC analysis using Q20 model TA instruments, Walters, USA with a double cycle of heating from 30 to 210 °C at 10 °C/min separated by a single cooling cycle at 10 °C/min kept at isothermal for 5 minutes at 210

and 30°C. Glass transition temperature, crystallisation temperature, melting point, crystallisation enthalpy and melting enthalpy were determined by heating and cooling scans. The percentage crystallinity of PLA and its bionanocomposites was determined using equation 5.1.

$$\frac{\Delta H_m - \Delta H_{cc}}{\Delta H_m \left(1 - \text{wt } \% \frac{\text{NFC}}{100}\right)} \times 100 \dots\dots\dots (5.1)$$

Where ΔH_m is the enthalpy of melting and ΔH_o is the enthalpy of crystallisation of 100% crystalline PLA (93.7 J /g) and NFC is nanofibrillated cellulose.

Thermo-gravimetric Analysis (TGA):

The thermal stability of the samples were investigated with Q50 , TA instruments, Walters, USA under nitrogen atmosphere from room temperature to 600 °C at a heating rate of 10 °C /min.

5.2.3.5 Testing of Mechanical Properties

The tensile properties of all the PLA/ MA-g-SEBS bionanocomposites were conducted as per ASTM D-638 (Shimadzu Autograph model AG-IS 50KN) using injection molded dumb bell-shaped specimens (165 mm × 13mm × 3.2 mm). The cross-head speed was fixed at 10 mm/min. Total of five specimens were tested and its average value was reported.

The Izod impact strength tests were carried out according to ASTM D-256 using Tinius Olsen IT 504 impact tester, USA. Five rectangular 347specimens with dimensions of 63.5 mm × 12.7 mm (notch depth of 2.54 mm and notch angle of 45⁰) were tested and its average value was reported.

5.3 Results and Discussions

5.3.1 XRD analysis of PLA, toughened PLA and its nanocomposites:

In fig. 5.1 (a) Two diffraction peaks were clearly detected at around 17.32° and 19.71° that corresponds to the typical α -crystallographic form of the crystalline phase of PLA described as pseudo-orthorhombic unit cell [26]. Also, the composite peaks at 16.75° and 19.04° corresponds to the combination of peaks for nano cellulose and polylactic acid (Fig. 5.1 b).

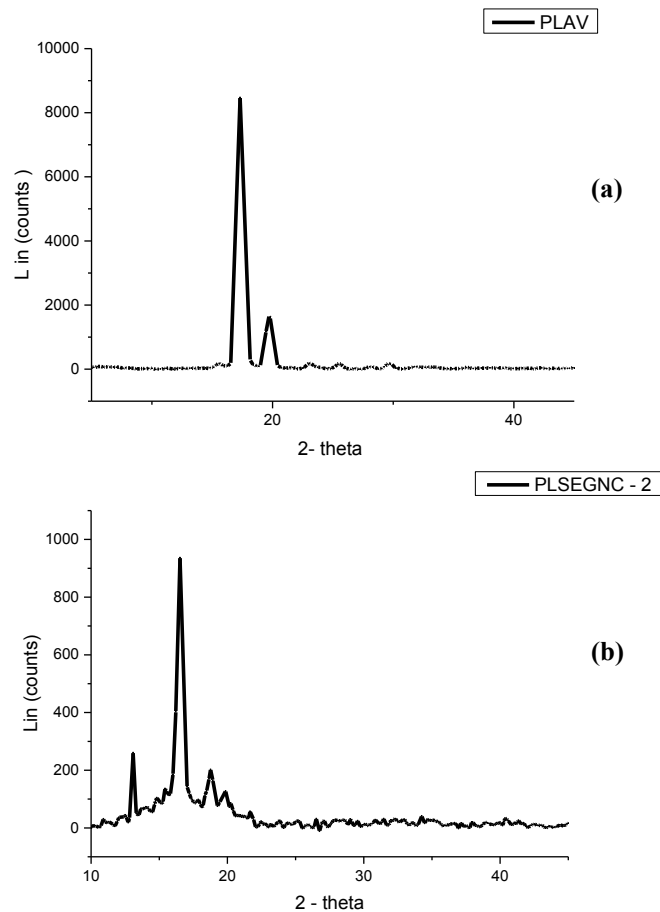


Figure 5.1 XRD of (a) virgin PLA (PLAV) (b) PLA bionanocomposite (PLSEGNC-2)

5.3.2 SEM Analysis of nanocomposites

Fig.5.2 shows the SEM images of PLA and maleated SEBS toughened PLA composites with different nano cellulose loading. The fracture surface of PLA and maleated sebs/cellulose toughened samples exhibited a distinct difference because of a plasticizing effect due to the presence of maleated SEBS[27]. At low concentration of nanocellulose loading (1 wt%), spherical rich domains of maleated SEBS along with PLA matrix was found more prominent.

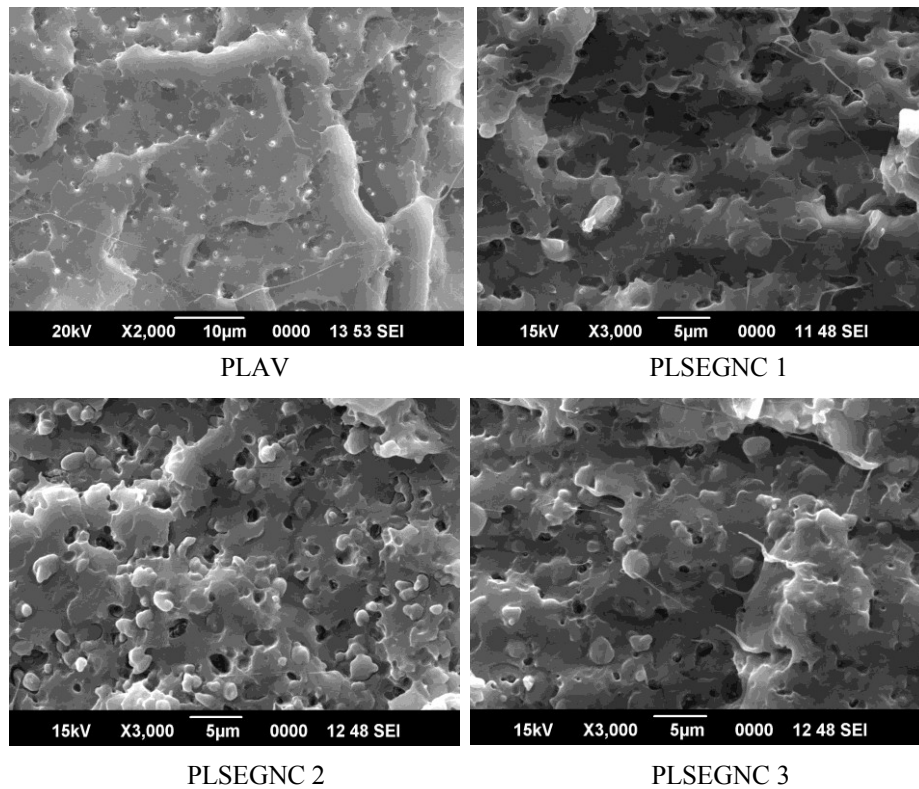
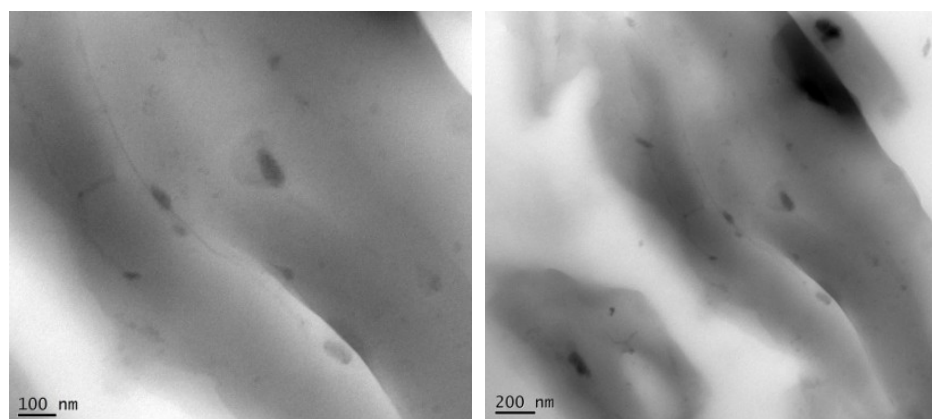


Figure 5.2 SEM Analysis of a) PLA b) PLSEGNC-1 c) PLSEGNC -2 d) PLSEGNC-3 PLSEGNC –PLA/MA-g-SEBS/Nanofibrillated cellulose

However, with the loading of 2wt% of cellulose nanofiber, spherical domains were comparatively smaller than other composition 1 wt % and 3 wt % filler loading may be due to improved interface adhesion between maleated SEBS, PLA and NFC. Surface traces and cracks could also be observed in PLSEGNC 1 and 3, which evidenced the more brittle tendency of this system to break. The observed morphological results were consistent with tensile impact test tests.

5.3.3 TEM analysis of PLA nano composites

Figure 5.3 shows the TEM images of maleated SEBS toughened polylactic acid nano composites taken at 100 nm and 200 nm magnification. Nano dispersed fibrils can be seen dispersed in toughened polylactic acid matrix. Dark grey region can be attributed as maleated Styrene Ethylene Butylene Styrene used as the impact modifier and grey regions corresponds to cellulose nano fibrils.



PLSEGNC-2 at 100 nm

PLSEGNC-2 at 200 nm

Figure 5.3 TEM analysis of toughened PLA nanocomposites under different magnifications

5.3.4 Mechanical properties

The mechanical properties of PLA and its nanocomposites are depicted in Figure 5.4. The incorporation of nano fibrillated cellulose into the toughened PLA did not bring any improvement in tensile strength due to poor stress transfer between cellulose fiber and the matrix. However, the tensile modulus was increased from 2888 MPa to 3080 MPa by the addition of 2 wt% nano cellulose. This increase in the modulus can be explained by the improved interface between PLA and NFC [28, 29,30, 31]. Also the percentage crystallinity effect of synthesised nano cellulose contributed to the stiffness of the biocomposite.

MA grafted SEBS substantially improved their strain-at-break and toughness for PLA/MA-g-SEBS system. The strain was increased by 428%, 502 % and 512% respectively by the addition of 1, 2 and wt 3% NFC respectively through MA-g-SEBS compatibilization, PLA was more compatible with hydrophilic nanocellulose. Therefore the number and size of the nanoparticle agglomerates were decreased, and the probability of premature sample failures initiated by these agglomerates was reduced accordingly. Therefore, an increase in average elongation of the samples was obtained [32]. The improvement in tensile toughness was especially important for the PLA/MA-g-SEBS binary system due to the better compatibilisation effect of maleated SEBS. The toughness increase by MA grafting afforded the NFC composites better-balanced overall performance with slight improvement in impact property. The impact property of all the three nanocomposites were found to be lesser than PLA/MA-g –SEBS blend system .The overall impact property of all the nanocomposites was higher than virgin PLA.

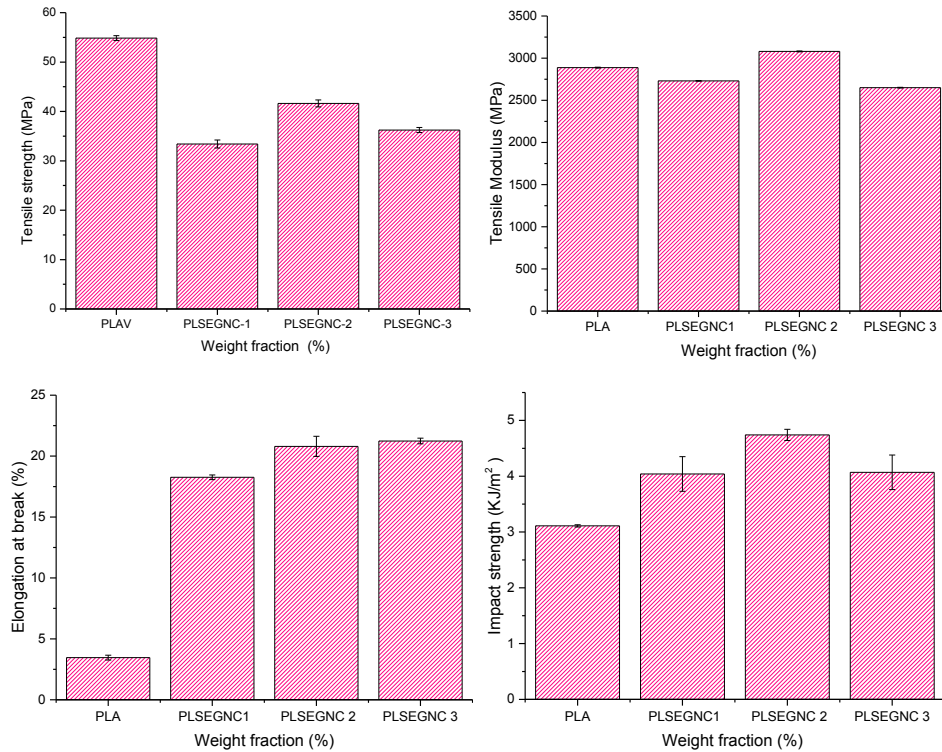


Figure 5.4 Mechanical Properties of PLA, PLA / MA-SEBS nanocomposites

5.3.5 Thermal properties

Differential Scanning Calorimetry (DSC)

DSC thermographs for PLA, PLA /SEBS and PLA/MA-g-SEBS and PLA/ MA-SEBS / nanocellulose composites are presented in Figure 5.5. The thermal properties such as melting, crystallization and glass transition temperature of PLA and PLA-SEBS nanocomposites are considered from the DSC thermograph obtained during the second heating cycle at a heating ramp of 10 °C/min and are reported in Table 5.2. In non-isothermal cold crystallization progression, the absence of

double melting peak is a sign of existence of stable crystal formation in PLA. This might be owing to the fact that homogeneous nucleation process took place in PLA.

Table 5.2 DSC characteristics of neat PLA and PLA/MA-g-SEBS nanocomposites

Materials designation	Tg (°C)	Tc (°C)	Tm (°C)	ΔHc ($\frac{J}{g}$)	ΔHm ($\frac{J}{g}$)	χc(%)
PLA	62.38	105.55	169.56	23.63	32.63	34.86
PLSEGNC1	56.98	101.61	171.39	22.07	29.4	31.41
PLSEGNC2	61.14	99.00	169.70	23.03	42.6	45.51
PLSEGNC 3	57.27	100.02	170.92	32.13	46.52	49.7

It can be seen from the table that crystallization temperature decreases with respect to increment in loading of nano cellulose in MA grafted SEBS - PLA matrix. This in turn reveals good compatibility between nanocellulose and MA-g- SEBS / PLA matrix [33]. Also, nanocellulose acts as a nucleating agent which initiates crystallization phenomenon at a lower T_{cc} resulting in the formation of stable as well as thick crystals. The lower T_{cc} means that less energy is required to achieve the desired degree of crystallinity[34]. The glass transition temperature of PLA also decreased by the incorporation of nano cellulose into the toughened matrix indicating the plasticising effect of nano cellulose. The non-isothermal melt crystallization temperature (T_{mc}) for PLA and PLA nanocomposites are reported in Table 5.2. It can be seen from the table that T_{mc} for PLA-nanocomposites tends to increase with nanocellulose loading as compared to neat PLA. These

results indicate that nanocellulose enhances the crystallization of PLA by heterogeneous nucleation effect.

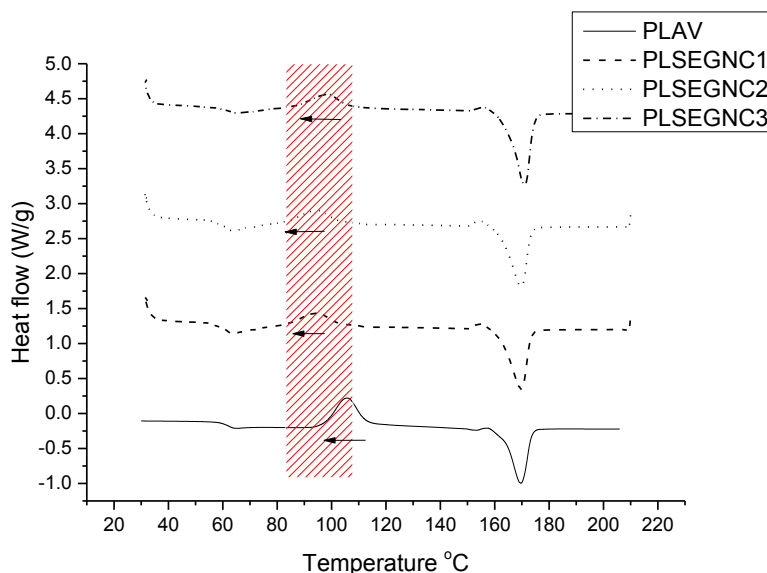


Figure 5.5 DSC curves for PLA, PLA / MA-SEBS nanocomposites

Therogravimetric analysis (TGA)

The TGA curves of neat PLA, PLA/SEBS and PLA/MA-g-SEBS and its nanocomposites are shown in Fig .5.6. TGA results are tabulated in Table 5.3. As evident from Table, SEBS is thermally stable than PLA with an onset degradation temperature of 419 °C. The onset degradation of virgin PLA was found to be 347 °C. T_{onset} , T_{50} and T_{95} of all the composites was lower than neat PLA. This may be due to lesser compatibility between maleic anhydride group and terminal groups of PLA in the presence of nano cellulose.

Table 5.3 TGA data of neat PLA and PLA/MA-g-SEBS nanocomposites

Materials designation	Thermal characteristics		
	T ₅₀ (°C)	T _{onset} (°C)	T _{peak} (°C)
PLA	365.14	347.64	371.18
SEBS	442.46	419.84	453.99
PLSEGNC-1	326.94	307.56	332.61
PLSEGNC-2	329.21	309.59	334.31
PLSEGNC-3	326.94	308.34	333.75

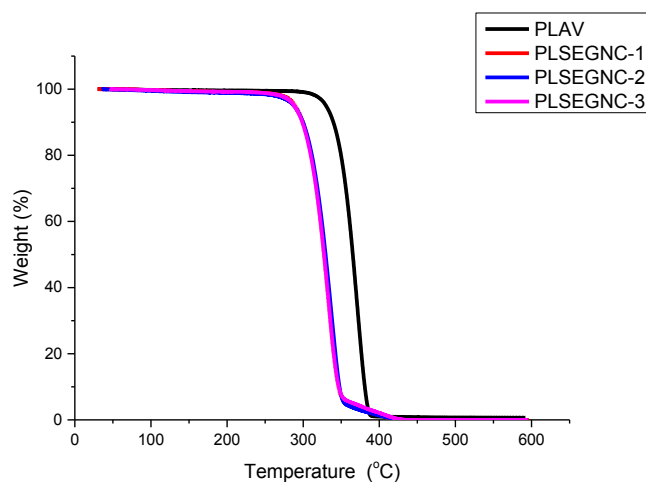


Figure 5.6 TGA curves for PLA, PLA/ MA-SEBS nanocomposites

5.4 Conclusions

PLA bionanocomposites containing both MA-g-SEBS and nano fibrillated cellulose (NFC) were prepared and its effect on toughening of PLA was also studied. The composites containing nanocellulose

exhibited higher modulus compared to virgin PLA and PLA binary blend system containing SEBS or MA-g-SEBS. Also the percentage crystallinity of synthesised nano cellulose contributed to the stiffness of the biocomposite. The increment in percentage elongation was also observed for the bionanocomposites. The impact strength was also found to be higher compared to virgin PLA. DSC measurements revealed the enhancement in crystallization of PLA by heterogeneous nucleation effect of NFC.

References

- [1] A.M. Garcia, S. Hooshmand, M. Skrifvars, J.M. Kenny, K. Oksman, L Peponi, *RSC Adv.* 6 (2016) 9221.
- [2] M. P. Arrieta, E.F. Fortunati, E. Dominici, J.L. Opezand , J.M. Kenny, *Carbohydr. Polym.* 107 (2014) 16.
- [3] E. Fortunati, M. Peltzer, I. Armentano, L. Torre, A. Jim´enez, J.M. Kenny, *Carbohydr. Polym.* 90 (2012) 948.
- [4] E. Fortunati, D. Puglia, F. Luzi, C. Santulli, J.M. Kenny, L. Torre, *Carbohydr. Polym.* 97 (2013) 825.
- [5] N. Johar, I. Ahmad, A. Dufresne, *Ind. Crops Prod.* 37 (2012) 93.
- [6] F. Lu, H. Yu, C. Yan, J. Yao, *RSC Adv.* 6 (2016) 46008.
- [7] E. Dinand, A. Maureaux, Chanzy, Vincent, M.R. Vignon, *Eur. Pat.* 0726356, 14 August 1996.
- [8] Y. Habibi, M. Vignon, *Cellulose.* (2008) 15177.
- [9] A Alemdar, M Sain, *Bioresour. Technol.* 99 (2008) 1664.
- [10] G. Siqueira, J. Bras, A. Dufresne, *Bio macromolecules.* 10 (2008) 10425.

- [11] D. Bhattacharya, L.T. Germinario, W.T. Winter, *Carbohydr. Polym* 73 (2008) 371.
- [12] A. Bendahou, H. Kaddami, A. Dufresne, *Eur. Polym. J.*46 (2010) 609.
- [13] G. Siqueira, S. Tadokoro, A.P. Mathew, K. Oksman, Carrot Nanofibers vs. Wood Pulp Nanofibers: Morphological and Mechanical Properties. Proceedings of the 2010 TAPPI International Conference on Nanotechnology for the Forest Product Industry, Espoo, Finland, 27–29 September 2010.
- [14] G. Siqueira, J. Bras, A. Dufresne, *Bioresources*. 5 (2010) 727.
- [15] M. A. Mamun , M. Rahman , G. M. Arifuzzaman Khan, M. H. Uddin, S. M. Abdur Razzaque , J. A. Foisal , M. Hasanuzzaman, S. Rahman, M. S. Alam, *CS J.* 16 (2016) 1.
- [16] F.W. Herrick, R.L Casebier, J.K Hamilton, K.R. Sandberg, *J. Appl. Polym. Sci.* 28 (1983) 797.
- [17] A.F Turbak, F.W. Snyder, K.R. Sandberg, *J. Appl. Polym. Sci.* 28 (1983) 815.
- [18] M.A. Hubbe, O.J.Rojas, L.A. Lucia, M. Sain Biores, *Bioresurces*,3 (2008)929.
- [19] I. Siró, D. Plackett, *Cellulose*. 17 (2010) 459.
- [20] S.Virtanen, J. Vartianen, H. Setälä, T. Tammelin, S. Vuoti, *RSC Adv.* 4 (2014) 11343.
- [21] Y. Srithep, T. Ellingham, J. Peng, R. Sabo, C. Clemons, L.S. Turng , S. Pilla, *Polym. Degrad. Stab.* 98 (2013) 1439.
- [22] K. Larsson L. A. Berglund, M. Ankerfors, T Lindström, *J. App. Polym. Sc.*125 (2012) 2460.
- [23] M. Bulota, K. Kreitsmann, M. Hughes, J. Paltakari, *J. App. Polym. Sc.* 126(2012) E449–E458.

- [24] A.P. Mathew, K.Oksman M. Sain, J.Appl. Polym. Sci. 97 (2005) 2014.
- [25] K. Oksman, A. P. Mathew, D. Bondeson, I. Kvien, Comp Sci. Technol. 66 (2006) 2776.
- [26] N. Burgos, P. Verónica, Martino, A. Jiménez, Polym.Degrad..Stab. 98 (2013) 651.
- [27] W.Yang, F. Dominici, E. Fortunati, J.M. Kenny, D.Puglia, RSC Advn, 5 (2015)32350.
- [28] M. S. Huda, L.T. Drzal, M. Misra, Ind. Eng. Chem. Res. 44 (2005) 5593.
- [29] R.F Landel, L.E. Nielsen, Mechanical Properties of Polymers and Composites, 2nd ed.; Taylor & Francis: London, UK, 1993.
- [30] Z. Jin, K.P. Pramoda, G. Xu, S.H. Goh, Chem. Phys. Lett. 337 (2001) 43.
- [31] A.M. Diez-Pascual, J.W. Guan, B. Simard, M.A. Gomez-Fatou, Compos. Part A Appl. Sci. Manuf. 43 (2012) 997.
- [32] J.H. Wu, M-S Yen, C.W. Chen, M. C. Kuo, Polym Environ 24 (2016) 318.
- [33] A.H. Pei, Q. Zhou, L.A. Berglund, Compos. Sci. Technol. 70 (2010) 815.
- [34] R.B. Valapa, G. Pugazhenthii, V. Katiyar, J. Appl. Polym. Sci. 132 (2015) 41320.

.....✂.....

Chapter 6

POLYLACTIC ACID (PLA)/ ETHYLENE VINYL ACETATE (EVA) BLENDS

Contents

- 6.1 Introduction
- 6.2 Experimental
- 6.3 Results and Discussion
- 6.4 Conclusion

In this chapter, a possible route to improve the toughness of PLA has been investigated by blending with ethylene vinyl acetate with a vinyl acetate content of 40 %. EVA is a copolymer of ethylene and vinyl acetate units with many benefits of excellent flexibility, toughness, light-transmission properties, good elongation at break, and good adhesion characteristics. Therefore, a systematic investigation on the mechanical properties, thermal degradation and crystallization behavior for PLA/EVA blends was carried out. The impact strength of binary blends of PLA-EVA was found to increase significantly by 176% for 15 wt. % of EVA compared to virgin PLA. This is due to the strong interfacial adhesion among PLA and EVA resulting in brittle to ductile transition. Scanning Electron Microscopy (SEM) analysis for impact fractured surfaces of binary blends of PLA implied the toughening effect of PLA by EVA. Thermogravimetry analysis (TGA) results revealed that the activation energy of PLA-EVA blends decreased with increase in EVA content in the PLA matrix. While, Differential Scanning Calorimetry (DSC) results obtained for PLA-EVA blends revealed the improvement in crystallinity when compared with neat PLA. The effect of EVA on non-isothermal melt crystallization kinetics of PLA was also examined via DSC at various heating rates. Decreasing trend in the $t_{1/2}$ values indicated the faster rate of crystallization mechanism after addition of EVA in the PLA matrix.

6.1 Introduction

Among all the biodegradable plastics, PLA has been considered as an effective alternative that can serve as a substitute for conventional polymers. However, PLA exhibits limitations like lower toughness, and slower rate of crystallization which limit its real time applications. To overcome these limitations, nano materials such as cellulose nano crystals (CNCs), [1] food additive, [2] carbon nanotubes (CNTs), [3] graphene (GR), [4] layered silicates and clays are used as reinforcements in the PLA matrix [5]. However, if incompatibility between PLA and the reinforcing agents affect the mechanical properties.

The properties of PLA can be improved by blending it with poly(hydroxyalkanoate)s (PHAs), [6] poly(caprolactone) (PCL), [7,8] poly(butylene succinate) (PBS), [9,10] poly(butylene adipate-co-terephthalate) (PBAT), [11,12] poly(ethylene-co-glycidyl methacrylate) (EGMA), [13] and poly(ethylene-co-octene) [14]. The utilization of PLA blends as composite materials by the addition of reinforcements provides several benefits such as improvement in terms of (i) processability, (ii) wide variety of end-use properties as well as applications. In addition to this, blending technique helps in considerable reduction in the cost for resultant composite materials. However, blending of PLA with the above mentioned polymers resulted in the formation of immiscible blends. This in turn, limited the enhancement in toughening properties, which is due to the action of physical blending alone. Therefore, in order to achieve high toughness, compatibilizers were utilized with the aim to avoid the inhomogeneity or phase separation behavior for the PLA blends.

The most economical way to enhance the toughening properties of PLA is to select the copolymer that exhibits compatibility with PLA in the absence of external or additional compatibilizer. Ethylene Vinyl Acetate (EVA) is one of the prospective copolymer which is found to be partially compatible with PLA matrix. The EVA co-polymer offers the advantage of both rubbery and resin characteristics, which are considered to be essential for enhancing the toughening properties of PLA. In simple terms, the toughening properties of PLA can be enhanced if there is good interfacial adhesion between PLA and the copolymer selected. Studies on PLA blends with EVA as toughening agents were reported. When ethylene-octene (EO) was used as a copolymer with PLA, it was found that the presence of EO in the PLA matrix led to inhomogeneity behavior of the blend due to the incompatibility nature of EO with the PLA. However, in case of EVA co-polymer, it was found that the compatibility with PLA was noticed to increase with respect to vinyl acetate (VA) content in the PLA matrix. For 40-50 wt. % VA content, the toughening properties were found to be enhanced by ~30%. EVA with 40 % vinyl acetate content is selected as the copolymer and the effect of EVA content on the toughening properties of PLA is investigated in detail. Also, the detailed studies on PLA/EVA blends and its thermal degradation kinetics are not reported. In this study, the influence of EVA loading on the thermal degradation behavior of PLA-EVA blends is also investigated. The kinetic studies for PLA-EVA blends are performed using Flynn-Wall-Ozawa and Kissinger models. Also, quantitative assessment of non-isothermal melt crystallization behavior for PLA-EVA blends is carried out in the present work. The crystallization rate parameters are determined using Avrami model.

6.2 Experimental

6.2.1 Materials

The details of the polymers and chemicals used for the study are discussed in Chapter 2 (sections 2.1.1, 2.1.2).

6.2.2 Preparation of PLA-EVA Blends

Virgin PLA was dried in a hot air oven at 80°C for 6 h. The PLA with different EVA content (PLA: EVA= 95:5, 90:10, 85:15 and 80:20) were melt blended in a microprocessor controlled twin screw co-rotating extruder with L/D ratio of 40:1. The processing temperature was optimized in the range of 165-190 °C and the screw speed of 60 rpm was maintained. The resulted extrudate strands were quenched in cold water and pelletized. The extruded granules were subjected to drying in a hot-air oven at 60 °C for 4 hrs and made into test specimen as per ASTM standard by injection moulding machine ((Electronica Endura 90). The moulding temperature and injection pressure were maintained in the range of 175-190 °C and 110 - 120 bar, respectively. The material designation and composition of PLA/EVA blends are presented in Table 6.1.

Table 6.1 Material designation and composition of PLA, PLA-EVA blends

Sample Name	PLA%	EVA%
PLA	100	-
PLA-EVA-5	95	5
PLA-EVA 10	90	10
PLA-EVA 15	85	15
PLA-EVA -20	80	20

6.2.3 Characterization

6.2.3.1 Scanning Electron Microscopy

The morphological analysis for tensile fractured specimens was carried out by using a scanning electron microscopy (Model: JEOL-6390LV, Make: Germany). Before subjecting to SEM analysis, the fractured samples were sputtered with platinum and dried for a period of 30 min.

6.2.3.2 Mechanical Properties

a) Tensile and flexural properties

The tensile properties for both PLA and PLA-EVA blends were determined at room temperature using Shimadzu Autograph (model: AG-IS 50KN) tensile tester as per ASTM D-638. Injection molded dumb bell-shaped specimens (165 mm × 13 mm × 3.2 mm) were used with cross-head speed of 50 mm/min for the analysis. The flexural properties for PLA and PLA-EVA blends were determined by three-point bending test using Universal testing machine and the analysis was performed in accordance with ASTM D790-Type B. The span length was set at about 96 mm. The testing speed was set at 3 mm/min and the flexural properties were determined at room temperature and specimen dimensions were 127 mm x 12.5 mm x 6.4 mm.

b) Impact strength properties

The Izod impact strength test for PLA and PLA-EVA blends were carried out according to ASTM D-256 using a Tinius Olsen IT 504 impact tester, USA. The specimen dimensions were of 63.5 mm × 12.7 mm with a notch depth of 2.54 mm and notch angle of 45°.

6.2.3.3 Thermal Properties

a) Thermo-gravimetric Analysis (TGA)

The thermal analysis for PLA and PLA-EVA blends were carried out using TGA analyzer (Model: Q50, Make: TA instruments, Walter, USA) in the temperature range of 30 to 600 °C at a heating rate of 10 °C /min under nitrogen atmosphere. To investigate the thermal degradation kinetics for PLA and PLA-EVA blends, TGA analysis was also carried out at different heating rates (10, 20, 30 and 40 °C/min).

b) DSC Analysis

Glass transition temperature (T_g), cold and melt crystallization temperatures (T_{cc} and T_{mc}), melting point (T_m), cold and melt crystallization enthalpy (ΔH_{cc} and ΔH_{mc}) and melting enthalpy (ΔH_m) for PLA and PLA-EVA blends were determined using DSC analysis (Model: Q50, Make: TA instruments, Walter, USA). Both PLA and PLA-EVA blends were subjected to double heating cycle in which the first heating cycle was performed in the temperature range of 35 to 210 °C at a heating rate of 10 °C/min. At 210 °C, the samples were kept at isothermal condition for 5 min. Followed by this, the samples were allowed to cool at a cooling rate of 10 °C/min. At 35 °C, the samples were kept at isothermal condition for 5 min. To investigate the non-isothermal melt crystallization kinetics, DSC analysis for PLA and PLA-EVA blends were also carried out at different heating rates (2.5, 5, 7.5 and 10 °C/min).

6.3 Results and Discussion

6.3.1 Scanning Electron Microscopy Analysis

The photo micrographs presented in Figure 6.1 shows the morphology of virgin PLA and PLA/EVA blends. The mechanical properties of the blends can be correlated with the morphology of the blends.

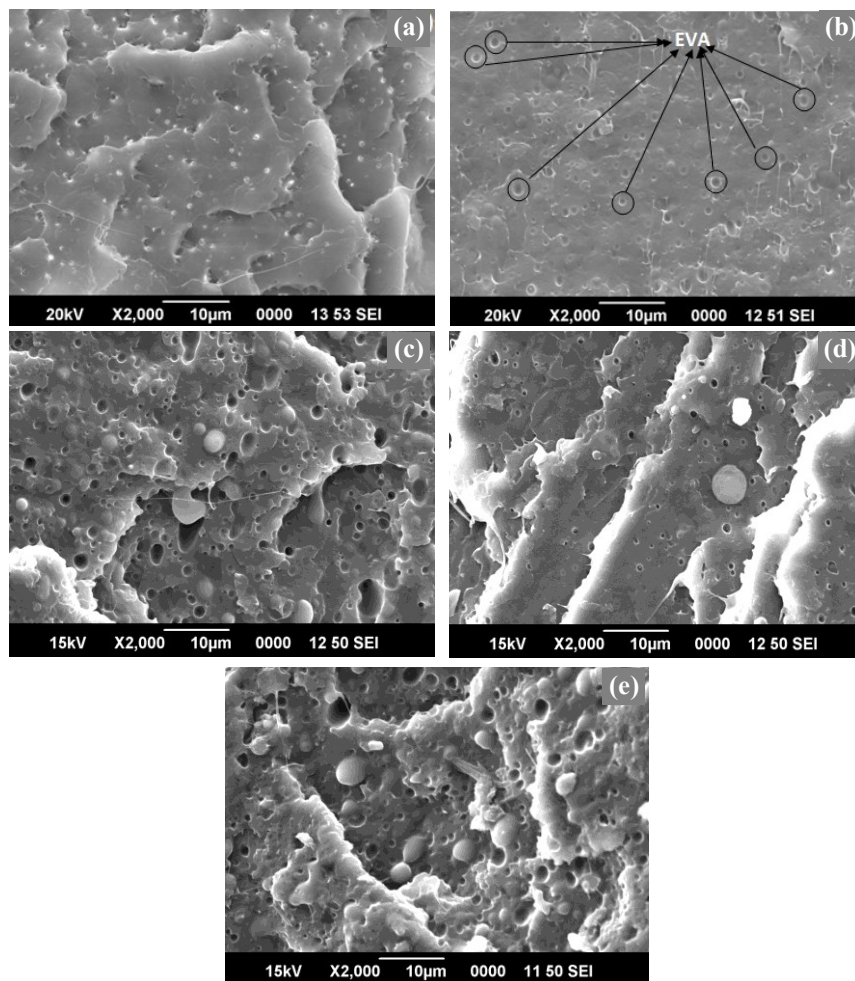


Figure 6.1. SEM images of (a) Neat PLA and (b) PLA/EVA (5wt %) (c) PLA/EVA (10wt %) (d) PLA/EVA (15wt %) (e) PLA/EVA (20 wt %)

It can be seen that surface of the dispersed phase has become rough by the addition of EVA. This indicates greater adhesion between PLA and toughening agent. The observation supports the increase in impact strength. The function of the rubber domains is not only to share the load with the matrix, but to contribute to energy dissipation and to prevent catastrophic cracks[15]. It is clear that the rubber domains were able to deflect the propagation of cracks which can contribute to energy dissipation responsible for toughness enhancement.

6.3.2 Mechanical Properties

The mechanical properties such as tensile strength, tensile modulus, percentage elongation-at-break, flexural strength, flexural modulus and impact strength values obtained for both PLA and PLA/EVA blends are presented in Table 6.2. Five samples were tested and its average value was taken. Five samples have been taken for each analysis and the data reported are from the average of five and is statistically analysed by standard deviation method. It can be seen from the Table that the tensile strength, tensile modulus, flexural strength and flexural modulus decreased with respect to increase in EVA content in the PLA matrix. This decrement can be attributed to the reduction in stiffness which is supposed to be due to the increase in flexibility induced by the addition of EVA in the PLA matrix. Thus, reduction in the tensile and flexural values is indicative of increase in flexibility caused by EVA present in the PLA matrix. Also, EVA being elastomeric in nature with high molecular weight, this phenomenon helps in enhancing the flexibility for PLA-EVA blends. Percentage elongation-at-break is found to be higher

than pristine PLA up to 15 wt. % of EVA content and gradually decreased for 20 wt. % of the EVA elastomer.

The impact strength of neat PLA is only 3.1 kJ/ m², and the samples are found to be fractured clearly in a brittle manner. The impact strength for all the compositions of PLA-EVA blends is higher than that of neat PLA. The addition of EVA resulted in greater toughness and the brittle-ductile transition is achieved at higher percentage of EVA. This may be due to the strong interfacial adhesion between the PLA matrix and EVA elastomer resulting in brittle to ductile transition. The elastomeric nature of EVA enabled to absorb impact energy and acted as stress concentrator during impact deformation. This in turn, retards the crack initiation and propagation and subsequently led to better toughness for PLA-EVA blends (85:15)[15]. The overall improvement in percentage elongation-at-break and impact toughness with respect to increase in EVA content may be due to increase in particle size of EVA, which in turn reduces the interfacial tension. The subsequent reduction in the interfacial tension might have helped in enhancing the compatibility between EVA and PLA matrix.

Table 6.2 Mechanical properties of pure PLA and PLA-EVA blends

Sample Name	Tensile strength (MPa)	Tensile modulus (MPa)	Elongation at break (%)	Flexural strength (MPa)	Flexural modulus (MPa)	Impact strength (kJ/m ²)
PLA	54.9±0.5	2883.7±0.5	3.5±0.2	107.5±0.59	3600±0.47	3.1±0.02
PLEV-5	50.18±1.5	1213±2	13.85±0.47	71.97±0.92	3012±0.71	4.11±0.06
PLEV-10	48.42±1	1050±0.83	27±0.44	66.69±0.56	2666±1.5	4.65±0.05
PLEV-15	37.1±0.78	1012±0.68	53.3±0.77	58.99±0.36	2379±1.7	8.55±0.17
PLEV-20	38.24±0.56	1016±0.42	16.12±0.43	58.13±0.40	2296.7±0.53	8.28±0.12

PLEV-PLA/EVA

6.3.3 Thermal Properties

Thermogravimetry analysis

The TGA curves for neat PLA and PLA-EVA blends are shown in Fig. 6.2. It can be seen from the Figure that neat PLA demonstrates single stage of degradation. The decomposition process which takes place in the temperature regime of 300-350 °C is due to the intramolecular transesterification reaction. In case of PLA-EVA blends, the TGA profile shows three stage decomposition processes. The first stage of degradation occurs in the temperature range of 300-350 °C, which corresponds to the decomposition of PLA backbone via back-biting reaction. The second stage of degradation can be observed in the temperature regime of 350-410 °C [16]. This is due to the removal of acetic acid from the EVA copolymer present in the blend [16]. In addition to this, the final stage of degradation can be observed for PLA-EVA blends in the temperature conditions ranging from 410-460 °C, which is mainly due to the escape of unsaturated butene as well as ethylene compounds in vapor form.

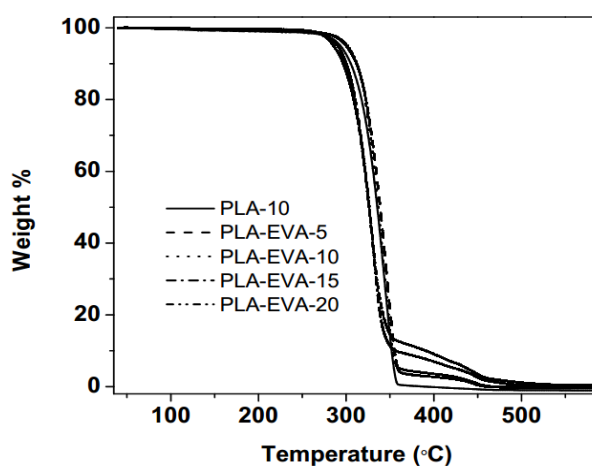


Figure 6.2 TGA curve for PLA and PLA-EVA blends obtained at 10 °C/min

The degradation profile of PLA-EVA blends is compared with neat PLA at two different degradation points i.e., the temperature at which degradation starts (T_{onset}) and temperature at which 50% weight loss occurs ($T_{50\%}$). In addition to this, the temperature at which maximum rate (T_{max}) of degradation occurs is interpolated from derivative weight loss curve for both PLA and PLA-EVA blends. The degradation temperature (T_{onset} , $T_{50\%}$ and T_{max}) results for EVA, PLA and PLA-EVA blends are tabulated in Table 6.3. It can be seen from Table that the onset temperature for thermal degradation (T_{onset}) of PLA and EVA is 347 °C and 308 °C, respectively. The temperature at which maximum degradation (T_{max}) takes place for PLA and EVA is 371 °C and 446 °C, respectively. It can be seen from the Table that the addition of EVA in the PLA matrix leads to slight decrement in T_{onset} , $T_{50\%}$ and T_{max} values as compared to neat PLA. However, the final decomposition temperature for PLA-EVA-20 blend is noticed to be 594 °C, at which the percentage char residue approached zero. While, in case of neat PLA, final decomposition temperature is observed to be at 475 °C with zero percentage char residue. This clearly indicates that the addition of EVA in the PLA matrix helps in sustaining the thermal degradation process by delaying the char formation.

Table 6.3 T_{onset} , $T_{50\%}$ and T_{max} of PLA and PLA-EVA blends

S. No.	Sample Name	T_{50} (°C)	T_{onset} (°C)	T_{max} (°C)
1	EVA	437	308	446
2	PLA	364	347	371
3	PLA-EVA-5	336	318	341
4	PLA-EVA-10	336	318	341
5	PLA-EVA-15	325	307	332
6	PLA-EVA-20	326	307	331

6.3.4 Thermal degradation Kinetics of PLA and PLA-EVA blends

The non-isothermal thermographs of TGA and DTG curves for PLA and PLA-EVA blends at four different heating rates (10, 20, 30, 40 °C/min) in inert atmosphere are shown in Fig. 6.3.

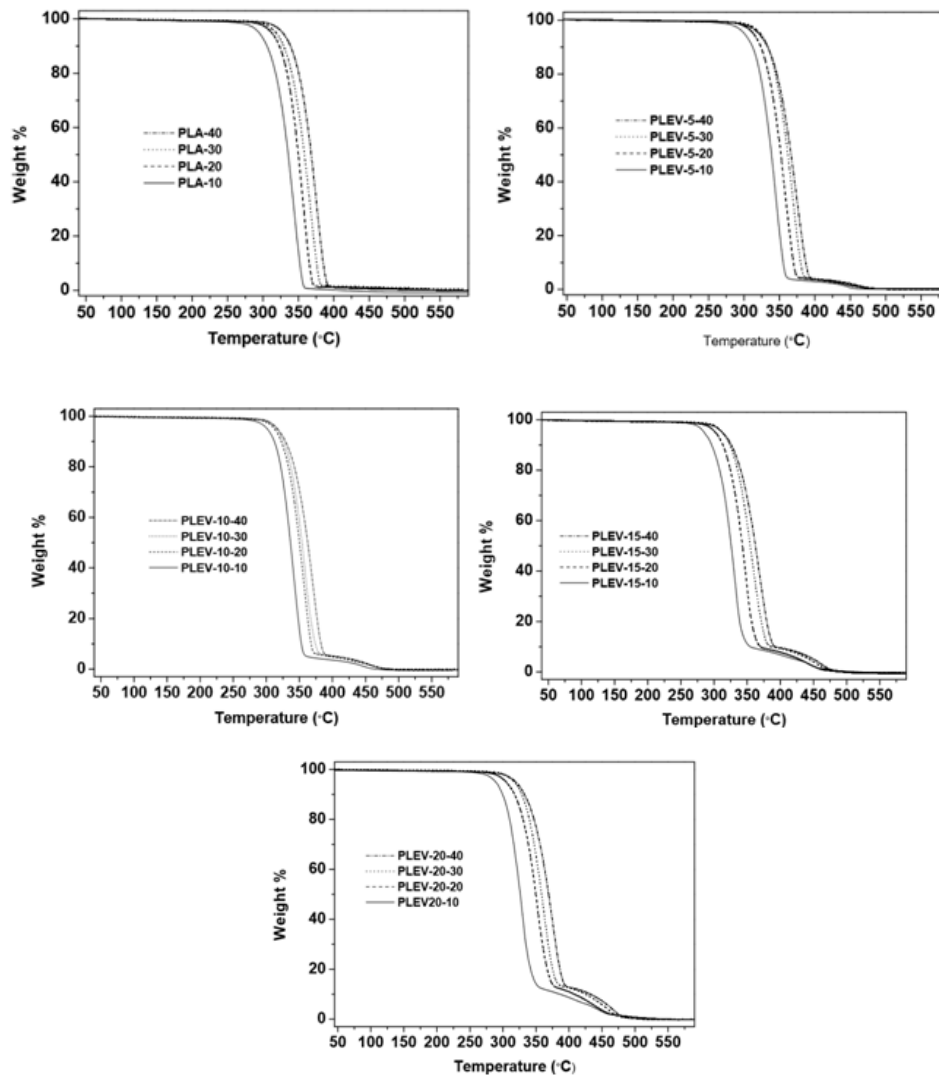


Figure 6.3 TGA graphs for PLA and PLA-EVA blends at different heating rates 10, 20, 30, 40°C/min.

It can be seen from the Fig. 6.3 that the thermal stability of PLA matrix slightly decreases with respect to increase in EVA content irrespective of the heating rate. DTG curves shown in Fig. 6.3(b) for PLA and PLA-EVA blends present various profiles depending on the wt% of EVA content and heating regime. It can be noticed that the maximum decomposition temperature (T_{max}) increases for all the samples with rise in temperature. Also, shift in the DTG curves to higher temperature side with respect to increase in heating rate can be noticed. This might be due to the lesser time provided to reach given temperature at higher heating rate [17-20].

For better understanding of thermal decomposition behavior of PLA and PLA-EVA blends, thermal degradation kinetic studies is performed. Thermal degradation kinetic studies for PLA and PLA-EVA blends can be given by the following expression.

$$\frac{d\alpha}{dt} = kf(\alpha) \dots\dots\dots (6.1)$$

where, ' α ' is the fraction decomposed or the conversion degree [$\alpha = (W_0 - W_t) / (W_0 - W_f)$], ' W_0 ' is the initial weight of the polymer, ' W_t ' is weight of PLA at time ' t ' and ' W_f ' is the final weight of PLA, ' $d\alpha/dt$ ' is the conversion rate, ' k ' is the rate constant and ' $f(\alpha)$ ' is the differential expression of a kinetic model function, which relies on the specific degradation mechanism [21].

Temperature dependent degradation rate constant (k) can be related to the Arrhenius equation by the following expression.

$$k = A \exp\left(\frac{-E_a}{RT}\right) \dots\dots\dots (6.2)$$

where, ‘ A ’ refers to the pre-exponential factor (S^{-1}), ‘ E_a ’ is apparent activation energy for degradation process (KJ/mol), ‘ R ’ is the universal gas constant ($8.314 \text{ J mol}^{-1} \text{ K}^{-1}$), and ‘ T ’ refers to the absolute temperature (K). The Eq. (2) is substituted in Eq. (6.1) to derive an expression that helps in understanding the degradation kinetic process and the expression as follows:

$$\frac{d\alpha}{dt} = A \exp\left(\frac{-E_a}{RT}\right) f(\alpha) \dots\dots\dots (6.3)$$

Non-isothermal thermal degradation kinetics can be predicted from Eq. (6.3) for single heating rate ($\beta = dT/dt$). In the current study, non-isothermal degradation kinetic study for PLA and PLA-EVA blends is carried out at a constant heating rate (β). Hence, Eq. (6.3) is rearranged into an Eq. (6.4) as follows.

$$\left(\frac{d\alpha}{dT}\right) = \frac{A}{\beta} \exp\left(\frac{-E_a}{RT}\right) f(\alpha) \dots\dots\dots (6.4)$$

Kinetic triplets of PLA and PLA-EVA blends can be calculated by TGA data by using Eq. (6.3) and Eq. (6.4) under isothermal and non-isothermal conditions, respectively. The order of reaction is proposed to be ‘ n^{th} ’ order and ‘ $f(\alpha)$ ’ as $(1 - \alpha)^n$ for measuring the kinetic triplets [21].

Flynn-Wall-Ozawa method

Flynn-Wall-Ozawa (F-W-O) method is a simple method for determining the activation energy directly from TGA data obtained at various heating rates. It is one of the integral methods which can

determine the activation energy without prior knowledge of the reaction mechanism. This method employs the Doyle's linear approximation and it is denoted by the following expression.

$$\log(\beta) = \left\{ \log \frac{AE}{g(\alpha)R} - 2.315 \right\} - \frac{0.457E_a}{RT} \dots\dots\dots (6.5)$$

where, ' β ' is the heating rate, ' A ' is the pre-exponential factor, ' E_a ' is the apparent activation energy, ' T ' is the absolute temperature, ' R ' is the relative gas constant and ' α ' is the conversion. From the slope of $\log(\beta)$ versus $-1/T$, the activation energy is calculated for the time value of conversion (α) [22].

The evaluation of activation energy for PLA and PLA-EVA blends is the primary footstep in better understanding of thermal degradation behavior of all samples. The TGA curves obtained at various heating rates (10, 20, 30 and 40 °C/min) are used to find out the activation energy for thermal degradation of all the samples. Fig. 6.4(a) displays $\log(\beta)$ versus $-1/T$ obtained via F-W-O method. For PLA and PLA-EVA blends, parallel straight lines are obtained at various ' α ' levels. This is an indication of suitability of F-W-O method for studying the thermal degradation kinetics at all stages of conversion.^{25,26} The plots of activation energy against conversion using F-W-O method for neat PLA and PLA-EVA blends can be seen from Fig. 6.4 (a-e). With respect to conversion, there is change in activation energy for all the samples throughout the degradation process. This reveals that the degradation process of both PLA and PLA-EVA blends does not proceed through simple degradation process.

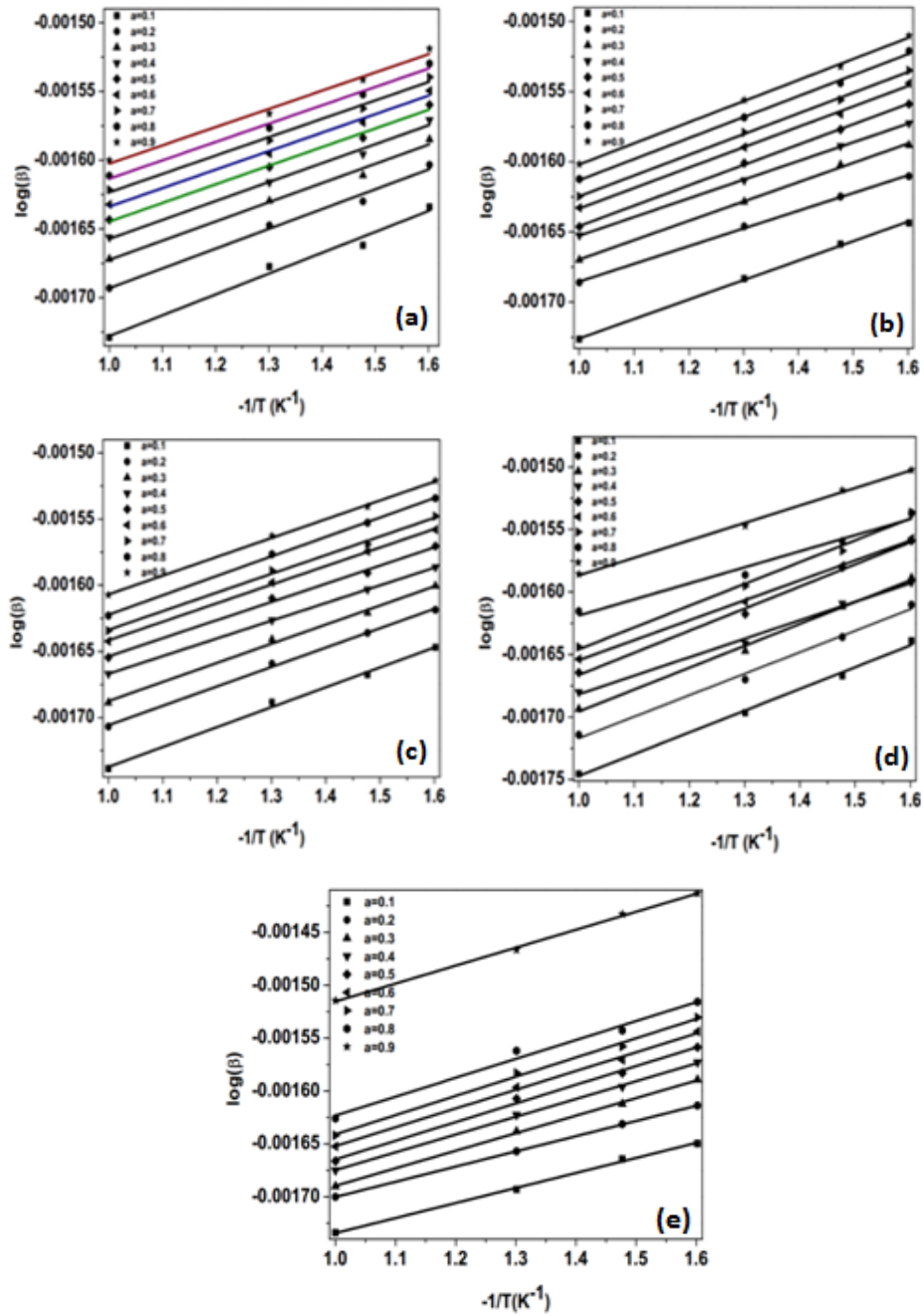


Figure 6.4. F-W-O plots for (a) PLA, (b) PLA-EVA-5, (c) PLA-EVA-10, (d) PLA-EVA-15, and (e) PLA-EVA-20.

The activation energy of PLA is found to be decreased after incorporation of EVA in the matrix, which is consistent with the TGA profile of PLA and PLA-EVA blends. The ‘ E_a ’ values of PLA and PLA-EVA blends are found to increase with respect to increase in conversion in the range of 0.1-0.7 and stay constant until complete degradation. The presence of EVA in the PLA matrix causes decrease in degradation rate for PLA-EVA blends.

Kissinger method

Kissinger method is the accepted model free system to get knowledge about degradation kinetics process. The advantage of this method is that the activation energy of any system can be obtained at a fixed conversion rate, without having any knowledge about degradation mechanism from the following expression.

$$\ln\left(\frac{\beta}{T_{max}^2}\right) = \left\{ \ln\frac{AR}{E_a} + \ln\left[n(1-\alpha_{max})^{n-1}\right] \right\} - \frac{E_a}{RT_{max}} \dots\dots\dots (6.6)$$

where, ‘ T_{max} ’, ‘ α_{max} ’ and ‘ n ’ refer to the temperature at which the maximum weight loss occurs, degree of conversion corresponding to the inflection point on the TGA thermographs and the order of reaction, respectively [22-24]. The slope that corresponds to linear plot when $\ln(\beta/T_{max}^2)$ is interpreted against $(-1/T_{max})$ is used to calculate ‘ E_a ’ for degradation process.

The TGA graphs of PLA and PLA-EVA blends obtained at various heating rate (10, 20, 30, 40 °C/min) are used to determine activation energies of PLA and its blends. In Kissinger method, the activation energy is determined from the slope of straight lines obtained when

$\ln(\beta/T_{\max}^2)$ against $1/T_{\max}$. The suitability of Kissinger method for PLA and PLA-EVA systems is confirmed by the various smooth fitted straight lines shown in Fig.6.5. The regression coefficient values obtained for PLA and PLA-EVA blends lie in between 0.9 to 0.999 which further support the applicability of this method. The activation energy values for PLA, PLA-EVA-5, PLA-EVA-10, PLA-EVA-15 and PLA-EVA-20 from the Kissinger method are 134, 129, 128, 116 and 113, respectively and shown in Table 6.4.

Table 6.4 Activation energy and regression coefficient from F-W-O and Kissinger methods for PLA and PLA-EVA blends

S. No.	Sample Name	F-W-O Method E_a (kJ/mol)	R^2 F-W-O Method	Kissinger Method E_a (kJ/mol)	R^2 Kissinger Method
1	PLA	131	0.998	134	0.999
2	PLA-EVA-5	129	0.999	129	0.999
3	PLA-EVA-10	127	0.994	128	0.998
4	PLA-EVA-15	114	0.999	116	0.999
5	PLA-EVA-20	111	0.999	113	0.997

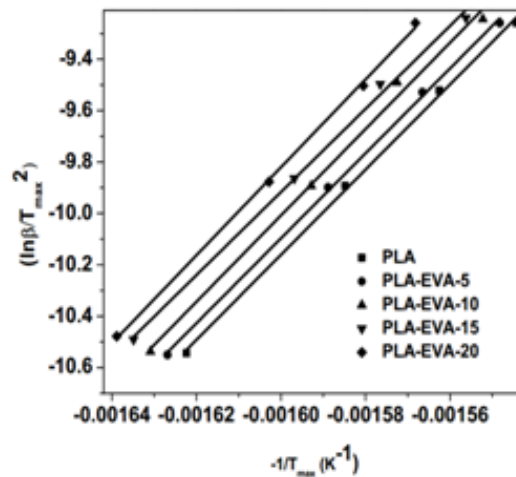


Figure 6.5 Kissinger plots for PLA and PLA-EVA blends.

6.3.5 Differential Scanning Calorimetry

DSC thermographs for PLA and PLA-EVA blends obtained during second heating and first cooling cycles are presented in Fig. 6.6. The thermal properties of PLA and PLA-EVA blends such as melting, crystallization and glass transition temperature are considered from the DSC thermograph obtained during the second heating cycle at a heating ramp of 10 °C/min and are reported in Table 6.5. While, the melt crystallization temperature for PLA and PLA-EVA blends is considered from the DSC thermograph which is obtained during the first cooling cycle at a cooling ramp of 10 °C/min and are reported in Table 6.5. The presence of unimodal endothermic peak at a melting temperature of 170 °C can be noticed for PLA in Figure 6.6(a), which is an indication of α -crystalline arrangement of PLA. In non-isothermal cold crystallization progression, the absence of double melting peak is an indication of existence of stable crystal formation in PLA. This might be owing to the fact that homogeneous nucleation process took place in PLA [25]. The melting peak for the PLA-EVA blends in Fig. 6.6(a) also reveals unimodally endothermic nature. This might be due to the stable crystals formed with identical thickness with the influence of EVA in the PLA matrix.

The non-isothermal cold crystallization temperature for PLA and PLA-EVA blends are reported in Table 6.5. It can be seen from the Table that crystallization temperature decreases with respect to increment in EVA loading in the PLA matrix. This in turn reveals good compatibility between EVA and PLA matrix. In addition, EVA acts as a

nucleating agent such that it initiates crystallization phenomenon at a lower T_{cc} resulting in the formation of stable as well as thick crystals. The lower T_{cc} means that less energy is required to achieve the desired degree of crystallinity[26]. The glass transition temperature of PLA is noticed to be unaffected with increase in EVA loading in the PLA matrix.

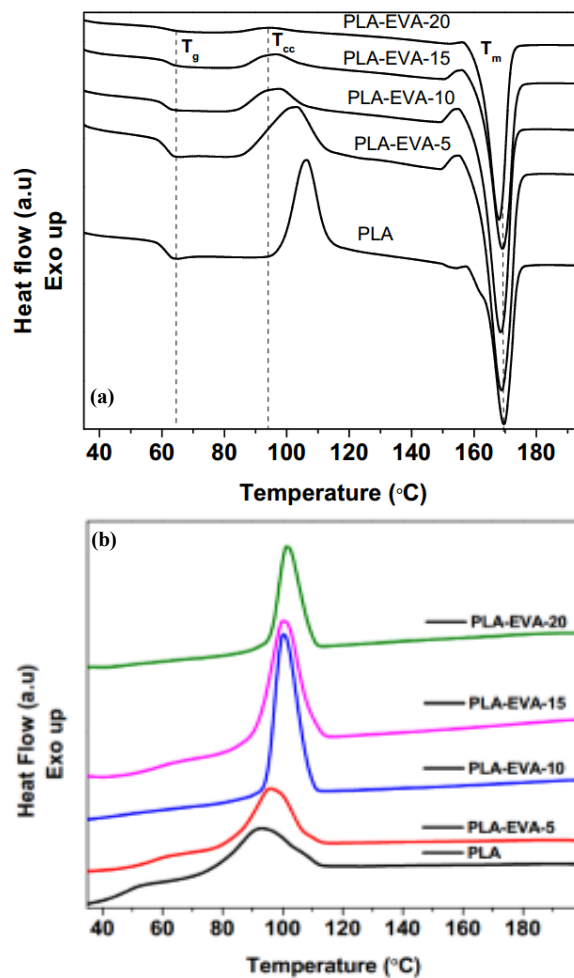


Figure 6.6 DSC thermographs for PLA and PLA-EVA blends with 10 °C/min (a) heating and (b) cooling curves

The non-isothermal melt crystallization temperature (T_{mc}) for PLA and PLA-EVA blends are reported in Table 6.5. It can be seen from the Table that T_{mc} for PLA-EVA blends tends to increase with EVA loading as compared to neat PLA. These results indicate that EVA enhances the crystallization of PLA by heterogeneous nucleation effect [27].

Table 6.5 Glass transition (T_g), cold and melt crystallization temperature (T_{cc} and T_{mc}) and melting temperature (T_m) for PLA and PLA-EVA blends

S. no.	Sample Name	T_g (°C)	T_{cc} (°C)	T_m (°C)	T_{mc} (°C)
1	PLA	62.38	105.55	170.87	92.1
2	PLA-EVA-5	62.03	102.72	168.92	93.2
3	PLA-EVA-10	61.94	98.59	169.27	94.1
4	PLA-EVA-15	62.24	96.77	169.32	95.3
5	PLA-EVA-20	61.48	95.33	168.87	98.0

6.3.6 Non-Isothermal melt crystallization for PLA and PLA/EVA blends

The non-isothermal melt crystallization behavior of PLA and PLA-EVA blends at various heating rates are illustrated through DSC thermographs shown in Fig. 6.7. For PLA the melt crystallization temperature (T_{mc}) is found in the range of 80 - 120°C at several heating conditions mentioned earlier. While PLA-EVA blends exhibited T_{mc} in the range of 100 – 126 °C under the similar heating conditions. It is observed that T_{mc} increases with increasing heating rate for both PLA and PLA-EVA blends. This is because, higher heating rates increase the time necessary for melt crystallization process [28].

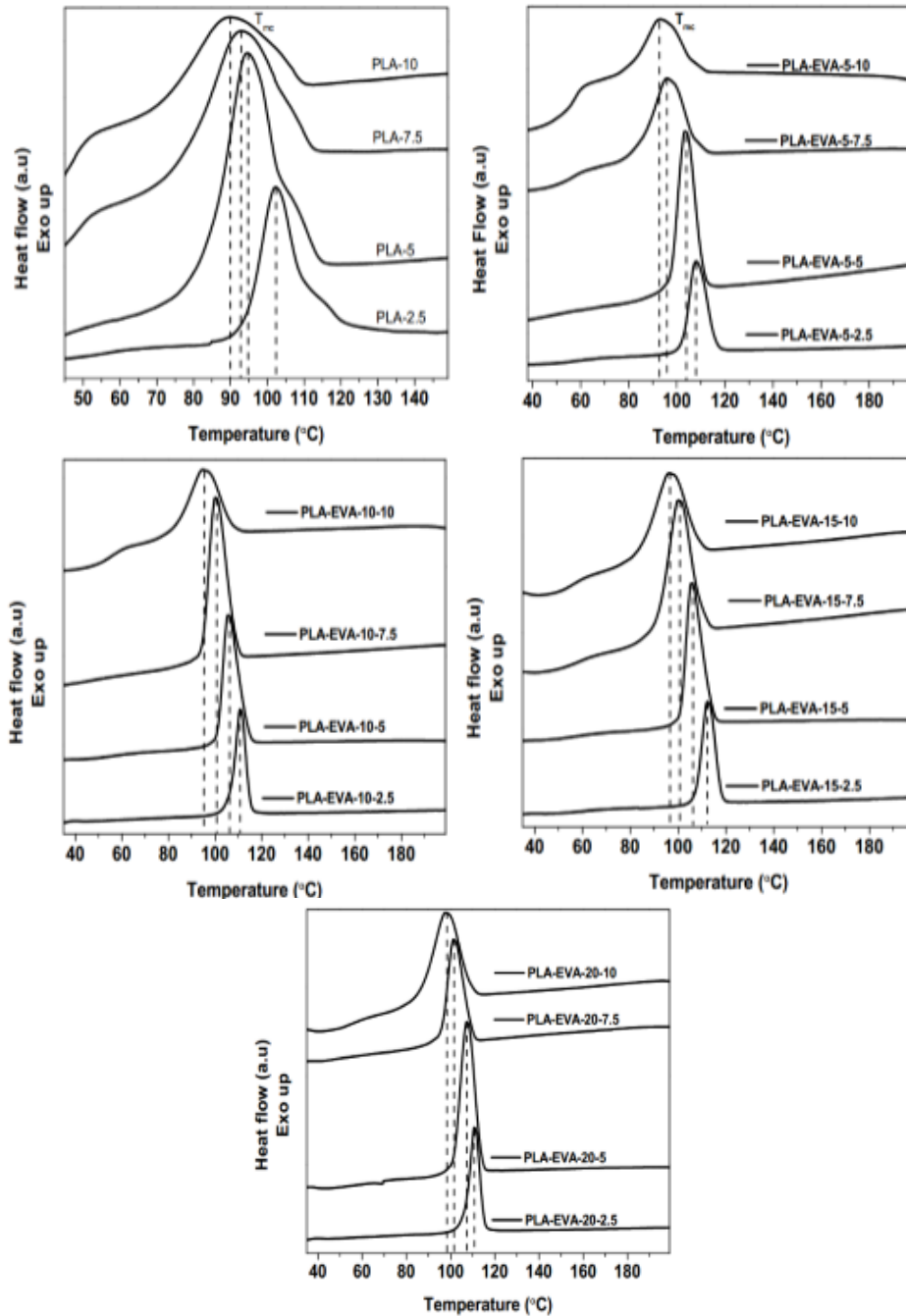


Figure 6.7 DSC thermographs for PLA and PLA-EVA blends with different cooling temperatures of 2.5, 5, 7.5, 10 °C/min

Relative crystallinity

Nonisothermal melt crystallization of PLA and PLA-EVA blends are integrated to determine their relative crystallinity ($X(t)$) as a function of time (t). The following equation relates $X(t)$ as a function of temperature.

$$X(t) = \frac{\int_{T_0}^T \left(\frac{dH_c}{dT} \right) dT}{\int_{T_0}^{T_\infty} \left(\frac{dH_c}{dT} \right) dT} \dots\dots\dots (6.7)$$

where, the onset and final melt crystallization temperatures for both PLA and PLA-EVA blends are indicated by T_0 and T_∞ respectively [29]. The following expression/equation relates the respective temperature (T) and the crystallization time (t).

$$t = \frac{T - T_0}{\phi} \dots\dots\dots (6.8)$$

where, ϕ is the heating rate [30]. For both PLA and PLA-EVA blends, relative crystallinity curves obtained at different heating rates (2.5, 5, 7.5 and 10 °C/min) are plotted as a function of crystallization time and the same is shown in Fig. 6.8 The sigmoidal shape of relative crystallinity curves indicate the phenomenon of impingement of spherulites that occurred at the later stage of melt crystallization process for both PLA and PLA-EVA blends. It can be seen from the Fig.6. 8 that lag effects are minimum for the faster heating rates as compared with the slower heating regime for both PLA and PLA-EVA blends.

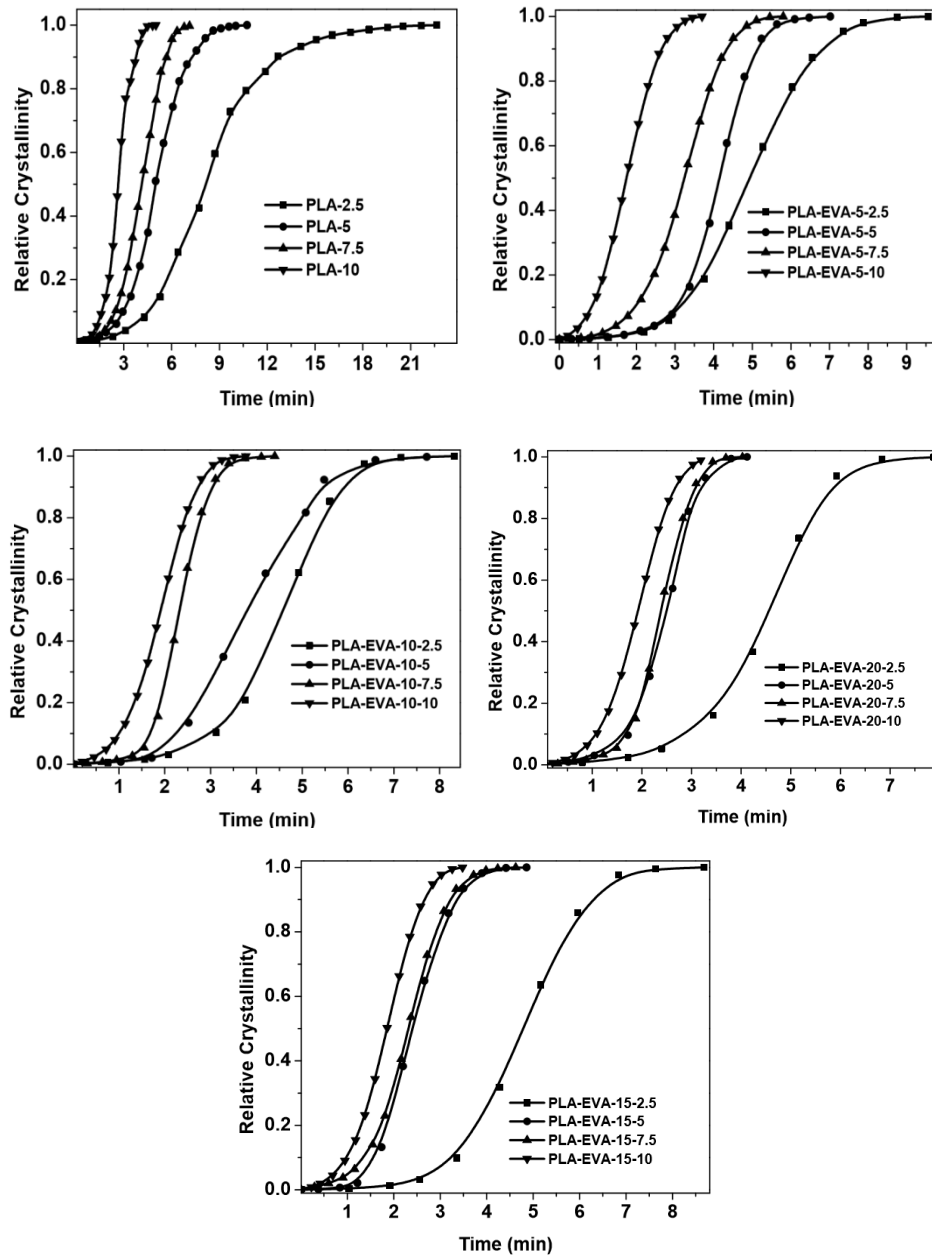


Figure 6.8 Relative crystallinity curves for PLA and PLA-EVA blends

Crystallization half-time

The time required to reach 50% of the crystallization process is denoted as crystallization half-time. Prime concern for determination of half time of crystallization is to better understand the kinetics of crystallization process. The half time of crystallization is obtained by the following equation.

$$t_{1/2} = \left(\frac{\ln 2}{k} \right)^{1/n} \dots\dots\dots (6.9)$$

The $t_{1/2}$ values obtained for both PLA and PLA-EVA blends are reported in Table 6.6. It can be observed from the Table that $t_{1/2}$ values shows decreasing trend with increment in heating rates which in turn indicates faster crystallization rate exhibited by PLA. It can be noticed from the Table 6.6 that $t_{1/2}$ values are even lower than neat PLA at all the heating rates. These results indicate the improvement in melt crystallization process for PLA after blending with EVA. In addition to this, secondary crystallization process is noticed for all the samples irrespective of PLA and PLA-EVA blends, which can be inferred from higher $t_{1/2}$ values at lower heating rates as shown in Table 6.6 [31-36].

Table 6.6 $t_{0.5}$ values for PLA and PLA-EVA blends

S.no.	Sample Name	$T_{0.5}$ (min)			
		2.5 (°C/min)	5 (°C/min)	7.5 (°C/min)	10 (°C/min)
1	PLA	2.6	2.5	2.2	2.0
2	PLA-EVA-5	2.48	2.3	2.08	2.0
3	PLA-EVA-10	2.5	2.1	2.03	1.8
4	PLA-EVA-15	2.42	2.15	1.95	1.68
5	PLA-EVA-20	2.3	2.0	1.92	1.47

In the present work, non-isothermal melt crystallization kinetic parameters for PLA and PLA-EVA blends are determined by the simplest Avrami kinetic model and the same is expressed by the following expression.

$$X(t) = 1 - \exp(-kt^n) \quad \dots\dots\dots (6.10)$$

Eq. (11) is presented in the non-linear form as follows

$$\log[-\ln(1 - X(t))] = \log k + n \log t \quad \dots\dots\dots (6.11)$$

where ‘*n*’ relates to the avrami parameter, which explains about crystal growth and nucleation effect, ‘*k*’ indicates the kinetic constant and ‘*X(t)*’ represents the relative crystallinity at time “*t*”. The avrami plots for PLA and PLA-EVA blends obtained at various heating rates are shown in Fig. 6.9, in which $\log[-\ln(1-X(t))]$ are plotted as a function of $\log t$. Relative crystallinity curves for neat PLA and PLA-EVA blends shown in Fig. 6.7 indicates Avrami plots for the same. It can be observed from the Fig. 6.8 that all the plots exhibits good linearity to each other. This indicates that the theory seems to be useful for evaluating the melt crystallization process of PLA and PLA-EVA blend systems.

The Avrami parameters (‘*K*’ and ‘*n*’) for both PLA and PLA-EVA blends are presented in Table 6.7. It is inferred that the ‘*n*’ values obtained for PLA lie in the range of 3.3-2.5, which corroborated with the reported literature. This clearly indicates that the non-isothermal melt crystallization process of PLA proceeds via three dimensional crystal growth due to homogeneous nucleation phenomenon. While in case of

PLA-EVA blends, the 'n' values lies in the range of 3.0-1.5, which are comparatively lesser than neat PLA. This decrease in 'n' values indicate that sufficient time is not provided for the crystals to grow in three dimensions. This phenomenon in turn leads to heterogeneous crystallization process in PLA after blending with EVA.

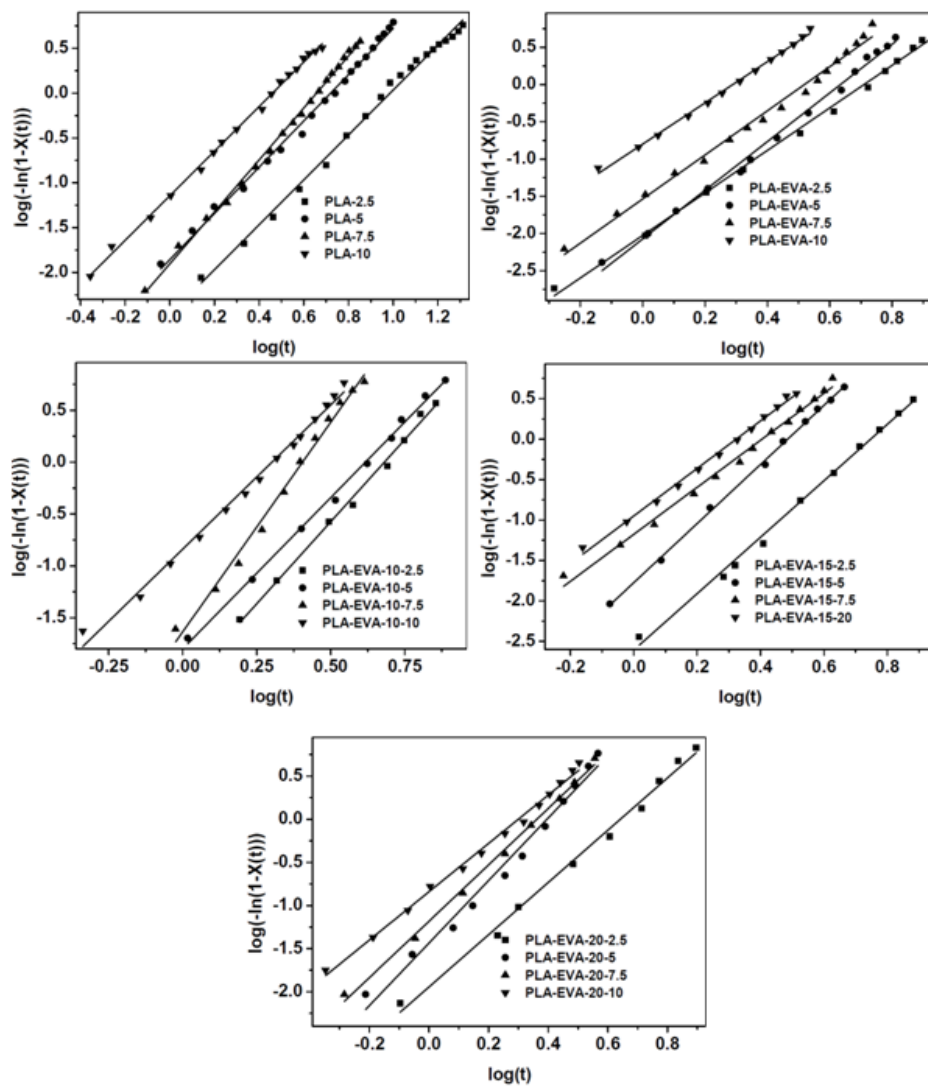


Figure 6.9 Avrami plots for PLA and PLA-EVA blends

Table 6.7. Avrami model parameters for PLA and PLA-EVA blends

S. No	Sample Name	n				Log K			
		2.5 °C/min	5 °C/min	7.5 °C/min	10 °C/min	2.5 °C/min	5 °C/min	7.5 °C/min	10 °C/min
1	PLA	3.3	2.9	2.7	2.5	-3.5	-3.1	-2.5	-2.1
2	PLA-EVA-5	3.0	2.8	2.5	2.2	-3.1	-2.7	-2.2	-1.9
3	PLA-EVA-10	2.8	2.6	2.3	2.0	-2.8	-2.3	-2.0	-1.5
4	PLA-EVA-15	2.7	2.4	2.0	1.8	-2.7	-2.2	-1.7	-1.3
5	PLA-EVA-20	2.5	2.1	1.9	1.5	-2.4	-2.0	-1.6	-1.1

6.4 Conclusion

EVA copolymer with 40% vinyl acetate content was used as the toughening agent in PLA. The impact strength for binary blends of PLA-EVA is increased significantly (176%) with 15 wt. % of EVA compared to virgin PLA due to the strong interfacial adhesion between the PLA matrix and EVA. SEM studies of impact fractured surfaces of binary blends of PLA implied the modification of PLA by EVA. However, the incorporation of EVA in PLA reduced thermal stability of PLA with a decrease in T_{onset} and T_{max} degradation temperatures. The presence of unimodal endothermic peak at a melting temperature of 170 °C is noticed for PLA and PLA-EVA blends, which is an indication of α -crystalline form of PLA. The effect of EVA on melt crystallization of PLA is investigated by using Avrami model. The Avrami coefficient for PLA-EVA blends are lower than the neat PLA which indicates that EVA acts as a nucleating agent.

The work included in this chapter has been published:

“Investigation on the influence of EVA content on the mechanical and thermal characteristics of poly(lactic acid) blends” -V H Sangeetha, Ravibabu Valppa, T O Varghese, S K Nayak, Journal of Polymers and Environment, 2016, 26 (1)2,1-14.

References

- [1] A. Muijica-Garcia, S. Hooshmand, M. Skrifvars, J.M. Kenny, K. Oksman, L. Peponi, *RSC. Adv.* 6, (2016) 9221.
- [2] X. Zhu, Y. yang, J. Feng, X. Zhang, C. Zhang, Z. Tang, J. Zhu, *Carbohydr. Polym.* 1 (2013), 810.
- [3] W. Chiu, Y. Chang, H. Kuo, M. Lin H. Wen, *J. App. Polym. Sci.* 5 (2008) 3024.
- [4] X. Li, Y. Xiao, A. Bergeret, M. Longerey J. Che, *Polym. Composite.* 2, (2013) 396.
- [5] K. Yao, X. Wen, H. Tan, J. Gong, J. Zheng, W. Zhao, Y. Wang, D. Cui, H. Na T. Tang, *Soft Matter.* 9(2013) 10891.
- [6] K.S. Anderson, K.M. Shreck , A.M. Hilmyer, *Polym. Rev.*, 48 (2008) 85.
- [7] I. Noda, M.M. Satkowski, A.E. Dowrey, C. Marcott, *Macromol. Biosci.* 4 (2004), 269.
- [8] M.E. Broz, D.L. Vander Hart N.R. Washburn, *Biomaterials.* 24 (2003) 4181.
- [9] T. K. Semba, U.S. Kitagawa, Ishiaku , H. Hamada, *J. App. Polym. Sci.*, 101 (2006) 1816.
- [10] R. Wang, S. Wang, Y. Zhang, C. Wan , P. Ma, *Polym .Eng. Sci.* 49 (2009) 26.
- [11] T. Yokohara and M. Yamaguchi, *Eur. Polym. J.* 44., (2008) 677-685.
- [12] L. Jiang, M. P. Wolcott and J. Zhang, *Biomacromolecules.*, 7 (2006) 199.
- [13] N. Zhang, J. Ren, Q. Wang. *J. Mater. Sci.* 44, (2009) , 250.
- [14] H.T. Oyama, *Polymer* 50 (2009) 747.

- [15] W. Hoogsteen, A. R. Postema, A. J. Penings, G. T. Brinke and P. Zugenmaier, *Macromolecules*. 1990, 23, 634.
- [16] L.M. Robeson, *Polym. Eng. Sci.* 8, (1984) 587.
- [17] R.B. Valapa, S. Hussain, P. K. Iyer, G. Pugazhenthii, V. Katiyar, *J. Polym. Res.* 2015, 22, 1572.
- [18] Q. Y. Han, Wang, C. Shao, G. Zheng, Q. Li and C. Shen, *J. Compos. Mater.* , 48 (2014) 2737.
- [19] S.N. Maiti and Hemalata, *J Polym Res.* 19, (2012) 1752.
- [20] I.E. Yuzay, R. Auras, H. Valdez and S. Selke, *Polym. Degrad. Stab.* 95 (2010) 1769.
- [21] J.H. Flynn and L.A. Wall, *J Polym Sci.* 4 (1996) 323.
- [22] K. Chrissafis, *Thermochim. Acta.* 511 (2010) 163.
- [23] Y. Fan, H. Nishida, Y. Shirai T. Endo. *Polym. Degrad. Stab.* 84, (2004) 143.
- [24] H. E. Kissinger, *Anal. Chem.* 29 (1957) 1702.
- [25] Y.Y. Leu, Z.A.M. Ishak W. S. Chow, *J.Appl. Polym. Sc.*, 124 (2012) 1200.
- [26] R.B. Valapa, G. Pugazhenthii and V. Katiyar, *J. Appl. Polym. Sci.* 2015, 132, 41320.
- [27] D. Sawai, K. Takahashi, A. Sasashige, T. Kanamoto and S. H. Hyon, *Macromolecules*. 2003, 36, 3601.
- [28] R.B. Valapa, G. Pugazhenthii and V. Katiyar, *RSC Adv.* 5, (2015) 28410.
- [29] R.B. Valapa, S. Hussain, P.K. Iyer, G. Pugazhenthii V. Katiyar, *Polym. Bull* (2016) 73, 21-38.

- [30] X. Shi, G. Zhang, T.V. Phuong and A. Lazzeri, *Molecules*. 20,(2015) 1579.
- [31] A.M. Diez-pascual and A. L. Díez-Vicente, *Int. J. Mol. Sci.* 15 (2014) 10950.
- [32] R.B. Valapa, S. Hussain, P. K. Iyer, G. Pugazhenthii and V. Katiyar. *J. Polym. Res.* 1 (2015) 175,
- [33] A. Pei, Q. Zhou and L.A. Berglund, *Compos. Sci. Technol.* 70, (2010) 815.
- [34] N. Vasanthan, H. Ly and S. Ghosh, *J Phys. Chem. B.* 115 (2011) 9556.
- [35] Liu Y, L. Wang, Y. He, Z. Fan and S. Lia. *Polym. Int.* 59 (2010) 1616.
- [36] F. Ravari, A. Mashak, M. Nekoomanesh and H. Mobedi. *Polym. Bull.* 70(2013) 2569.

.....✂.....

Chapter 7

PLA /EVA/EVOH TERNARY BLEND SYSTEM: EFFECT OF DEGREE OF HYDROLYSIS OF ETHYLENE VINYL ACETATE

Contents

- 7.1 Introduction
- 7.2 Experimental
- 7.3 Results and Discussion
- 7.4 Conclusion

In order to modify the properties of PLA like low impact strength and slow crystallization rate, an attempt has been made in the present study to prepare ternary blends of PLA with Ethylene Vinyl Acetate (EVA) and Ethylene Vinyl Alcohol (EVOH). The effect of degree of hydrolysis of EVA on the thermal and mechanical properties of PLA is investigated. Differential scanning calorimetry results disclose the prominent decrement in cold crystallization temperature and display a distinct melt crystallization peak in comparison with neat PLA. This is a clear indication that EVOH acted as a nucleating agent to increase the crystallization rate of PLA. The decrement in terms of tensile properties clearly indicated the reduction in stiffness after addition of EVOH in the PLA matrix. For the ternary blends of PLA, four and eight folds increment in terms of elongation at break (%) and impact strength properties are observed as compared to neat PLA, respectively. Morphological studies revealed the presence of good adhesion between the PLA matrix and EVOH in presence of EVA.

7.1 Introduction

Amidst of all the biopolymers, PLA is being currently explored intensively for its potential in biomedical, automobile, electronics and packaging applications [1]. This is due to the excellent process ability of PLA as compared to other biopolymers. Despite this, PLA exhibits disadvantages such as high brittleness, slow crystallization rate and poor impact resistance, which in turn limit its wide-spread applications [2]. In order to address these drawbacks, incorporation of several nanoscale reinforcements namely cellulose nanocrystals (CNCs) [3], graphene (GR) [4], carbon nanotubes (CNTs) [5] and clay [6] is practiced in the PLA matrix. The drawback associated with the incorporation of nanofillers is that enhancement in terms of impact and crystallization properties can be expected only if there exists compatibility between nanofillers and the PLA matrix.

An alternative approach envisaged in order to overcome the drawbacks associated with PLA is blending technology in which PLA is blended with certain other polymers namely PHB, PCL and PBS [7-9]. The blending technology finds wide-spread utilization in industrial sectors due to its potential in combining the characteristics of individual polymers into a unique end use product. Blending of PLA with other polymers can help in significantly reducing the cost for the final product as compared with developing a new polymer [10]. The selection of co-polymer used for blending with PLA should be circumspectly selected. In other words, the co-polymer should exhibit compatibility with the PLA matrix or otherwise can end up in phase separation or immiscible blends [11].

There are reports envisaged for addition of external compatibilizers in order to enhance the miscibility of the PLA blends [12]. However, the most economically attractive method to enhance the miscibility of the PLA blend is to select a co-polymer which exhibits high compatibility with PLA in devoid of external compatibilizer.

Ethylene Vinyl Acetate (EVA) is one such co-polymer which is reported to exhibit compatibility with PLA matrix. The rubbery as well as resin properties offered by EVA make it as an attractive material to be used as a co-polymer in order to improve the impact properties of PLA. Therefore, investigation on blending of EVA as a co-polymer with PLA has been carried out by several researchers [13, 14]. It was found that increment in terms of vinyl acetate (VA) content in the PLA matrix helped in enhancing the compatibility between EVA and PLA [14]. With 40-50 wt. % of VA content, it was found that the impact strength was increased by 176%. Therefore, in the current work, EVA containing 40 wt.% of VA content is considered as a co-polymer for blending with PLA. The main aim of this work is to enhance the impact strength and crystallization properties of PLA. In order to achieve this, EVA is modified into ethylene vinyl alcohol (EVOH) via hydrolysis and subsequently used for blending with PLA matrix. Even though, there are reports on direct blending of PLA with EVOH co-polymer, studies on the modification of EVA into EVOH and comparative analysis on the properties of PLA-EVA and PLA-EVA-EVOH blends are not yet reported to the best of our knowledge. The novelty of the current work lies in examining the effect of degree of hydrolysis on compatibility, impact strength and crystallization properties of PLA-EVA-EVOH

blends in comparison with PLA-EVA blend and neat PLA. In the current work, binary blend of PLA-EVA (90/10 wt.%) and ternary blends of PLA-EVA-EVOH (90/5/5 wt.%) are developed and studied the effect of EVA under different degree of hydroxyl content. The blend samples were prepared via melt mixing technique and are then subjected to injection molding process. The influence of degree of hydrolysis of EVA on the toughening properties as well as phase behavior of injection molded PLA-EVA-EVOH blends is studied in comparison with PLA-EVA and neat PLA samples. The toughening mechanism is also explained based on the morphological analysis and impact strength properties of the prepared blends. Thermal degradation kinetics of PLA blends was studied using Coats-Redfern method for the better understanding of degradation behavior.

7.2 Experimental

7.2.1 Materials

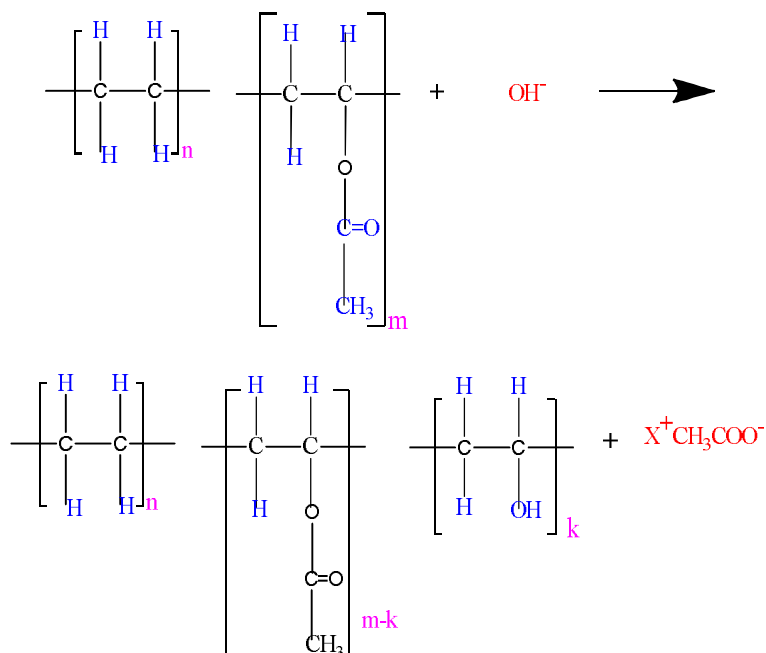
The details of the polymers and chemicals used for the study are discussed in Chapter 2 (sections 2.1.)

7.2.2 Modification of EVA

Hydrolyzed EVA was synthesized according to the following procedure.

Initially, 50 g of EVA was dissolved in 250 mL of THF. Thereafter, 80 mL of 0.5 M NaOH was added to the reaction mixture and was heated under nitrogen atmosphere at 50°C for different time intervals 1h, 2h and 3h respectively. The reaction mixture was neutralized by 1N HCl, then precipitated in chilled distilled water. The precipitate

was washed thoroughly with distilled water and was dried at 80°C till constant weight was achieved. The hydrolysis reaction of EVA with NaOH and its subsequent conversion to EVOH is illustrated in Figure 7.1.



Where n is the number of ethylene monomers, m is the number of vinyl acetate monomers, k is the number of vinyl alcohol monomers

Figure 7.1 Hydrolysis reaction of EVA with NaOH

7.2.3 Determination of hydroxyl content of hydrolysed EVA

The hydroxyl content was determined by titration method using phthalic anhydride in presence of pyridine. One gram of hydrolysed EVA was dissolved in toluene (25 mL) and 5 mL of phthalic anhydride /distilled pyridine (70:30) was added and the mixture was refluxed for 24 h. Unreacted phthalic anhydride was determined by titrating against 0.5 N NaOH using phenolphthalein as an indicator.

7.2.4 Blend Preparation

Prior to blending, virgin PLA was dried in a hot air oven at 80°C for 6 h. Binary blend of PLA with EVA (10 wt%) composition was melt mixed in a microprocessor controlled twin screw co-rotating extruder with L/D ratio of 40:1. The temperature condition in the range of 165-190 °C and the screw speed with 60 rpm were optimized for processing the blend. The extrudate strands obtained after processing were pelletized by quenching in cold water. The drying process for the extruded granules was carried in a hot-air oven, which was maintained at 60 °C. The drying process lasted for 6 h and further, the granules were subjected to injection molding using Electronica Endura 90 in order to prepare the test specimen as per ASTM standard. The temperature and injection pressure used for injection molding process were maintained in the range of 175-190 °C and 110 - 120 bar, respectively. The ternary blends of PLA (90 wt.%) /EVA (5 wt. %)/ EVOH (5 wt.%) were also prepared using injection molding process. The temperature and injection pressure conditions for preparation of ternary blends were maintained in the range of 165-190 °C and 110 - 120 bar, respectively. The various blend compositions are shown in Table 7.1. The numerical values (1, 2, 3) followed after EVOH in the ternary blends corresponds to EVA hydrolyzed at different intervals i.e., 1 h, 2 h and 3 h, respectively.

Table 7.1: Material designation, composition of PLA, PLA-EVA and PLA-EVA-EVOH blends

Blend Composition	PLA (wt. %)	EVA (wt. %)	EVOH (wt. %)
PLA	100	-	-
PLA-EVA	90	10	-
PLA-EVA-EVOH-1	90	5	5
PLA-EVA-EVOH-2	90	5	5
PLA-EVA-EVOH-3	90	5	5

7.2.5 Characterization Techniques

Fourier Transform Infrared (FTIR) Spectroscopy Analysis. All the samples such as EVA, EVOH, PLA, PLA-EVA and PLA-EVA-EVOH blends were subjected to FTIR analysis (Model: Avatar 370 Make: Thermo Nicolet). The FTIR spectra for these samples were recorded in the wavenumber region ranging from 400 to 4000 cm^{-1} .

Scanning Electron Microscopy Analysis. The morphological analysis for tensile fractured specimens was carried out by scanning electron microscopy (Model: JEOL-6390LV, Make: Germany). Before subjecting to SEM analysis, the fractured samples were sputtered with platinum and dried for a period of 30 min.

Thermogravimetric Analysis (TGA). The thermal analysis for PLA, PLA-EVA, PLA-EVA-EVOH blends were carried out using a TGA analyzer (Model: Q50, Make: TA instruments, Walter, USA) in the temperature range of 30 to 600 $^{\circ}\text{C}$ at a heating rate of 10 $^{\circ}\text{C}/\text{min}$ under nitrogen atmosphere. The thermal degradation kinetics for PLA and PLA blends was carried with the data obtained at a heating rate of 10 $^{\circ}\text{C}/\text{min}$ using Coats-Redfern method.

Differential Scanning Calorimetry (DSC) Analysis. Glass transition temperature (T_g), cold and melt crystallization temperatures (T_{cc} and T_{mc}), melting point (T_m), cold and melt crystallization enthalpy (ΔH_{cc} and ΔH_{mc}) and melting enthalpy (ΔH_m) for PLA, PLA-EVA and PLA-EVA-EVOH blends were determined using DSC analysis (Model: Q50, Make: TA instruments, Walter, USA). The PLA, PLA-EVA and PLA-EVA-EVOH blends were subjected to double heating cycle in which the first

heating cycle was performed in the temperature range of 35 to 210 °C at a heating rate of 10 °C/min. At 210 °C, the samples were kept at isothermal condition for 5 min. Followed by this; the samples were allowed to cool at a cooling rate of 10 °C/min. At 35 °C, the samples were kept at isothermal condition for 5 min. The percentage crystallinity for PLA PLA-EVA, PLA-EVA-EVOH blends was determined using the following equation.

$$\chi_c = \frac{\Delta H_m}{\Delta H_o} * 100 \dots\dots\dots (7.1)$$

where, ΔH_m is the melting enthalpy and ΔH_o is the crystallization enthalpy for 100% crystalline PLA (93.7 J /g).

7.3 Results and Discussion

7.3.1 EVA Hydrolysis

The hydrolysed EVA samples were designated as EVOH-1, EVOH-2 and EVOH -3 based on the degree of hydrolysis. The hydroxyl content present in the hydrolysed EVA was determined by reaction with excess acetic anhydride and successive titration [15]. The degree of hydrolysis (DOH) was calculated by taking theoretical value of OH into consideration. The hydroxyl value and the extent of hydrolysis with respect to reaction time are presented in Table7.2. The values indicated that the hydrolysis of EVA is a time dependent reaction since both OH value and degree of hydrolysis value increased with increase in reaction time. In case of EVOH-1, the DOH was obtained to be 32% with a hydroxyl value of 163. While, the DOH for EVOH-2 and EVOH-3, was found to be 58% and 80%, respectively. The corresponding hydroxyl

values for EVOH-2 and EVOH-3 were 297 and 412, respectively. From the DOH and hydroxyl values, it is clear that the maximum degree of hydrolysis is achieved for EVOH-3.

Table 7.2 Effect of reaction time on hydroxyl value and extent of reaction

Polymer	Reaction time (min)	Hydroxyl value (A)	DOH (%)
PLA/EVA/EVOH-1	60	163	32
PLA/EVA/EVOH-2	120	297	58
PLA/EVA/EVOH-3	180	413	81

7.3.2 FTIR Analysis

The FTIR spectra for EVA and EVOH samples are presented in Figure 7.2. The FTIR analysis revealed the modification of EVA into EVOH via hydrolysis reaction. It is observed from FTIR spectra of EVA that the peak present at 1735 cm^{-1} corresponds to the presence of acetate group [16]. It can be seen from the Figure that the intensity of the acetate peak decreases with respect to hydrolysis time for EVOH samples. In addition to this, peak due to OH stretching can be seen in the wave number region of $3200\text{-}3400\text{ cm}^{-1}$ [17]. The appearance of OH peak in EVOH samples confirms the occurrence of hydrolysis process. The increase in the intensity of the hydroxyl peak with respect to hydrolysis time reveals the increase in hydroxyl content due to maximum extent of degree of hydrolysis, which in turn, confirms the modification of EVA into EVOH.

The FTIR spectra for PLA, PLA-EVA and PLA-EVA-EVOH samples are depicted in Figure 7.2. The appearance of peaks at 3000 and 2950 cm^{-1} is attributed to the asymmetric and symmetric mode of C-H

groups present in PLA, respectively. The presence of absorption band in the wavenumber region ranging from 1700-1800 cm^{-1} corresponds to the carbonyl group available in the PLA [18]. The availability of CH_3 band in the PLA is confirmed by the appearance of peak at 1450 cm^{-1} . The existence of band at 1386 cm^{-1} is attributed to the C-H deformation. The C-O-C asymmetric stretching of ester groups is confirmed by the presence of band around 1020 cm^{-1} . The presence of band at 922 cm^{-1} corresponds to the rocking mode of CH_3 groups. The presence of EVA in the PLA matrix is confirmed by the appearance of acetate peak position at $\sim 1735 \text{ cm}^{-1}$ in the case of PLA-EVA blend. The presence of EVOH in the PLA matrix is confirmed by the presence of hydroxyl peak in the wavenumber region ranging from 3000-3300 cm^{-1} in the case of PLA-EVA-EVOH blends. Otherwise, the FTIR spectra for PLA and its blends remain almost unaltered due to the existence of similar functionalities in both the cases.

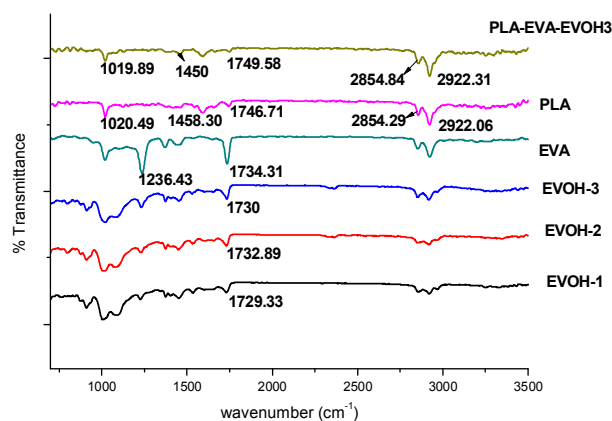


Figure 7.2 FTIR Spectra for EVA, EVOH with different hydroxyl value, PLA and PLA-EVA- EVOH-3.

7.3.3 Mechanical Properties

The tensile, flexural, elongation-at-break (%) and impact strength properties obtained for neat PLA, PLA-EVA and PLA-EVA-EVOH blends are presented in Figure 7.3. It can be seen from the Figure that the tensile strength and tensile modulus values for PLA-EVA and PLA-EVA-EVOH decreased as compared to neat PLA. This is due to the reduction in stiffness induced by the addition of EVA and EVOH in the PLA matrix. In addition to this, it can also be seen from the Figure that the flexural properties for PLA-EVA and PLA-EVA-EVOH blends are found to be reduced as compared to neat PLA. This is an excellent indication of improvement in flexibility for the PLA blends. This is further confirmed by the enhancement in terms of elongation-at-break (%) for PLA-EVA and PLA-EVA-EVOH blends when compared with neat PLA (Figure). The elongation at break (%) values was found to be higher than that of neat PLA for both binary and ternary blends of PLA. In case of PLA, the elongation-at-break (%) is obtained to be 3.5. After addition of EVA in the PLA matrix, the elongation-at-break (%) is found to increase up to 27. With respect to increase in the degree of hydrolysis, the elongation-at-break (%) values were tending to show increment. For, PLA-EVA-EVOH-1, PLA-EVA-EVOH-2 and PLA-EVA-EVOH-3, the elongation-at-break (%) values are found to be 8.8, 11.8 and 12.5, respectively. This improvement in elongation-at-break (%) values for both PLA-EVA and PLA-EVA-EVOH blends is attributed to the enhancement in ductility of PLA.

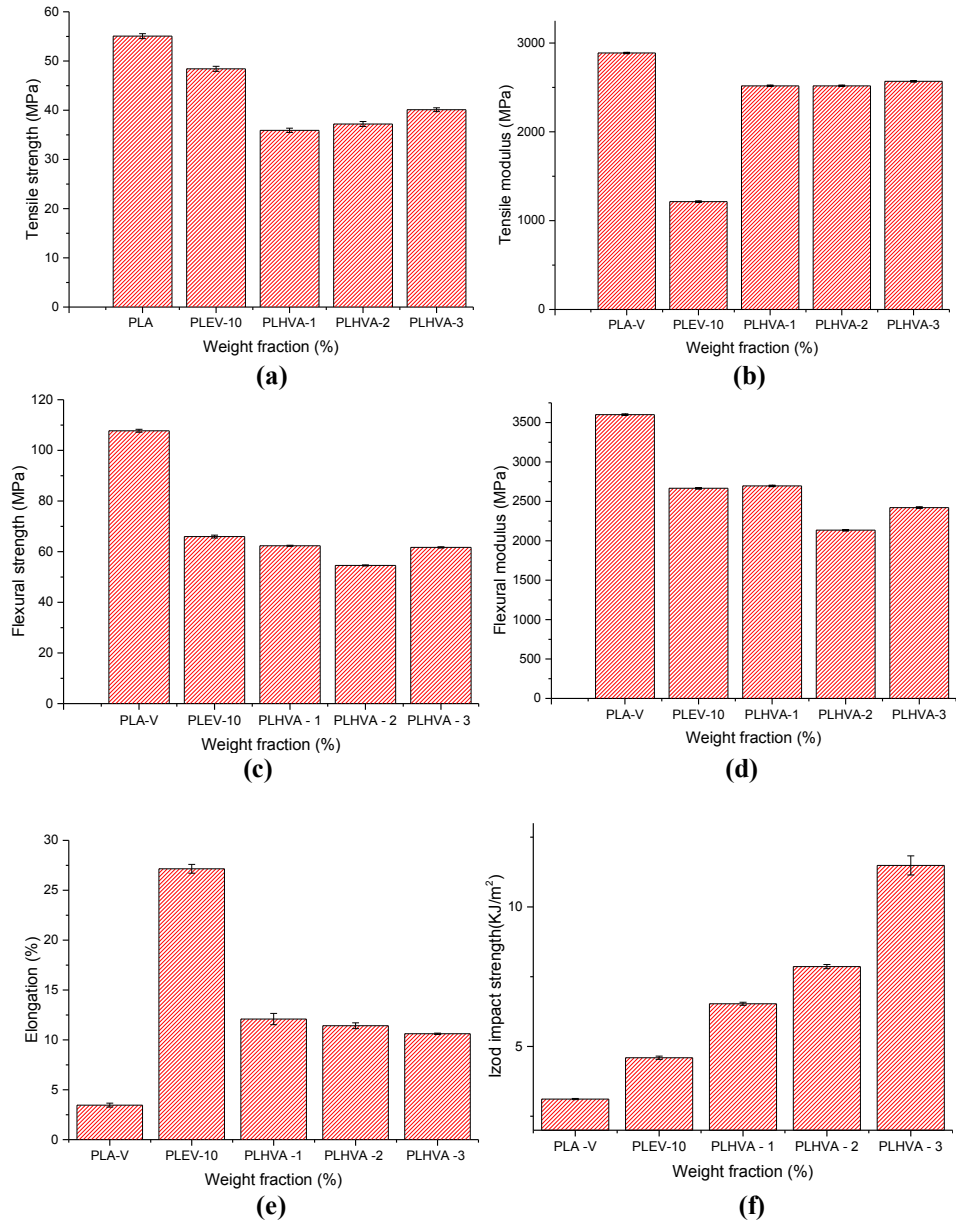


Figure 7.3 Mechanical properties of PLA, PLA-EVA and PLA-EVA-hydrolysed EVA with different degree of hydrolysis as a function of weight fraction a)Tensile strength b)Tensile modulus c) % Elongation d) Flexural strength e)Flexural modulus f)Impact strength

plev

The impact strength (Figure 7.3.f.) of neat PLA was only 3.1 kJ/ m², and the samples fractured clearly in a brittle manner. The impact strength of PLA-EVA with 10 wt% of EVA was higher (4.65 KJ/m²) than that of neat PLA. It can be seen from the Figure that remarkable increase in terms of impact strength was obtained for PLA-EVA-EVOH blends. Like elongation-at-break (%) values, the impact strength also tends to increase with respect to increase in degree of hydrolysis. The impact strength for ternary blend of PLA-EVA-EVOH-1 with hydroxyl value of 32 is found to be 6.58 KJ/m². The impact strength values for PLA-EVA-EVOH-2 (hydroxyl value: 58) and PLA-EVA-EVOH-3 (hydroxyl value: 81) are found to be 7.9 and 11.73 KJ/m², respectively. The results indicate that the impact strength for PLA-EVA-EVOH-3 blend is increased by ~4 fold in comparison with neat PLA. This may be due to the strong interfacial adhesion between the PLA matrix and the EVOH resulting in brittle to ductile transition. The phase behavior of the ternary blend also played an important role in increasing the toughness of PLA. The elastomeric nature of EVOH enabled to absorb impact energy and acted as stress concentrator during impact deformation which retarded the crack initiation and propagation and subsequently led to better toughness for PLA-EVA-EVOH blends [19].

7.3.4 Toughening mechanism via surface morphology of impact fractured surface

To further study the toughening effect of PLA binary and ternary blends, the fracture surface of impact specimens was investigated using SEM analysis. The morphology images obtained for PLA, PLA-EVA

and PLA-EVA-EVOH blends are shown in Figure 7.4. It can be seen from the Figure 7.4 (a) that the neat PLA showed a smooth and featureless brittle fracture surface with no plastic deformation. The PLA-EVA blend with 10 wt. % of EVA content showed a clear stress-whitening surface (Figure 7.4(b)). In addition to this, presence of oval cavities around the matrix can also be seen from Figure 7.4 (b), which is indicative of deformation. The dispersed EVA in the PLA matrix cavitates and de-bond upon application of load. Particulate cavitation and void formation generate new stress whitening that facilitates the deformation of matrix. The plastic deformation effectively helps in energy dissipation and attaining high impact strength for PLA matrix [20, 21].

The Figure 7.4(c) shows the morphology of ternary blend of PLA containing EVOH with a DOH value of 81%. The mechanical properties of the blends can be correlated with the morphology of the blends. It can be seen that surface of the dispersed phase contained more and longer fibril threads by the addition of EVA and EVOH. This indicates greater adhesion between PLA and toughening agent. The observation supports the increase in impact strength. The addition of EVA and EVOH helps in sharing the load. Along with this, the presence of EVA and EVOH make substantial contribution towards energy dissipation and there by prevents the formation of cracks. This is due to this reason; enhancement in terms of toughness is achieved for the PLA blends. There is no observation regarding “pulling out phenomenon” for both PLA-EVA and PLA-EVA-EVOH blends. This reveals the fact that PLA exhibits excellent compatibility with EVA and EVOH elastomers [22].

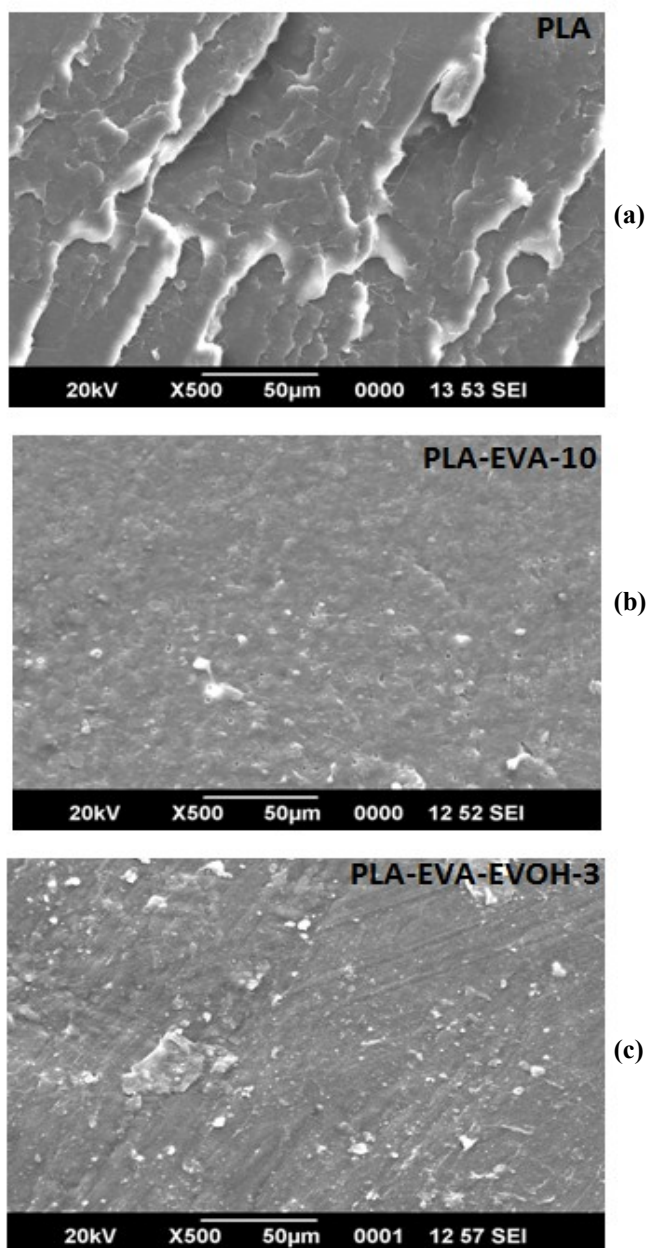


Figure 7.4 SEM micrographs of impact fracture surfaces of (a) neat PLA, (b) PLA-EVA-10 and (c) PLA-EVA-EVOH-3

7.3.5 Thermogravimetry Analysis

The thermal properties for neat PLA, PLA-EVA and PLA-EVA-EVOH blends are investigated using TG analysis. The TGA and DTG curves for PLA and its blends are presented in Figure 7.5. It can be seen from the Figure 7.5(a) that thermal degradation of PLA starts around 347 °C. The degradation of PLA corresponds to hydrolysis, lactide reformation, oxidative main chain scission, and inter or intramolecular transesterification reactions [23]. Unlike PLA, PLA-EVA blend exhibits two stages of degradation. The first stage of degradation for PLA-EVA blend is found to be in the temperature range of 310-355 °C. This weight loss that occurs in this region corresponds to the removal of acetic acid from EVA. As a part of de-acetylation process, small fractions of ketone, carbon dioxide and carbon monoxide also evolve during the degradation process of EVA [24]. The second stage of degradation for PLA-EVA blend occurs in the temperature range of 355-450 °C. The weight loss that corresponds to this degradation step is due to the chain scission reaction. Similar to PLA-EVA blend, PLA-EVA-EVOH blends also exhibit two stage degradation process. However, the slightly earlier degradation of PLA-EVA-EVOH (300-440 °C) blend may be due to the decomposition of PLA induced by the presence of hydroxyl groups in the EVOH.

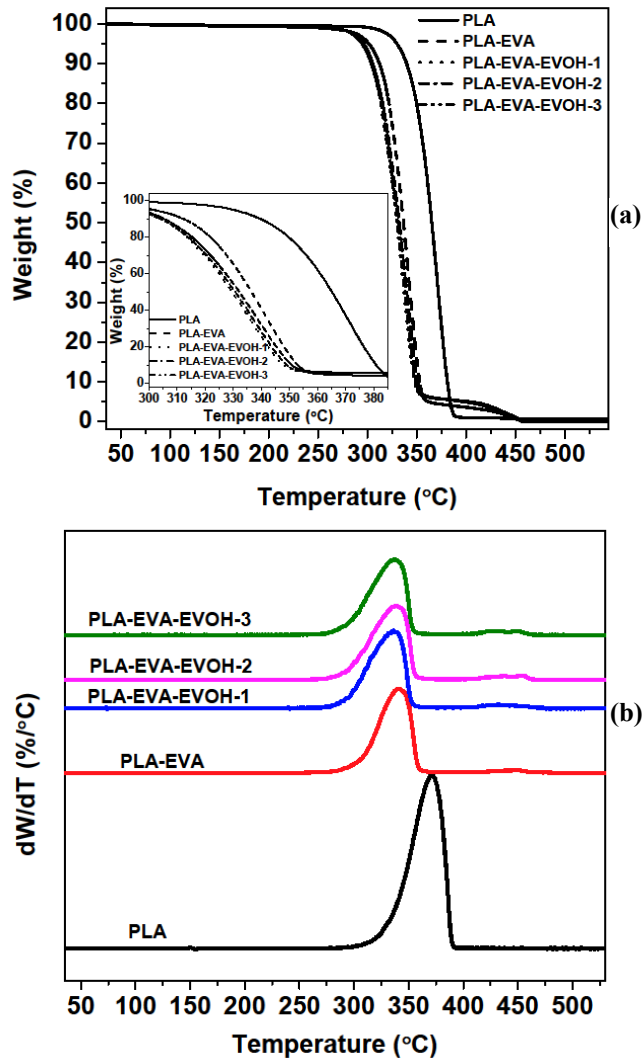


Figure 7.5 (a) TGA and (b) DTG curves for PLA, PLA-EVA and PLA-EVA-EVOH blends

The comparative investigation of thermal degradation profiles of PLA, PLA-EVA and PLA-EVA-EVOH blends was carried out at various degradation points. The degradation points include the temperature at which degradation starts (T_{onset}) and temperature at which 50% weight

loss occurs ($T_{50\%}$). Also, the temperature at which maximum rate (T_{\max}) of degradation occurs is interpolated from the derivative weight loss curve for PLA, PLA-EVA and PLA-EVA-EVOH blends. The temperature at various degradation points (T_{onset} , $T_{50\%}$ and T_{\max}) for PLA, PLA-EVA and PLA-EVA-EVOH blends are tabulated in Table 7.3. In case of PLA, the T_{onset} , $T_{50\%}$ and T_{\max} values are found to be 347 °C, 364 °C and 371 °C, respectively. While case of PLA-EVA blend, the T_{onset} , $T_{50\%}$ and T_{\max} values are found to be 318 °C, 336 °C and 341 °C, respectively. After addition of EVOH in the PLA-EVA blend, further reduction in the T_{onset} , $T_{50\%}$ and T_{\max} values are observed as compared to neat PLA and PLA-EVA blend. It can be seen from the Table 7.3. that the thermal stability of PLA-EVA-EVOH blends decreases with increase in hydrolysis time. However, the final decomposition temperature in case of PLA-EVA and PLA-EVA-EVOH blends can be noticed at 450 °C. While in case of PLA, complete decomposition occurs at 400 °C. This indicates that addition of EVA and EVOH in the PLA matrix helps to prolong the complete degradation process.

Table 7.3 TGA results for PLA, PLA-EVA and PLA-EVA-EVOH blends

Sample Name	T_{onset}	$T_{50\%}$	T_{\max}
PLA	347.10	364.01	371.01
PLA-EVA	318.20	336.02	341.12
PLA-EVA-EVOH-1	314.81	334.30	338.85
PLA-EVA-EVOH-2	311.49	332.17	336.58
PLA-EVA-EVOH-3	310.23	330.57	336.58

Thermal Degradation Kinetic Analysis

The thermal degradation kinetic analysis for PLA, PLA-EVA and PLA-EVA-EVOH blends is carried out in order to have knowledge about degradation behavior of the blends as compared to neat PLA. The thermal degradation of PLA, PLA-EVA and PLA-EVA-EVOH blends can be given by the following expression:

$$\frac{d\alpha}{dt} = kf(\alpha) \dots\dots\dots (7.2)$$

where, “ α ” represents the degree of conversion or the fraction decomposed [$\alpha = (w_0 - w_t) / (w_0 - w_f)$, w_0 , w_t , and w_f correspond to the polymer weight present at initial, time t , and final conditions], $d\alpha/dt$ represents the conversion rate, “ k ” is the temperature-degradation rate constant, and $f(\alpha)$ represents the differential expression of a kinetic model function and is dependent on the particular degradation mechanism [25-28].

The temperature dependent degradation rate constant (k) is given by the following Arrhenius equation:

$$k = A \exp\left(\frac{-E_a}{RT}\right) \dots\dots\dots (7.3)$$

where, “ A ” is the pre-exponential factor (s^{-1}), “ E_a ” corresponds to the apparent activation energy of the degradation reaction (kJ/mol), “ R ” refers the universal gas constant ($8.314 \text{ J mol}^{-1} \text{ K}^{-1}$), and “ T ” is the absolute temperature (K). Substituting “ k ” from Eq. (3) into Eq. (2), a general expression for the kinetic process under isothermal conditions can be derived and expressed as

$$\frac{d\alpha}{dt} = A \exp\left(\frac{-E_a}{RT}\right) f(\alpha) \quad \dots\dots\dots (7.4)$$

In the current work, the thermal degradation kinetic study of PLA and PLA blends is carried out under non-isothermal conditions, where samples are heated with a constant heating rate, $\beta = dT/dt$. Hence, Eq. (4) is transformed into an equation that can describe the degradation reaction rate as a function of temperature and then expressed as follows:

$$\left(\frac{d\alpha}{dT}\right) = \frac{A}{\beta} \exp\left(\frac{-E_a}{RT}\right) f(\alpha) \quad \dots\dots\dots (7.5)$$

Eqs. (4) and (5) are the fundamental expressions useful for calculation of kinetic triplets on the basis of data obtained by TGA. The degradation reaction is assumed to be a simple n^{th} order reaction and kinetic model function, $f(\alpha)$, as $(1-\alpha)^n$, where “ n ” is the order of reaction [29,30].

Integration on both sides of the equation (5) and rearrangement results in the following expression

$$g(\alpha) = \int_0^\alpha \frac{d\alpha}{f(\alpha)} = \frac{A}{\beta} \int_0^T e^{\frac{-E_a}{RT}} dT \quad \dots\dots\dots (7.6)$$

where, $g(\alpha)$ corresponds to the integral function of conversion degree, α .

Coats-Redfern method

Using eq. (6) and putting $f(\alpha) = (1-\alpha)^n$ and $x = E_a/RT$ and rearranging, we get:

$$g(\alpha) = \frac{ART^2}{\beta E_a} \left(1 - \frac{2RT}{E_a}\right) \exp\left(\frac{E_a}{RT}\right) \dots\dots\dots (7.7)$$

$g(\alpha)$ can be written in different ways for different n values.

When

$$n = 1, g(\alpha) = -\ln(1 - \alpha) \dots\dots\dots (7.8)$$

When

$$n \neq 1, g(\alpha) = \frac{1}{n-1} \left[(1 - \alpha)^{1-n} - 1 \right] \dots\dots\dots (7.9)$$

The combination of equations (8) and (9) and by rearrangement, we get:

$$n = 1, \ln\left(\frac{-\ln(1 - \alpha)}{T^2}\right) = \ln\left[\frac{AR}{\beta E_a} \left(1 - \frac{2RT}{E_a}\right)\right] - \frac{E_a}{RT} \dots\dots\dots (7.10a)$$

$$n \neq 1, \ln\left(\frac{1 - (1 - \alpha)^{1-n}}{(1 - n)T^2}\right) = \ln\left[\frac{AR}{\beta E_a} \left(1 - \frac{2RT}{E_a}\right)\right] - \frac{E_a}{RT} \dots\dots\dots (7.10b)$$

Plotting the left hand side term versus $-1/T$ gives the straight line and activation energy is obtained from the slope of the straight line. The value of the pre-exponential factor, A is obtained from intercept of the straight line, by considering the expression $\left(1 - \frac{2RT}{E_a}\right)$ inside the parenthesis as 1. Analysis is done using only single heating data, which is different from other kinetic models where multiple heating data are required for analysis.

The Coats-Redfern method requires TG data with only one heating rate to calculate kinetic parameters such as activation energy (E_a), reaction order (n) and pre-exponential factor (A). In this study, TGA data of PLA and PLA blends are obtained at a single heating rate (10 °C/min). For this method, a reaction order “ n ” is assumed and the assumed value is substituted in eq. (10a) and (10b). The plot of the left hand side of the eq. (10a) and (10b) versus $-1/T$ is fitted to calculate the R^2 values. This process is repeated until the best R^2 value is obtained.

Figure 4 represents the linear fitted graph for neat PLA, PLA-EVA and PLA-EVA-EVOH blends for different “ n ” values. The reaction order which is obtained at the best R^2 value is regarded as the reaction order for PLA, PLA-EVA and PLA-EVA-EVOH blends (Table 7.4). Then the activation energy and the pre-exponential factor are obtained from the slope and intercept of the fitted straight line. The activation energy of neat PLA, PLA-EVA, PLA-EVA-EVOH-1, PLA-EVA-EVOH-2 and PLA-EVA-EVOH-3 is found to be 176, 173, 150, 146 and 145 kJ/mol, respectively. The decrement in the activation energy is an indication of reduction in thermal stability for PLA matrix upon addition of EVA and EVOH elastomers.

Table 7.4 Activation energy (E_a) and Regression coefficient (R^2) for PLA, PLA-EVA and PLA-EVA-EVOH blends

Sample Name	Activation energy (E_a)	Regression coefficient (R^2)
PLA	175	0.993
PLA-EVA	173	0.995
PLA-EVA-EVOH-1	150	0.995
PLA-EVA-EVOH-2	146	0.996
PLA-EVA-EVOH-3	145	0.993

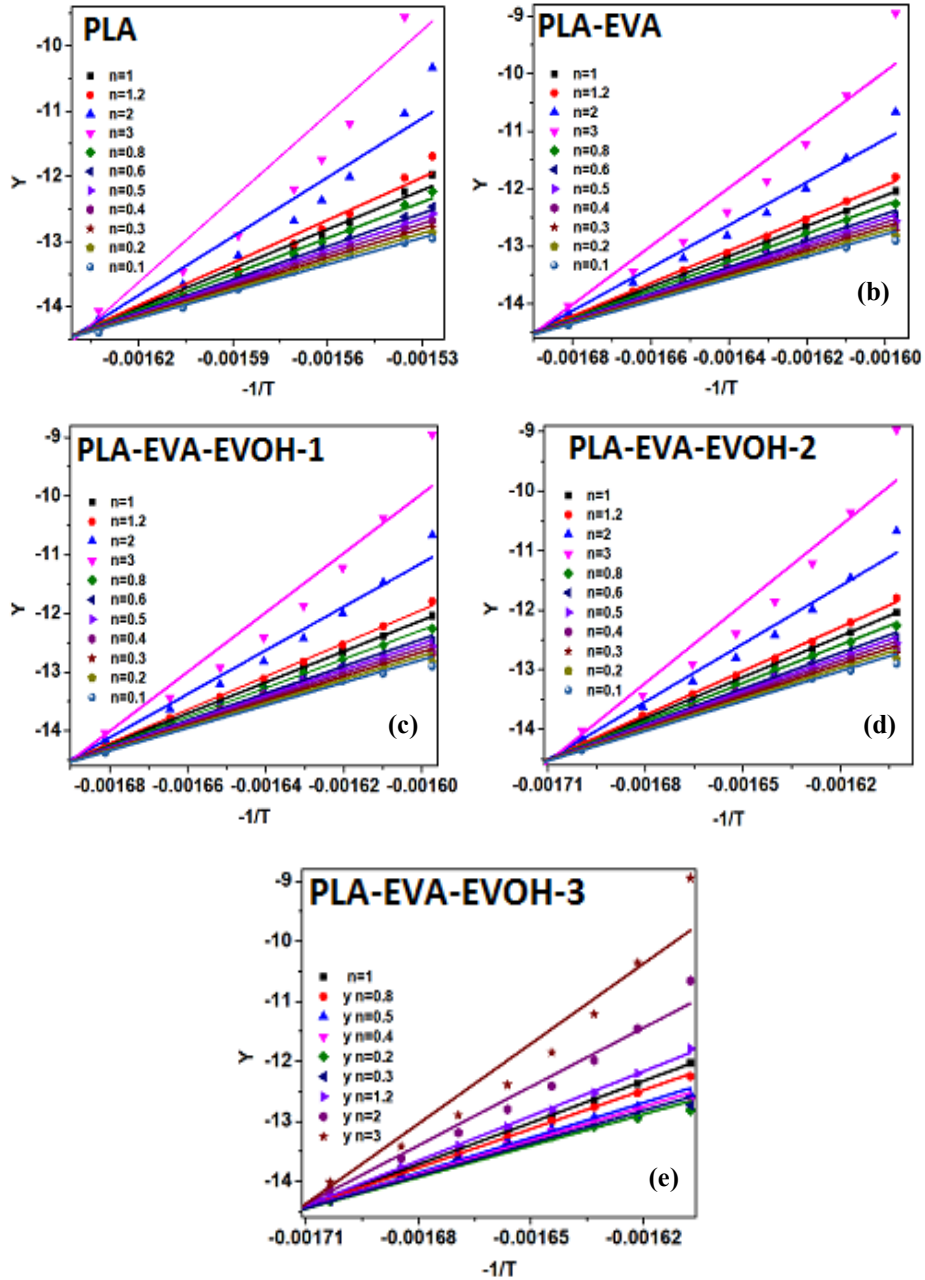


Figure 7.6 Determination of kinetic parameters by left part in eqn (10 a and b) against using coats-redfern method: (a) PLA, (b) PLA-EVA and (c) PLA-EVA-EVOH blends

7.3.6 Differential Scanning Calorimetry (DSC)

DSC thermographs for PLA, PLA-EVA and PLA-EVA-EVOH blends during second heating and first cooling cycles are represented in Figure 7.7 (a) and (b), respectively. The thermal properties for PLA, PLA-EVA and PLA-EVA-EVOH blends such as glass transition temperature (T_g), melting temperature (T_m), and cold crystallization temperature (T_{cc}) are considered from the DSC thermograph obtained during the second heating cycle at a heating ramp of 10 °C/min and are reported in Table 7.5. While, the melt crystallization temperature (T_{mc}) for PLA, PLA-EVA and PLA-EVA-EVOH blends is considered from the DSC thermograph which is obtained during the first cooling cycle at a cooling ramp of 10 °C/min and are reported in Table 7.5. It can be noticed from the Figure that the peak that corresponds to melting temperature of PLA appears at 170 °C. The melting peak of PLA is unimodal and endothermic in nature, which in turn indicates the α -crystalline arrangement of PLA [29-31]. The stable crystal formation in PLA is confirmed by the absence of double melting peak. This may be due to the occurrence of homogeneous nucleation process in PLA [32]. The melting peak obtained for PLA-EVA and PLA-EVA-EVOH blends is also found to be unimodal and endothermic in nature. The unimodal nature of endothermic peak confirms the formation of stable crystals with uniform thickness with the addition of EVA and EVOH in the PLA matrix.

The non-isothermal cold crystallization temperature for PLA, PLA-EVA and PLA-EVA-EVOH blends are reported in Table 7.5. It can be noticed that crystallization temperature for PLA-EVA and PLA-

EVA-EVOH decreases as compared to neat PLA (Table 7.5). With respect to increase in the degree of hydrolysis, it is observed that the prominent reduction in the crystallization temperature for PLA-EVA-EVOH blends. Due to the nucleating effect of EVOH, crystallization phenomenon is initiated at a lower T_{cc} which in turn resulted in the development of stable and thick crystals. The reduction in the T_{cc} values is an indication of requirement of less energy for achieving desired degree of crystallinity. In case of glass transition temperature, it remains unaffected for both PLA-EVA and PLA-EVA-EVOH blends in comparison with PLA. The non-isothermal melt crystallization temperature (T_{mc}) for PLA, PLA-EVA and PLA-EVA-EVOH blends are reported in Table 7.5. The T_{mc} values for PLA-EVA and PLA-EVA-EVOH blends seem to increase as compared to neat PLA. With respect to increase in degree of hydrolysis, further increment in the T_{mc} values for PLA-EVA-EVOH blends can be seen in comparison with PLA-EVA blend. This is due to the fact that EVOH helps in enhancing the crystallization of PLA by promoting the heterogeneous nucleation process. The crystallinity (%) for PLA matrix is increased after blending with EVA and EVOH.

Table 7.5 DSC results for PLA, PLA-EVA and PLA-EVA-EVOH blends

Sample Name	T_g	T_{cc}	ΔH_c	T_m	ΔH_m	χ
PLA	62.17	106.13	25.55	170.87	35.44	37.86
PLA-EVA	58.88	97.39	8.95	168.81	50.31	53.75
PLA-EVA-EVOH-1	59.20	84.78	16.25	169.11	48.87	51.89
PLA-EVA-EVOH-2	60.85	79.86	12.79	166.22	44.07	47.09
PLA-EVA-EVOH-3	63.70	83.32	16.12	167.24	44.53	47.57

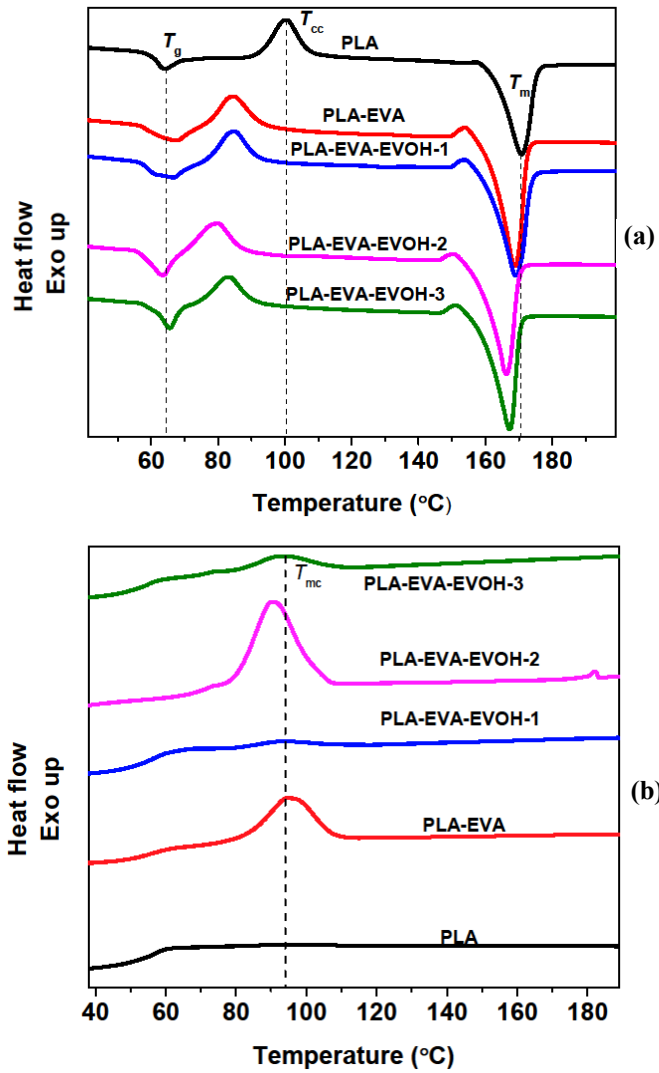


Figure 7.7 DSC curves of (a) second heating and (b) first cooling thermographs for PLA, PLA-EVA and PLA-EVA-EVOH blends

7.4 Conclusions

The FTIR results elucidate the increase in intensity of the hydroxyl peak ($3200\text{-}3400\text{ cm}^{-1}$) with increase in degree of hydrolysis. The highest degree of hydrolysis (81%) is achieved for EVOH-3. The increase in the degree of hydrolysis has brought prominent improvement in the mechanical properties such as elongation at break (12.5 %) and impact strength (11.73 (KJ/m²)) for ternary blends of PLA matrix. The DSC results confirm the nucleation effect of EVOH by reducing the cold crystallization temperature for PLA. The decrement in the activation energy for PLA-EVA-EVOH blends is observed when compared with neat PLA. This is an indication of reduction in thermal stability due to decomposition of hydroxyl group present in the EVOH. The SEM images depict good compatibility among PLA and its blends.

The work included in this chapter has been published:

“Super Toughened Renewable Poly(lactic acid) Based Ternary Blends System: Effect of Degree of Hydrolysis of Ethylene Vinyl Acetate on Impact and Thermal Properties” - V H Sangeetha, Ravibabu Valppa, T O Varghese, S K Nayak, RSC Advances, 2016, 76 (6)72681-72691

References

- [1] E. T. H. Vink, K. r. Rabago, D. A. Glassner and P. R. Gruber, *Polym Degrad Stabil*, 2003, 80, 403-419
- [2] S. Corneillie and M. Smet, *Polym Chem*, 6 (2015) 850.
- [3] A. Mujica-Garcia, S. Hooshmand, M. Skrifvars, J. M. Kenny, K. Okasman, L. Peponi, *RSC Adv*, 6 (2016) 9221.
- [4] R. B. Valapa, G. Pgazhenthil, V. Katiyar, *RSC Adv*, 5 (2015) 28410.
- [5] Z. J. Zhang, W. Cui, H. Xu, L. Xie, H. Liu, L. M. Zhu, H. Li, R. Ran, *RSC Adv*, 5 (2015) 16604.
- [6] M. R. Aghjeh, M. Nazari, H. A. Khonakdar, S. H. Jafari, U. Wagenknecht, G. Heinrich, *Mater Design*, 88 (2015) 1277.
- [7] M. P. Arrieta, J. Lopez, D. Lopez, J. M. Kenny, L. Peponi, *Eur Polym J*, 73 (2015) 433.
- [8] J. P. Mofokeng, I. Kelnar, A. S. Luyt, *Polym Test*, 50(2016) 9.
- [9] T. Yokohara, M. Yamaguchi, *Eur Polym J*, 44 (2008) 677.
- [10] J. P. Mofokeng and A. S. Luyt, *Thermochim Acta*, 613 (2015) 41.
- [11] Q. Lv, D. Wu, H. Xie, S. Peng, Y. Chen, C. Xu, *RSC Adv*, 6 (2016) 37721.
- [12] J. D. Martin, S. S. Velankar, *J. Rheol.* 2007, 51, 669.
- [13] M. Pracella, M. M. Haque, M. Paci, V. Alvarez, *Carbohydr Polym*, 137 (2016) 515.
- [14] P. Ma, D.G. Hristova-Bogaerds, J. G. P. Goossens, A. B. Spoelstra, Y. Zhang, P. J. Lemstra, *Eur Polym J*, 48 (2012) 146.

- [15] S. P. Tambe, S. K. Singh, M. Patri, D. Kumar, *Prog. Org. Coat.* 62 (2008) 382.
- [16] M. A. Rodriguez-Perez, R. D. Simoes, C. J. L. Constantino, J. A. De Saja, *J Appl Polm Sci*, 121(2011) 2324.
- [17] H. S. Mobarakeh, A. Yadegari, J. Didehvar and F. Khakzad-Esfahalm, *J. Polym. Eng*, 33 (2013) 843.
- [18] R. B. Valapa, G. Pugazhenthii, V. Katiyar, *J. Appl. Polym. Sci.*, 2015, 132, 41320.
- [19] Y. Y. Leu, Z. A. M. Ishak and W. S. Chow, *J Appl Poly Sci.* 124 (2012) 1200
- [20] P. Choudhary, S. Mohanty, S. K. Nayak and Unnikrishnan, *J Appl Poly Sci*, 121, (2011) 3223.
- [21] Z. A. Kusmono M. Ishak W. S. Chow, T. Takeichi and Rochmadi, *Composites Part A*, 95(2008) 627.
- [22] Y. Wang, K. Chen, C. Xu and Y. Chen, *J Phys Chem B*, 119(2015) 12138.
- [23] Jamshidi, S. H. Hyon, Y. Ikada, 29 (1988) 2229.
- [24] S. B. Mishra, A. S. Luyt, *J Appl Polym Sci*, 112(2009) 218.
- [25] I. Armentano, N. Bitinis, E. Fortunati, S. Mattioli, N. Rescignano, R. Verdejo, M. A. Lopez-Manchado, and J. M. Kenny, *Prog Polym Sci* (2013)38, 1720.
- [26] D. F. Wu, L. Wu, L. F. Wu, M. Zhang, *Polym Degrad Stab*, 91 (2006) 3149.
- [27] A. Khawan, D. R. Flanagan, *J Phys Chem B*, 110 (2006)17315.
- [28] R. B. Valapa, G. Pugazhenthii, V. Katiyar, *Int J Biol Macromol*, 65 (2014) 275

- [29] E.I Yuzay, R. Auras, H. Valdez, S. Selke, *Polym Degrad Stab*, 95 (2010) 1769.
- [30] Y. S. Hirata, Q. T. Marais, C. Nguyen, J. Cabot, Suvage, *J. Membr. Sci.* (1993) 32, 295
- [31] W. Hoogsteen, A. R. Postema, A. J. Pennings, and G. T Brinke, *Macromolecules*, 1990, 23 634-642
- [32] F. Peng, M. T. Shaw, J. R. Olson and M. J. Wei, *J Phys Chem C*, 2011, 115, 15743-1575.

.....❧.....

**EFFECT OF NANOCELLULOSE ON TOUGHENED
PLA / EVA /HYDROLYSED EVA TERNARY
BLEND SYSTEM**

Contents	8.1 <i>Introduction</i>
	8.2 <i>Experimental</i>
	8.3 <i>Testing and Characterisation</i>
	8.4 <i>Results and Discussion</i>
	8.5 <i>Conclusion</i>

Nanofibrillated cellulose was isolated from cotton waste via steam explosion technique. The effect of nanocellulose on mechanical, thermal and morphological properties of EVA/EVOH toughened PLA was investigated. The composites of nanocellulose filled toughened PLA was prepared by melt mixing technique using twin screw extruder and subsequent injection molding. Nanocomposites prepared were characterised by SEM, TEM, DSC, TGA etc. For PLA/EVA/EVOH nanocellulose composites, the tensile modulus and percentage elongation was increased significantly by the addition of 2 wt. % of nanocellulose. The impact strength was increased upto 89 % by the addition of 2 wt. % of nanocellulose. However, the crystallization temperature decreased by the addition of nanocellulose upto 2 wt. % in the PLA matrix.

8.1 Introduction

Cellulose and nanocellulose including nano fibrillated cellulose and nanocrystals can act as biological reinforcing agents for biopolymers. The addition of renewable and biodegradable fillers like cellulose or cellulose derivatives could optimize the cost performance balance and also improve the mechanical and thermal behaviors [1].

In most cases, the addition of toughening agent like elastomers at low weight percentage alone results in the decline in tensile strength and modulus of PLA. For PLA systems toughened with another resin, good toughness-strength balance may be obtained using nanoparticles as a third component, which strongly depends on the morphology of dispersed phase and also on the interfacial adhesion between the components [2,3]. Nanocellulose with PLA or PLA copolymers as matrix significantly help to improve its properties and overcome its shortcomings. Several studies have been performed using some fillers such as clay minerals, carbon nanotubes, graphene and its precursor to obtain nanocomposite materials[4–7].

Several research and development units have targeted on developing toughened PLA biodegradable polymer. In this chapter, studies on the mechanical, thermal, barrier and biodegradability properties of nanofibrillated cellulose (NFC) filled toughened PLA nanocomposites.

8.2 Experimental

8.2.1 Materials

The details of the polymers and chemicals used for the study are discussed in Chapter 2 (section 2.1) Nanofibrillated cellulose was isolated from waste cotton via steam explosion technique (chapter 3).

8.2.2 Preparation of Nanocomposites

The nanocomposites whose composition as given in Table 8.1 were prepared by simultaneous addition of all components to twin screw extruder. The screw speed was 60 rpm and extrusion barrel temperatures were fixed in the range of 165-190 °C from the feed section to the die head. The extruded materials were injection molded into standard tensile, flexural and Izod impact test specimens. All test specimens were dried and kept in desiccator prior to analysis.

Table 8.1 Material composition of nanocomposites

Material designation	PLA (%)	EVA (%)	EVOH (%)	NC (%)
PLA/EVA/EVOH	90	5	5	-
PLA/EVA/EVOH/NC 1	90	5	5	1
PLA/EVA/EVOH/NC 2	90	5	5	2
PLA/EVA/EVOH/NC 3	90	5	5	3

8.3 Testing and characterisation

8.3.1 Mechanical Properties

The tensile properties of all the composite samples were performed at standard laboratory atmosphere as per ASTM D-638 using Shimadzu Autograph model AG-IS 50KN with a cross-head speed of 10mm/min.

The flexural properties were determined by three-point bending test and were performed in accordance with ASTM D790-Type B using Universal testing machine. The span length was set at about 96mm. Testing speed was set at 2 mm/min.

The Izod impact strength tests of all composites were carried using Tinius Olsen IT 504 impact tester, USA as per ASTM D-256. The specimen dimensions were of 63.5 mm x 12.7 mm with a notch depth of 2.54 mm and notch angle of 45°.

8.3.2 Scanning Electron Microscopy

The SEM of tensile fractured specimens was carried out using JEOL-6390LV (Germany). The samples were sputtered with platinum and were dried for half an hour in vacuum, prior to study.

8.3.3 Transmission Electron Microscopy

TEM was used to characterise the prepared nanocomposites. TEM images of nanocomposites were performed in a Transmission Electron Microscope, J, JEM 2100 TEM mode, JEOL, Japan, operated at an accelerated voltage of 200 kV. The ultra thin size samples of less than 100 nm for the imaging have been prepared using a Cryo Leica EM UC6 instrument (Leica Microsystems, Switzerland) with diamond knife and viewed without staining.

8.3.4 Thermal properties

DSC Analysis:

Thermal characterisation of all the nanocomposites were performed using Q20 model TA instruments, Walters, USA with a

double cycle of heating from 30 to 210 °C at 10 °C/min separated by a single cooling cycle at 10°C/min kept at isothermal for 5 minutes at 210 and 30°C. Glass transition temperature, crystallisation temperature, melting point, crystallisation enthalpy and melting enthalpy were determined by heating and cooling scans. The percentage crystalline of PLA/EVA/EVOH/NFC was determined using the following equation [8.1].

$$\chi_c = \frac{\Delta H_m - \Delta H_{cc}}{\Delta H_o (1 - wt\% \frac{nfc}{100})} * 100 \dots\dots\dots (8.1)$$

Where ΔHm is the enthalpy of melting, ΔHcc is the cold crystallisation temperature and ΔHo is the enthalpy of crystallisation of 100% crystalline PLA (93.7 J /g) and nfc is nano fibrillated cellulose added as reinforcement.

Thermo-gravimetric Analysis (TGA):

The thermal stability of the samples were investigated by TGA analysis using Q50, TA instruments, Walters, USA under nitrogen atmosphere from room temperature to 600 °C at a heating rate of 10 °C /min

8.4 Results and discussions

8.4.1 Mechanical Properties

The effect of nanofibrillated cellulose on mechanical properties of PLA/EVA/EVOH ternary blend system is shown in Figure 8.1. The mechanical parameters such as tensile strength, modulus, and elongation at break are key factors in evaluating polymeric nanocomposites. The nanofibrillated cellulose was added at 1, 2, and 3 wt. % in PLA /EVA/ EVOH ternary blend system. The tensile strength values were decreased

from 54.9 for virgin PLA to 34.3 by the addition of 3 wt % of nanocellulose in toughened PLA matrix. The decrease in tensile strength for the biocomposites may be ascribed to aggregation of the NFC due to Vander Waal's forces of attraction.[8]but the addition of nano cellulose upto 2 wt % retained the tensile strength of PLA/EVA/ EVOH ternary blend systems.

At 1 wt.% nano fibrillated cellulose addition, modulus was found to be 2480 MPa. With the incorporation of 2 wt.% nano fibrillated cellulose, the modulus increased to 2920 MPa compared to virgin PLA. With increase in nanocellulose again (3 wt.%) decreased the modulus. This means that a particular weight of loading of nanocellulose contributed to the stiffness and thereby enhancement of modulus by forming a fibrillated network structure. Also high percentage crystallinity of nanocellulose might have contributed in improved stiffness in the biocomposites [9,10]

However, higher concentration of nanocellulose in ternary blends resulted in decrease of mechanical properties which may be due to incompatibility of the system. The percentage elongation at break showed 214 % increase in the case of PLA/EVA/EVOH/NC 2 system in comparison to virgin PLA. The sudden enhancement in the percentage elongation can be due to the combined effect that is plasticisation by EVA/EVOH together with the strong interactions between polymeric groups of PLA and hydroxyl groups of nano cellulose. [11, 12]. It reduced drastically with the addition of 3 wt % nanocellulose may be due to less compatibility and wettability with the toughened system. Flexural strength and flexural modulus were also lowered by the addition of nanofibrillated cellulose to toughened blend system.

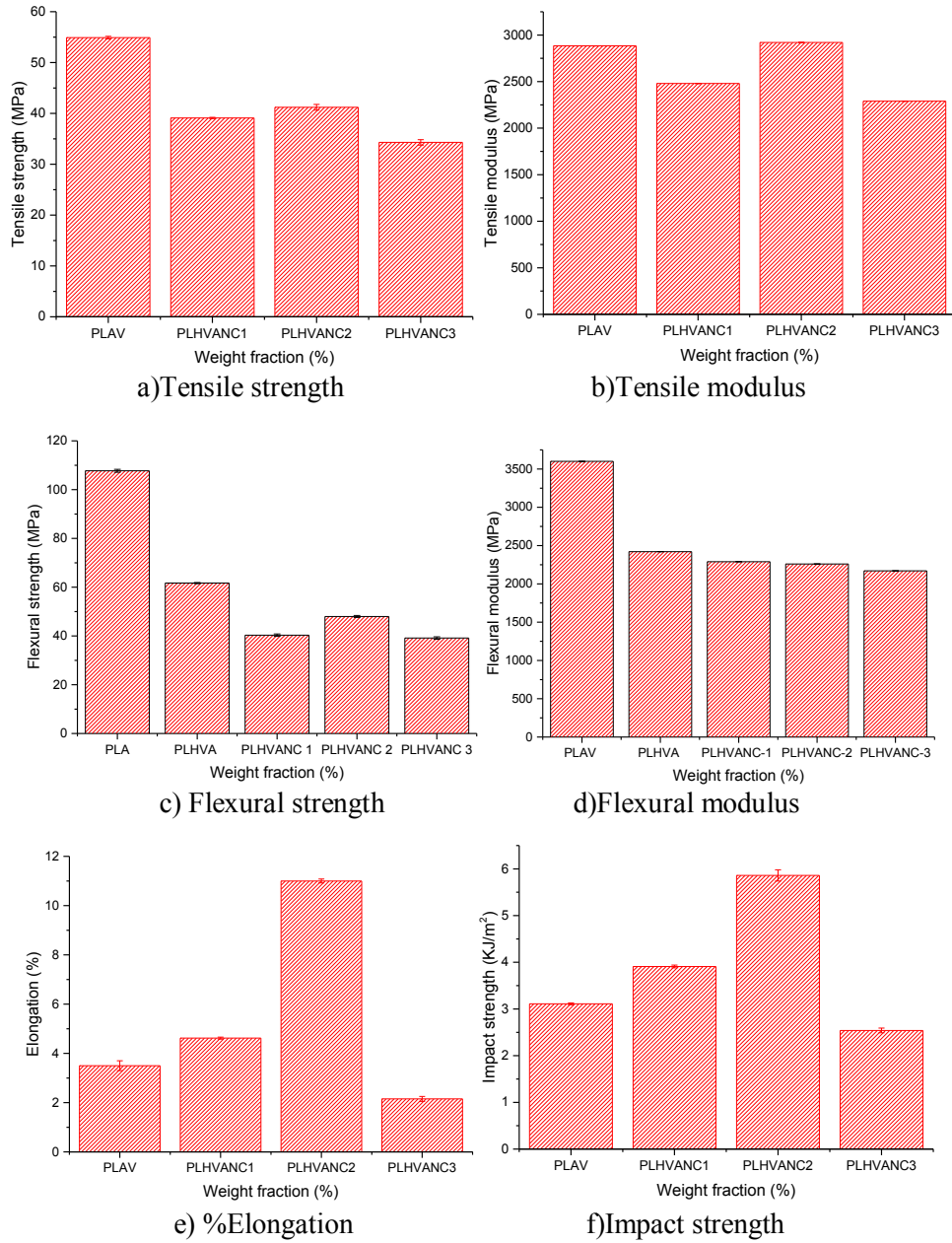


Figure 8.1 Effect of nanofibrillated cellulose on mechanical properties of PLA/EVA/EVOH blend system a) Tensile strength b) Tensile modulus c) Flexural strength d)Flexural modulus e) % Elongation f) Impact strength

The impact value for virgin PLA was found to be 3.1 KJ/m². The impact strength of ternary blends increased to 10.61 KJ/m² in case of PLA/EVA/EVOH ternary blend system in which the degree of hydrolysis of EVOH (81%) contributed to greater compatibility between EVA and PLA. However, with the addition of nanofibrillated cellulose to the ternary blend system, the impact strength got reduced. But impact strength of all the three biocomposites (PLHVANC 1, PLHVANC 2, PLHVANC 3) also showed an enhancement as compared to VPLA. This may be due to the increased energy absorption capacity of PLA biocomposite in the presence of nanocellulose.

8.4.2 Scanning Electron Microscope (SEM):

Scanning electron microscope (SEM) was used to analyse the surfaces of impact fractured samples of PLA and PLA based bionanocomposites (Fig 8.2). All the three concentrations of nanocellulose (1 - 3 wt%) forms a continuous phase with toughened PLA. Partial interfacial adhesion between PLA and cellulose fibres has been reported [14]. This might have brought increase in percentage elongation at optimum weight loading of 2 wt. %, thereafter the elongation also got decreased. SEM observations indicate that a good dispersion of nano cellulose with 2wt% is shown in toughened PLA. The moderate wetting of cellulose in PLA/EVA/EVOH blends may be due to the presence of OH groups in hydrolysed EVA which can react with the hydroxyl groups of cellulose and carboxyl/hydroxyl groups present in PLA. But higher concentration of nanocellulose may get interbonding which restricts the mobility of molecules and hence reduced the elongation.

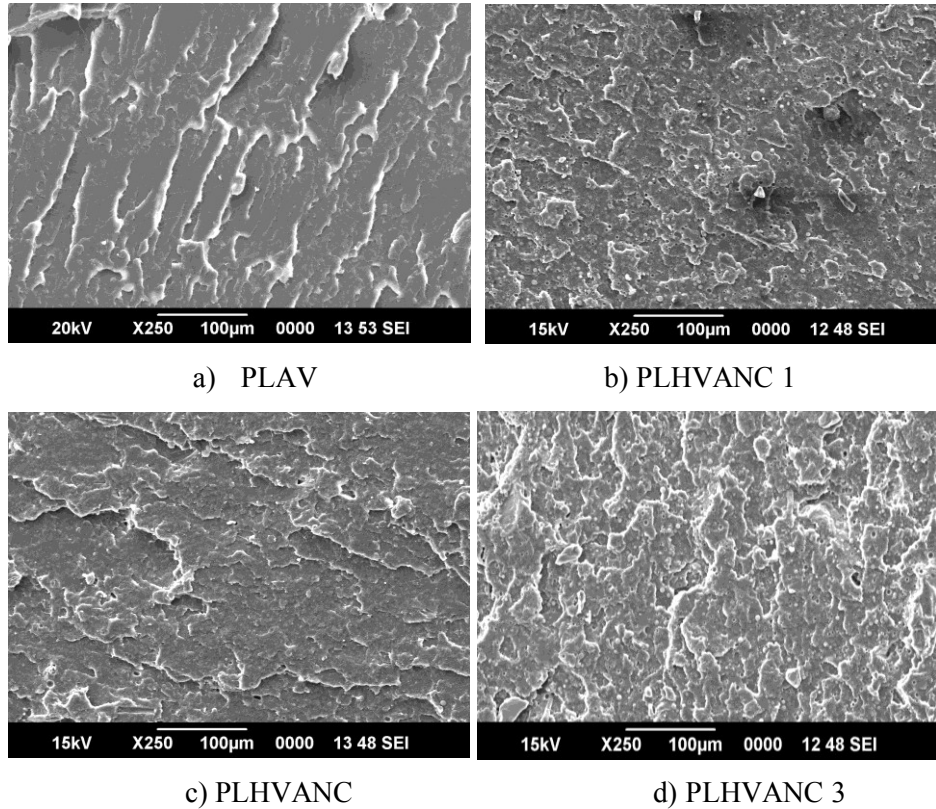


Figure 8.2 SEM images of a) Virgin PLA b) PLHVANC -1 (PLA/EVA/EVOH/NFC-1) c) PLHVANC -2 (PLA/EVA/EVOH/NFC-2) d) PLHVANC -3 (PLA/EVA/EVOH/NFC-3)

8.4.3 Transmission Electron Microscope

Fig. 8.3 shows the TEM images of EVA/EVOH toughened polylactic acid nano composites (PLHVANC 2) taken at 100 nm and 200 nm magnification. Dark region represent the toughened polylactic acid matrix in which nano fibrillated cellulose (grey regions) is dispersed homogenously.

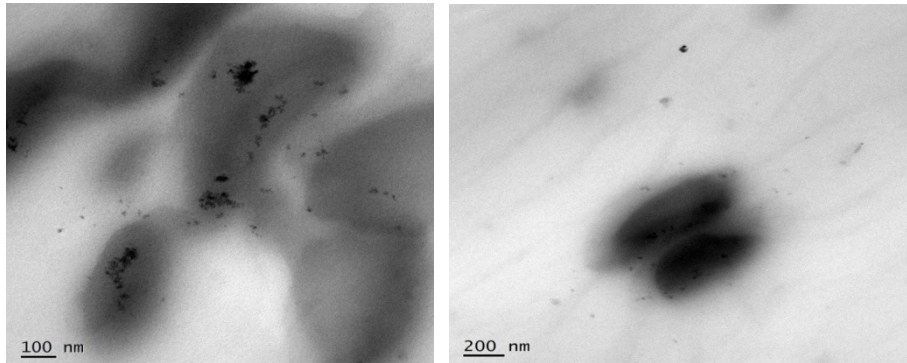


Figure 8.3 TEM images of PLHVANC2 at two different magnifications

8.4.4 Differential Scanning Calorimetry

The non-isothermal cold crystallization temperature for PLA and PLA-EVA/EVOH/NFC composites are reported in Table 8.3. It can be seen from the table that crystallization temperature decreases with respect to increment in nanocellulose loading in the PLA matrix which indicates good compatibility between toughened matrix and nanocellulose. Also, nanocellulose acts as a nucleating agent such that it initiates crystallization phenomenon at a lower T_{cc} resulting in the formation of stable as well as thick crystals. The lower T_{cc} means that less energy is required to achieve the desired degree of crystallinity [13]. The glass transition temperature of PLA decreased with increase in nanocellulose loading in the PLA matrix. Dsc curves for PLA, PLA/EVA/EVOH AND its nanocomposites are shown in Figure 8.4.

Table 8.3 Glass transition (T_g), cold and melt crystallization temperature (T_{cc} and T_{mc}) and melting temperature (T_m) for PLA and its nanocomposites

Materials designation	T_g (°C)	T_{mc} (°C)	T_{cc} (°C)	T_m (°C)	ΔH_c ($\frac{J}{g}$)	ΔH_m ($\frac{J}{g}$)	χ_c (%)
PLA	62.38	89.22	106.13	169.56	23.63	32.63	34.86
PLA/EVA/EVOH	63.70	92.82	83.32	167.24	16.12	44.53	47.57
PLA/EVA/EVOH/NC 1	60.85	91.60	91.47	168.94	20.07	37.52	40.15
PLA/EVA/EVOH/NC 2	61.22	92.23	90.31	168.87	18.02	39.86	42.59
PLA/EVA/EVOH/NC 3	60.09	92.53	89.91	169.23	25.90	50.05	53.47

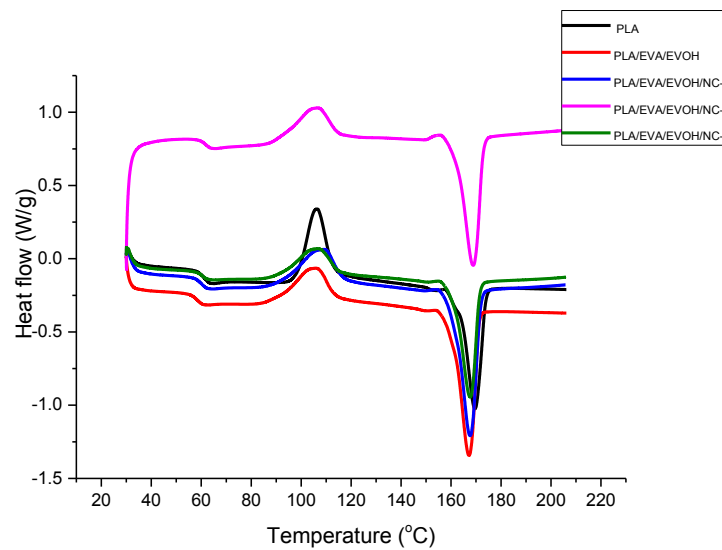


Figure 8.4 DSC curves of PLA and PLA/EVA/EVOH nanocomposites

8.4.5 Thermogravimetric analysis: (TGA)

The table 8.4 shows the thermal degradation characteristics of PLA and its nanocomposites. It was seen that the thermal stability of PLA decreases with respect to increase in nano fibrillated cellulose content. PLA undergoes thermal degradation above 300°C by hydrolysis, lactide reformation, oxidative main chain scission, and inter or intramolecular transesterification reactions [15]. The onset degradation temperature for all the three nanocomposites was found lesser than that of

virgin PLA. The presence of nanofibrillated cellulose and humidity in the nanocomposites results in multiple-stage degradation. From Figure 8.5, it is seen that the nanocomposite with 1 wt % NFC shows a first step degradation at around 310 °C, which is probably related to the degradation of cellulose. The second degradation step is related to PLA chains which has its maximum temperature at around 347°C, almost same thermal stability of pristine PLA. Similarly is the case of 2 and 3 wt% added nanocellulose composites.

Table 8.4 T_{onset} , $T_{50\%}$ and T_{max} for PLA and its nanocomposites

Sample code	T_{onset} (°C)	$T_{50\%}$ (°C)	T_{max} (°C)
PLAV	347.64	365.14	371.18
PLHVA	310.23	330.57	336.58
PLHVANC 1	300.97	323.64	329.78
PLHVANC 2	300.92	322.04	326.37
PLHVANC 3	302.96	323.64	328.64

PLHVANC:PLA/EVA/EVOH/Nanocellulose

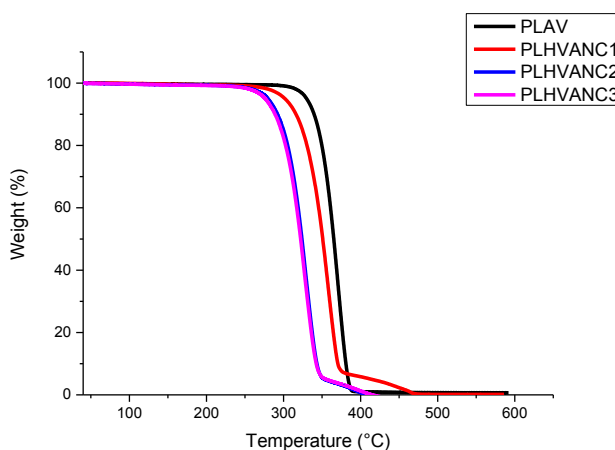


Figure 8.5 TGA curves of PLA and PLA/EVA/EVOH nanocomposites

8.5 Conclusion

PLA /EVA/EVOH nanocomposites were prepared by the addition of nanofibrillated cellulose under different weight loadings of 1, 2 and 3 wt% respectively to toughened PLA blend systems. The addition of nano cellulose upto 2 wt % retained the tensile strength of PLA/EVA/ EVOH ternary blend systems whereas for further weight loadings the tensile strength decreased significantly. Also, the addition of nano cellulose upto 2 wt% loading increased the modulus compared to PLA. The addition of nanofibrillated cellulose increased the stiffness of the composite. The percentage elongation at break showed 214 % increase in the case of PLA/EVA/EVOH/NC 2 system in comparison to virgin PLA. This may be due to the combined effect that is plasticisation by EVA/EVOH together with the strong interactions between polymeric groups of PLA and hydroxyl groups of nanocellulose.

References

- [1] K. Oksman, M., Skrifvars, J.F. Selin, *Comp. Sci. and Tech.* 63 (2003) 1317.
- [2] F. Yu, H. X. Huang, , *Polym. Test.*, 45 (2015) 107..
- [3] J.R. S.Y. Gu, B. Dong, *J. Polym. Sci. B-Polym. Phys.*, 45 (2007) 3189.
- [4] M. Keshtkar, M. Nofar, C. B. Park, and P. J. Carreau, *Polymer*, 55 (2014) 4077.
- [5] F.Mai, Y. Habibi, J.-M. Raquez, , *Polymer*, 54 (2013) 6818.
- [6] E. Narimissa, R. K. Gupta, N. Kao, H. J. Choi, M. Jollands, S. N. Bhattacharya, *Polym.Eng. Sc.* 54, (2014) 175.
- [7] B. Wang, T. Wan, and W. Zeng, *J. App. Polym.Sci.*, 125 (2012) pp. E364.

- [8] G.H. Yew, A.M.M. Yusof, Z.A.M. Ishak, U.S. Ishiaku, *Polym. Degrad. Stab.* 90 (2005) 488.
- [9] Q. Cheng, S. Wang, T.G. Rials, T, *Compos. Part A Appl. Sci. Manufact.* 40 (2009) 218.
- [10] Kemala, E. Budiando, B. Soegiyono, *Arab J. Chem.* 5 (2012) 103.
- [11] S-Y Lee, D.J. Mohan, I-A Kang, G-H Doh, S. Lee, S.O. Han *Fibers Polym* 10 (2009). 77.
- [12] W.Yang, F. Dominici, E. Fortunati, J.M. Kenny, D.Puglia, *RSC Advn*, , (2015) 32350-32357.]
- [13] R.B. Valapa, G. Pugazhenthii and V. Katiyar, *J. Appl. Polym. Sci.* 5, 132 (2015) 41320.
- [14] M. S. Huda, A. K. Mohanty, L. T. Drzal, E. Schut, M. Misra, *J.Mat.Sc* 40 (2005) 4221.
- [15] K. Jamshidi,S.-H.Hyon, Y.Ikada, *Polymer* 29 (1988)2229.

.....✂.....

SUMMARY AND CONCLUSION

This chapter provides a brief summary and conclusion of the work described in this thesis and the scope of future work is also presented herewith.

PLA is a biodegradable, biocompatible and bioactive thermoplastic aliphatic polyester produced from renewable sources of starch such as sugar feed stocks, corn wheat, potato etc., by fermentation to lactic acid, followed by ring-opening polymerization or condensation polymerization. PLA showcases excellent inherent properties such as good tensile strength and modulus of elasticity, low toxicity, excellent transparency, biocompatibility etc., in addition to being fully biodegradable and compostable; whereby it is one of the most promising biopolymer serving as a potential high-performance and eco-friendly alternative for petroleum derived thermoplastics. Currently PLA is used in the production of compostable bags, mulch films and as materials for controlled release of fertilizers, pesticides, drugs etc., wherein biodegradability of PLA is the major highlight than its mechanical property attributes. However, establishment of PLA as a durable material is hindered by its inherent brittleness and consequent low impact resistance, low melt viscosity, low heat deflection temperature etc.

In this context, many researchers have dedicated their work to the improvement of ductility and toughness of PLA via plasticization, copolymerization and by melt blending with various toughening agents viz. rubbers, elastomers, thermoplastics etc. Melt blending has been proven to be an efficient technique for its relative easiness in performing and cost-effectiveness compared to solution mixing. Also, the use of rubbers and elastomers in improving ductility and toughness of PLA is of special interest as they facilitate increased dissipation of energy through the material during deformation without adversely affecting its stiffness or thermal stability. However, it is found that toughening efficiency of the modifiers varied depending upon their miscibility with the matrix, processing temperature, interfacial adhesion between the dispersed and continuous phase within the blend.

In this study, two different types of elastomers, Poly(styrene-*b*-(ethylene-co-butylene)-*b*-styrene) (SEBS), Poly (ethylene-vinyl acetate) (EVAc) and their chemically modified forms, Maleic Anhydride grafted SEBS (MA-g-SEBS) and hydrolysed EVA (EVOH) were used as toughening agents for PLA employing melt blending technique. Mechanical, thermal and morphological characteristics of the blends were investigated and characterised in comparison to that of the virgin PLA and furthermore, nanocellulose isolated from cotton waste were incorporated in the blends so as to enhance the thermal and mechanical properties of PLA.

PLA/SEBS blends were prepared in four compositions by melt mixing in a twin screw extruder and its morphological, physico-mechanical

and thermal properties were evaluated and studied. The properties of these blends did not reveal any significant improvement in impact strength of PLA which may be due to poor miscibility of the blend system. However, SEBS had imparted plasticisation effect on base matrix (PLA) with prominent improvement in % Elongation. Therefore, SEBS was chemically modified using maleic anhydride by melt grafting technique termed as MA-g-SEBS which was used as toughening agent in four different compositions to study its effect on PLA. PLA with 20 wt% of maleated SEBS elastomer showed remarkable improvement in especially impact strength (134 %) compared to virgin PLA. SEM study revealed that high impact property was due to multiple crazing and cavitations toughening mechanisms. The percentage elongation of PLA / MA-g-SEBS (80:20) blend was also increased considerably in comparison with neat PLA which indicated a brittle to ductile transition. However tensile and flexural properties were reduced in comparison with virgin PLA.

Nanomaterials have numerous applications in the field of healthcare, electronics, cosmetics etc. The issues such as renewability, sustainability, biocompatibility and cost efficiency have resulted significant interest towards cellulose based nanomaterials over synthetic nanomaterials. Nanocelluloses, mainly, nanofibrillated cellulose (NFC) was isolated from waste cotton and characterised by various techniques such as SEM, TEM, XRD etc. SEM images showed highly entangled nanofibrils with diameters in nano dimensions. TEM results revealed size reduction of fiber from micro to nano upon mild acid treatment followed by steam explosion. Nanofibrillated cellulose was incorporated in PLA toughened by using

two impact modifiers such as MA-g-SEBS and EVA/EVOH. Both the PLA toughened systems were investigated for its thermal, mechanical and morphological properties.

Nanofibrillated cellulose under three different compositions viz 1, 2 and 3 wt. % was incorporated in PLA /MA -g- SEBS blend by melt mixing technique and its effect on thermo-mechanical properties and morphological behaviour of PLA blends were studied. The nanocomposites containing 2 wt. % of nanocellulose (PLA/MA-g-SEBS/nanocellulose) exhibited higher modulus compared to virgin PLA. An increase in percentage elongation was also observed for PLSEGNC composites containing 2 wt.% of nanocellulose. The impact strength was found to be higher for all the PLA/MA-g-SEBS /nanocellulose composites compared to virgin PLA. DSC measurements revealed the improved impact strength due to the enhancement in crystallization of PLA by heterogeneous nucleation effect of nanofibrillated cellulose.

EVA and modified EVA (hydrolysed EVA) in various compositions were also used as toughening agents for PLA and investigated its effect on mechanical, thermal and morphological properties. The impact strength of binary blends PLA/EVA increased significantly (176%) for 15 wt. % of EVA compared to pristine PLA. This was due to good interfacial adhesion between the PLA matrix and EVA. From SEM studies, surface of the continuous phase (PLA) was found more rougher by the addition of EVA indicating greater adhesion between PLA and toughening agent. However, PLA blends with EVA reduced the thermal stability of PLA with a decrease in onset and maximum degradation temperatures.

The effect of EVA on melt crystallization of PLA was investigated by using Avrami model. Avrami coefficient for PLA-EVA blends was found lower than neat PLA which indicated that EVA acted as a nucleating agent.

Modification of EVA was carried out to form ethylene vinyl alcohol (EVOH) via hydrolysis at varying time (1, 2 and 3 hrs) which was subsequently blended with PLA to make more compatible and toughened PLA and EVA system. FTIR results show an increase in intensity of the hydroxyl peak ($3200\text{-}3400\text{ cm}^{-1}$) with increase in degree of hydrolysis. The highest degree of hydrolysis (81%) was achieved for EVA hydrolysed for 3 hrs (EVOH-3). The higher degree of hydrolysis has brought higher improvement in the mechanical properties such as elongation at break (12.5 %) and impact strength ($11.73\text{ (KJ/m}^2\text{)}$) for ternary blends of PLA. DSC results confirmed the nucleation effect of EVOH by reducing the cold crystallization temperature of PLA. The decrement in the activation energy for PLA/EVA/EVOH blends indicated reduction in thermal stability due to decomposition of hydroxyl group present in EVOH. The SEM images of PLA/EVA/EVOH shows PLA/EVA blends in the presence of EVOH.

Nanofibrillated cellulose on the toughened ternary blend system of PLA (PLA/EVA/EVOH) was investigated for its effect on thermo-mechanical properties. In this system, tensile modulus and percentage elongation increased significantly upto addition of 2 wt% of nanocellulose. The impact strength increased upto 89 % by the incorporation of 2 wt% of nanocellulose. The crystallization temperature decreased with respect to

increment in nanocellulose loading upto 2% in the PLA matrix, which revealed good compatibility between toughened matrix and nanocellulose.

To summarize, PLA blends and nanocomposites prepared using SEBS, EVA, MA-g-SEBS, EVOH based toughening agents via melt blending technique produces vast improvement in mechanical properties, especially impact strength which will strengthen its applicability to promote environmental sustainable PLA based blends and composites.

Future scope of the work:

- 1) **Studies on the effect of green compatibilisers:** Instead of using chemical compatibilisers, some compatibilisers derived from renewable resources may be used for producing fully green composite systems based on PLA.
- 2) **Prototype development:** A prototype product of toughened PLA blends and composites with higher properties can be used for different applications like automotive interior parts like door trim.
- 3) **Life cycle analysis** of PLA blends and nanocomposites.

.....✂.....

||| List of Publications |||

- [1] V H Sangeetha, H Deka, T O Varghese, S K Nayak. ***“State of the art and future prospective of Poly (lactic acid) based blends and composites”*** in Polymer Composites, Wiley Interscience, 2016, 39 (1) 81-101.
- [2] V H Sangeetha, T O Varghese, S K Nayak ***“Toughening of Polylactic Acid (PLA) Using Styrene Ethylene Butylene Styrene (SEBS) By Melt Blending: Mechanical, Thermal And Morphological studies”*** in Polymer Science and Engineering, Wiley Interscience, 2016, 56 (6), 669-675.
- [3] V H Sangeetha, Ravibabu Valppa, T O Varghese, S K Nayak ***“Super Toughened Renewable Poly(lactic acid) Based Ternary Blends System: Effect of Degree of Hydrolysis of Ethylene Vinyl Acetate on Impact and Thermal Properties”*** in RSC Advances, 2016, 76 (6) 72681-72691.
- [4] V H Sangeetha, Ravibabu Valppa, T O Varghese, S K Nayak ***Investigation on the influence of EVA content on the mechanical and thermal characteristics of poly(lactic acid) blends –Journal of Polymers and Environment*** 2016, 26 (1) 1-14.

Paper communicated: *Isolation and characterisation of nanofibrillated cellulose from waste cotton: Effect of nanocellulose on thermo-mechanical properties of PLA/MA-g- SEBS blends”-V H Sangeetha, S K Nayak, T O Varghese, Polymer Bulletin, Springer on 19th Sept 2017*

Presentations in Seminar and Conferences(National/international):

- [1] Toughening of Polylactic Acid (PLA) With Styrene Ethylene Butylene Styrene (SEBS): Physico-mechanical properties by V H Sangeetha, T O Varghese, S K Nayak, in APM-2015 at IISC Bangalore on March 1-3 2015.
- [2] Analysis and characterization of Epoxidised Cis-1,4-Polybutadiene rubber by different methods and study of PVC-EPBR multiphase blends by V H Sangeetha, T O Varghese, S K Nayak, G in APM-2014 at CIPET-Lucknow on Feb 14-15, 2014.

- [3] "Synthesis of Nanocellulose from Cotton Waste," by V H Sangeetha, H Deka, T O Varghese, S K Nayak in National Seminar on Biopolymers and Green Composites (BPGC -2013) organised by CBPST, Kochi on 27th September 2013.
- [4] "Synthesis and Characterisation of Nanofillers from Renewable Resources," by V H Sangeetha, Jayavani S, H. Deka, T O Varghese, S K Nayak in International Conference on Advance Polymeric Materials on 11th October 2013 at M G University Kottayam.
- [5] "Synthesis, Characterization and Curing Of Vinyl Fuctionalised PolysiloxaneAdhesives for Aerospace Applications," by V H Sangeetha, T O Varghese, S K Nayak, G Prabhakaran in APM-2013 at CIPET-Lucknow on 1 st March 2013.

.....✪.....

Curriculum Vitae

V H Sangeetha

Vellaparambil House
Anapuzha P O
Kodungallur,
Thrsissur, Kerala 680667
Ph: 04802812744
Mob: 9846500397,9400512744
E-mail: sangeetha.vh2006@gmail.com



Personal Details:

Nationality : Indian
Religion : Hindu
Sex and Marital Status : Female, Single
Language Proficiency : English, Malayalam, Hindi

Present address:

Research Scholar
Centre for Biopolymer Science and Technology (CBPST)
FACT Township, Eloor, Udyogamandal PO ,Kochi 683501
Ph:9846500397
Email: sangeetha.vh2006@gmail.com

Educational Qualifications:

M. Tech Polymer Technology(Cochin University of Science and Technology)
M.Sc. Polymer Chemistry (University of Calicut)
B.Ed. (University of Calicut)

Achievements:

First Rank in B.Sc. Polymer Chemistry (University of Calicut)
First Rank in M.Sc. Polymer Chemistry (University of Calicut)
Second Position in M.Tech Polymer Technology (CUSAT)
Selected for Inspire Fellowship (DST) -2011
State Eligibility Test (2010)

Research Experience:

Five Years in the field of Polymers

Teaching Experience:

Five years in the field of Polymers and Biopolymers

.....&O&.....